METAL TO CERAMIC JOINING FOR HIGH TEMPERTURE APPLICATIONS

A thesis submitted for the degree of Doctor of Philosophy

by

Ammer Khan Jadoon

B.Sc (Hons)., M.Sc., DIC., AMIM

Department of Mechanical Engineering
Brunel University
February 2003

Sūra CX.

Naṣr, or Help.

In the name of God, Most Gracious,
Most Merciful.

1. When comes the Help
   Of God, and Victory,

2. And thou dost see
   The People enter God's Religion
   In crowds,

3. Celebrate the Praises
   Of thy Lord, and pray
   For His Forgiveness:
   For He is Oft-Returning
   (In Grace and Mercy).

بِسْمِ اللّٰهِ الرَّحْمٰنِ الرَّحِيمِ

١- اِذَا جَآءَ نَصْرُ اللّٰهِ وَالْفَتْحُ ۙ

٢- وَرَاَيْتَ النَّاسَ يَدْخُلُوْنَ فِىْ دِيْنِ اللّٰهِ اَفْوَاجًا ۙ

٣- فَسَبِّحْ بِحَمْدِ رَبِّكَ وَاسْتَغْفِرْهُ ؕ اِنَّهٗ كَانَ تَوَّابًا ۞

Publications

Work from this thesis has been presented at:

• 6th International Symposium on Advanced Materials, September 1999. Paper was publ'shed in the conference proceedings.

A. K. JADOON, in Proceedings of the 6th International Symposium on Advanced Materials, Pakistan, September 1999, edited by M. A. Khan, K. Hussain and A. Q .Khan, p.304-309

• 7th International Symposium on Advanced Materials, September 2001. Paper was published in the conference proceedings.

A. K. JADOON, in Proceedings of the 7th International Symposium on Advanced Materials, Pakistan, September 2001, edited by A. A. MAZHAR, M. A. KHAN, J. A. MIRZA and A. Q. KHAN, p.129-136.

To be presented:

• Euromat 2003 Congress, "A novel approach for metal to ceramic joining".

The following papers have been submitted for journal publication.

• A. K. JADOON, "Employing reactive synthesis for metal to ceramic joining for high temperature applications". Journal of Materials Science.

• A. K. JADOON, "Metal to ceramic joining via a eutectic bonding technique". Science and Technology of Welding and Joining.

• A. K. JADOON, "NiAl as a metal to ceramic joining interlayer". Journal of High-Temperature Materials.

i

Abstract

The phenomenal growth rate for the use of engineering ceramics is attributed to successful scientific responses to industrial demand. These materials are replacing metal and its alloys in diverse applications from cutting tools and heat engine components to integrated circuits.

Joining technology plays a vital role in this changing and evolving technology as success and failure comes with breaking new barriers. It is important to improve existing techniques and to develop new techniques that reliably join simple shape components to form complex assemblies or join dissimilar materials such as metal to ceramic.

Joining of ceramics is not simple due to their high chemical stability and low coefficient of thermal expansion (CTE). Joining between metal and ceramic is usually carried out at elevated temperatures and upon cooling thermal residual stresses are induced that lead to joint failure or poor strength.

Most metal-ceramic joints cannot be used over 500°C primarily due to the low melting temperature of the interlayer.

This investigation was concerned with the successful joining for higher temperature applications (above 500°C) of two dissimilar high temperature oxidation and corrosion resistant materials, Fecralloy and silicon nitride. The primary focus was on the effects of process conditions upon the microstructure and mechanical properties of the joint and to also study/identify the joining mechanism.

Two novel techniques were employed to join successfully the metal to ceramic. The first was by use of a thin Cu foil that did not remain after joining. Joining occurs by a process that results in partial melting of the Fecralloy interface, where Fe, Cr, Al and Cu reactively infiltrate into the silicon nitride. This liquid mixture causes partial dissolution of the silicon nitride interface, where Si and N diffuse into the Fecralloy. A thin reaction product layer was formed at the silicon nitride interface and our results suggested that this was AlN. The free surface Si and porosity of the silicon nitride along with the eutectic temperatures above 1100°C are all vital for this joining process. The highest average shear strength of a Fecralloy-silicon nitride joint produced by the method was 67.5 MPa.

ii

The second route was that of a powder metallurgy one, where cold pressed Ni-Al (1:1 molar) compacts were used to join successfully the Fecralloy to silicon nitride. The formation of NiAl from its constituents is highly exothermic and this is initiated between 500-650°C The high temperature reached causes partial melting of the Fecralloy interface and dissolution/reactive wetting at the silicon nitride interface. Mostly Fe infiltrates the NiAl improving room temperature ductility, fracture toughness and yield strength. Molten Al from the interlayer reacts and wets the silicon nitride interface with small amount of infiltration and no reaction product forming. The reaction synthesis of NiAl was studied using DTA and TGA, where the effects of Ni particle size and heating rate were investigated.

This joining process is highly dependant upon process conditions, the most important of which are applied pressure, heating rate and Ni/Al particle size. The highest average shear strength attained was 94.30 MPa and this is attributed to good interfacial bonding, high pressure, moderate process temperature and dwell time. The exothermic formation of the NiAl interlayer that is densified and monophase was paramount for this joining process.

The Bansal-Doremus kinetic model for evaluating the kinetic parameters from non-isothermal DTA data was shown to be valid. The results obtained were identical to those by other authors who used a different model and approach.

Acknowledgements

Contents Page

1. *Introduction*

Since the dawn of time, the ability to join similar and dissimilar materials to produce tools, devices and structures has been a vital technology for the survival and progression of humankind [1].

With the passage of time and advances in Materials Engineering, the need for joining has not abated, but in fact, has grown. This is due to the development of new materials with desirable properties and the demand for the incorporation of these into new components and structures [2].

Ideally, a structure would be made without joints, as they are points of weakness. However, the major reasons of why joining becomes necessary are: to achieve function, to achieve structural efficiency and to minimise cost.

When joining dissimilar materials it is important that the engineering compatibility of the two components be considered. A mismatch of the elastic modulus is a common form of mechanical incompatibility, leading to stress concentrations and stress discontinuities at the interface. The higher modulus (stiffer) component restricts the lateral contraction of the lower modulus component, generating shear stress at the joint interface leading to possible failure.

A mismatch in the coefficient of thermal expansion (CTE) represents a lack of physical compatibility and is commonly associated with metal-ceramic joints. This mismatch leads to the generation of thermal stresses at the joint interface and to eventual failure.

Poor chemical compatibility usually leads to undesirable interfacial reactions and unwanted products, which tend to be brittle. Some reactions are accompanied by a volume change, generating local stresses, which can lead to eventual failure.
From this it is apparent that great consideration is and should be taken when joining dissimilar materials.

In the past few years engineering ceramics such as silicon nitride and silicon carbide have gained considerable use in a number of demanding applications. This is due to their superior strength, high impedance to wear, excellent corrosion/chemical resistance, good thermal

1

properties and their ability to maintain strength at elevated temperatures. Applications include various wear-reducing parts such as seals, valves and nozzles in engines; turbine rotors that can reach moderately high temperatures and heat exchangers to recover waste heat that is lost in corrosive exhausts of industrial furnaces [3].

There is a need to further incorporate such engineering ceramics into new devices and structures. Joining is the key enabling technology that will lead to the successful commercial production of such new devices and structures. Thus, there is a need to improve and develop joining techniques that produce integral (high shear strength and resistance to thermal shock) metal-ceramic joints, yet, which are simple and commercially viable.

Most conventional metal-ceramic joining techniques produce joints that cannot be used for higher temperature applications with a ceiling limit of around 500°C [4]. This is due to the relatively low melting temperature of the interlayer. Thus, a need has been identified to develop and study a metal-ceramic joining technique(s) that produce integral joints for higher temperature applications (above 500°C) by a simple and commercially viable process. This has been the primary aim of this work. The overall theme of the work was that of a processing-microstructure-property-performance-relationship.

Silicon nitride is strong, hard, wear resistant, stable to high temperatures and has excellent thermal shock resistance due to its low CTE and high thermal conductivity. These properties in addition to its low density (half that of steel) make it a very attractive engineering ceramic. Reaction bonded silicon nitride (brand name of nitrasil) was chosen for the investigation, as it is cheaper than sintered silicon nitride and little work has been carried out on it. Although not as strong as sintered silicon nitride, its strength is held up to 1400°C, with long-term oxidation resistance up to 1150°C. The thermal and electrical properties of the two forms of silicon nitride are very similar.

The high temperature oxidation resistant iron-chromium-aluminium alloy (brand name of Fecralloy) is an oxidation and corrosion resistant variant of stainless steel. These properties make it an attractive choice for possible high temperature applications.

To date, there have been no reports of successful joining between Fecralloy and silicon nitride. This is believed to be mainly due to the large difference in CTE (Fecralloy=$12 \times 10^{-6} K^-$ and

2

silicon nitride $3.4 \times 10^{6} K^{-1}$) that induces thermal stresses in the joint, which do not produce integral metal-ceramic joints. The weak joints produced after processing usually break under handling. The major obstacles to successful metal-ceramic joining are the mismatched CTE and ability of the interlayer to wet adequately the ceramic interface.

These two materials have outstanding individual properties and if combined in an assembly could find use in numerous high temperature applications (eg. gas turbines). The potential can only be utilised by developing a joining technique that produces integral metal-ceramic joints by a commercially viable technique.

Two different techniques were employed to join these two materials. The first was by use of metallic foil, where pure Cu and then a Ti/Cu/Ti multi-layer was investigated. The second route was a powder metallurgy one, where cold pressed compacts of Ni-Al powder (1:1 molar ratio) were used to exothermically form nickel aluminide, NiAl, as a joining interlayer. The mechanisms of joining were studied and correlated to various factors such as joint strength and processing parameters.

An outline of the thesis is as follows;

• Chapter 2 presents an in-depth and critical literature review into Joining Technology with respect to metal-ceramic joining. Recent advances are presented and discussed, in addition to covering the relevant theoretical background.

• Chapter 3 covers the experimental section, where the joining equipment and procedures are presented, along with the joint characterisation methodology.

• Chapter 4 presents the results and discussion of joining by use of metallic foil.

• Chapter 5 looks into joining via a powder metallurgy route using a NiAl interlayer.

• Chapter 6 is a summary of the conclusions.

• Chapter 7 present the recommendations for future work.

3

2. *Joining Technology: Literature Review of Techniques and Advances*

The techniques and advances discussed in this chapter are most relevant to metal-ceramic joining.

2.1 *Diffusion Bonding*

This joining technique is more commonly associated with metal-metal joining and less so with metal-ceramic joining. The surface conditions of the sample, namely flatness, roughness and cleanliness are vital factors during the diffusion bonding process. Joining temperature, pressure and atmosphere are also important variables of this joining process [5].

Diffusion bonding can be subdivided into two major categories, Solid State and Transient Liquid Phase (TLP) bonding.

2.1.1 *Solid State Diffusion Bonding*

This is a micro-deformation process, which involves holding the components under considerable pressure for a certain time at an elevated temperature, usually in an inert atmosphere or vacuum. A metallic interlayer may or may not be used between the joining surfaces. This interlayer does not melt but aids the joining process by reducing bond line voids.

Solid state diffusion bonding can be used to join a wide range of materials and in cases where an interlayer is not required, offers the possibility of a relatively low degree of micrstructural disruption. A major limitation is the presence of continuous oxide layers on the joining surface which have a strong detrimental effect on the ability to produce strong joints.

Successful joining is dependant on the following factors:

1. Absence of contamination at the joint surfaces and an adequate surface finish. The surfaces must be polished and cleaned ultrasonically before joining.

2. The ability of at least one component to undergo sufficient plastic micro-deformation in order to develop complete contact across the interface between the two components.

3. Sufficient time for diffusion to occur in the interface region to eliminate micrstructural instability and to establish adequate interfacial bonding.

Adherence between dissimilar materials results from atomic and molecular interactions at the interface. These interactions derive from the differences in co-ordination between the atoms at the surface (asymmetrically co-ordinated) and those in the bulk (symmetrically co-ordinated) of the material. Surface atoms contain excess energy and this is considerably higher for metals. As a consequence in metal-ceramic joining, the metal surface energy produces a strong driving force for shape changes that reduce the non-contacting area and for chemical changes that lower the surface energy [6].

The development of a diffusion bond in the solid state depends on both thermally-activated plastic micro-deformation and diffusion-controlled mass transfer. The growth of the contact areas in the early stages of joining occurs by plastic micro-deformation of the more ductile component. Mass transfer and surface diffusion involve the elimination of interfacial voids, while an adhesion process gives the interface boundary strength.

A possible third step involves chemical reactions between the two materials and formation of new phases at the interface. These interfacial reactions are dependant upon joining conditions and on the chemical composition of the materials involved. These reaction products can be either detrimental (due to their brittleness) or decisive to joint strength.

Direct joining between metal and ceramic (i.e. no interlayer) is possible in certain cases, but usually does not result in joining/poor strength. This is mainly due to the presence of thermal residual stresses, which develop during cooling after the diffusion bonding process as a result of the difference in CTE.

Work by Krugers and Den Ouden [7,8] looked at joining silicon carbide to austenitic stainless steel (800-1000°C, 5-30 MPa, up to 24 hours dwel time). They found that joining was only possible by use of a metallic interlayer, as this serves as a barrier for uncontrolled diffusion and reduces thermal stresses. The strongest joint produced had an average strength of 30 MPa and Finite element analysis (FEA) calculations were carried out to evaluate the residual stress. It

was shown that the stress level at the metal-ceramic interface was greatly reduced by use of a metallic interlayer.

In addition to the residual stresses, formation of brittle and unwanted phases (usually silicides) can be detrimental to joint strength/joining. This was found to be the case by Suganama *et al.* when trying to join iron to silicon nitride (1200°C, 100 MPa, 30 minutes). No interlayer was used and the excess formation of the brittle iron-silicide, Fe_5Si_3, was believed to be the main reason for poor joint strength [9].

There was a report of successful direct joining between silicon nitride and the 253MA wear resistant steel, without any interlayer (1200°C, 1-10 MPa, 30 minutes) [10]. An average shear strength of 75 MPa was attained and this was increased to 87 MPa by application of increased pressure during cooling. However, cuboidal modification of the surface steel gave a value of 97.5 MPa, an increase of some 20% when compared to flat steel surfaces.

While the results are encouraging and the process conditions are very modest (low pressure and low dwell time), no thermal cycling was carried out to see how the joints would behave under possible service-like conditions and to see the effects of oxidation. There has also been no further work published by Krajewski or anyone else on this topic [10].

Stoop and Den Ouden [11] looked into joining hot-pressed silicon nitride with austenitic stainless steel by use of Fe, Ni and invar interlayers. The strongest joints with an average shear strength of 95 MPa were produced using an invar interlayer (1000-1100°C, 7-20 MPa, 90-1440 minutes). A reaction layer was formed at the ceramic-interlayer interface. This consisted of a porous zone into the silicon nitride and a diffusion zone extending into the interlayer. Although the average shear strength values are good, it is felt that the presence of the porous zone could act as stress concentration sites for crack propagation during thermal cycling. This was indicated during the processing where a moderately high heating rate (25 K/minute) was used but a low cooling rate (5 K/minute).

It was reported possible to control the residual thermal stresses that are induced upon processing cooling due to the CTE mismatch. Esposito *et al.* [12] found that by controlling experimental conditions, in particular a low vacuum, a joining temperature of 1200°C and a dwell times of 30-3600 minutes, good joining was achieved between Ni foil and silicon nitride.

Shear strength testing was not carried out, rather flexural strength testing, highlighting the lack of international testing standards for metal-ceramic joints. The controlled experimental conditions resulted in the formation of no metal silicides at the joint interface.

The biggest drawback of this work was that it was not very representative of commercial demands, as the Ni foil was 50 μm thick. The flexural strength decreased by some 50% when the foil thickness was increased to 1mm. With the 50 μm foil favourable geometrical effects gave good flexural strength values, which decreased with foil thickness.

The same authors used Ni and Cu foils to join alumina to itself [13]. Very low amounts of interfacial compounds were formed and were dependant on the processing conditions and on the presence of oxygen in the system. This is an interesting study and highlights the importance of studying metal-ceramic interfaces and relating them to the properties of the joint.

Joining technology is not simply applicable to metal-ceramic systems, but to various groups of materials. Metal matrix composites (MMC's) are an important group of such materials with many desirable properties. To achieve commercial success additional processing such as machining or joining will be required. Mechanical methods of joining (bolting or riveting) are not possible as they would disrupt the reinforcement or create sites of stress concentration. High temperature methods (e.g. fusion welding) lead to chemical reactions between the reinforcement and the metal matrix. Aluminium-based composites present an additional problem owing to the tenacious oxide film on the metal, which inhibits joining.

Work by Bushby *et al.* [14] successfully joined, by diffusion bonding in air, the Al-Cu-Mg (2124) alloy reinforced with particulate silicon carbide, to itself (500°C, 10 MPa, 60 minutes). This was achieved using an unreinforced 2124 alloy as the joining interlayer. The Mg present in the interlayer was vital for joining as it disrupted the surface oxide, allowing metal inter-diffusion to occur.

One of the major difficulties in producing complex-shaped ceramic-only components is the lack of suitable joining techniques. Current techniques include joining with glasses, metals and reactive metal brazes [15]. All of these produce joints where the high temperature strength and oxidation/corrosion resistance are inferior to those of the ceramic being joined, due to the less refractory nature of the joining material itself.

7

Diffusion bonding has been successfully used as an alternative to join silicon nitride to itself and silicon carbide to itself by use of different types of interlayers [16,17,18,19].

One novel approach has used electrophoretic deposition (EPD) to deposit a 3Y-TZP interlayer onto an MgO stabilised-Zirconia sample. This was then joined in air by diffusion bonding to another MgO stabilised-Zirconia sample (1400-1475°C, 0.2 MPa, 120 minutes) [20] Although this technique does offer an alternate means of fabricating conformal powder interlayers for diffusion bonding, especially in non-planar geometries, further work is required to quantify joint integrity (shear strength and thermal cycling).

2.1.2   Transient Liquid Phase (TLP) Bonding

This is a diffusion bonding process that has some similarities with brazing. This process has been recently modified and used in the aerospace industry for the joining of high temperature nickel and cobalt-based superalloys [21]. The biggest advantage of this technique is the moderate processing temperatures and low pressures, and this is particularly attractive for the joining of MMCs, as minimal disruption to the composite microstructure is attained. A drawback can be the sometimes long processing dwell time, as this is a diffusion process.

TLP bonding is primarily used for metal-metal joining and employs a thin and chemically different metallic interlayer between the components [22]. The interlayer completely melts and then wets the solid surface before solidifying as a result of the inter-diffusion with the base material. The solidified bond region consists of a primary solid solution similar in composition to the base material. This generally rules out the formation of brittle phases at the interface, as can be formed during solid-state diffusion bonding or brazing.

TLP bonding is applicable to eutectic or peritectic alloy systems, where a lowering of the liquidus temperature occurs during alloying [23]. Let us consider a hypothetical eutectic system, as illustrated in Figure 2.1, of an interlayer of pure metal A sandwiched between components of pure metal B brought into contact at temperature T_1, that is lower than the melting point of either A or B. Diffusion of B into A and of A and into B initially causes the formation of the *Ass* and *Bss* solid solutions. Ultimately the solubility limits, identified as *a* and *d* in the figure, are exceeded and a liquid phase is formed with a composition between *b* and *c* that wets and spreads over the whole solid surfaces. Formation of this liquid increases the rate of inter-diffusion and eventually all the interlayer is consumed. However, inter-diffusion does

not stop and the liquid becomes richer in B and starts to resolidify isothermally when its composition becomes d [24].
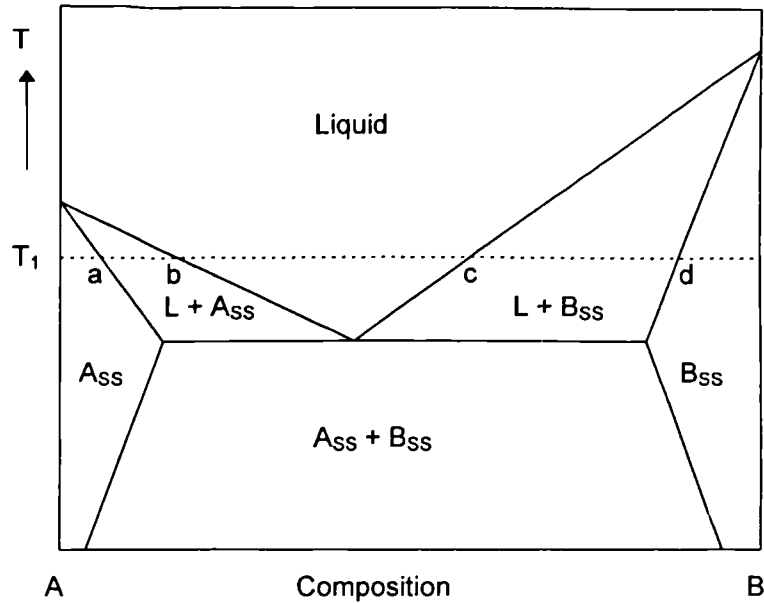
Figure 2.1   **Hypothetical eutetic binary phase diagram [24]**

The TLP bonding process can be summarised in four stages:

1.   Dissolution of the interlayer A

2.   Homogenisation of the liquid

3.   Isothermal solidification

4.   Homogenisation of the joint region

A pre-stage, which is not usually mentioned, is the removal of the oxide surface layer and this is important. The liquid phase disrupts the oxide film and once metal-metal contact has been established in at least one location, the volume changes associated with inter-diffusion and penetration of oxide/substrate interfaces by the liquid phase disrupts the oxide film. Whilst oxide removal can be a relatively slow process, the time taken is only a small fraction of that needed for the whole joining process.

Recent work has primarily focused on TLP bonding to join MMCs and ODS (oxide dispersion strengthened) alloys. Other viable joining techniques disrupt the composite microstructure, causing a segregation of the reinforced particles to the bond region and poor joint strength. Work by Askew and Khan [25,26] has overcome this problem by use of a Ni foil and slightly

higher joining temperature (655°C, 10-60 minutes, 7.5 MPa) when joining a 2124 aluminium MMC alloy, which contains 20 vol% silicon carbide.

Li *et al.* [27] considered the same problem when joining 6061 MMC (Al-Mg-Si with 20 Vol% Al_2O_3). They found the use of a very thin Cu interlayer (< 15μm) and increased pressure at dwell temperature prevented particle segregation and hence good joint strength.

ODS alloys posses very high strength and heat resistance and are promising structural materials for high temperature applications. These alloys are usually produced using mechanical alloying (MA) and contain finely dispersed oxide particles in fine-grained microstructures.

Nakoa and Shinozaki [28] successfully joined the Fe-based ODS alloy, MA 956, to itself by use of a Fe-based filler material IM 7 (1290°C, 5 MPa, 36 minutes). The joints were free of interfacial microvoids and room temperature tensile strength and elongation values were almost equal to those of the parent metal. The best joints were produced at 1290°C, which dispels the notion that TLP is always a low temperature process. However, this is due to the high liquidus temperature of the interlayer metal being 1143°C.

A variant of TLP bonding known as partial transient liquid phase (PTLP) bonding has been looked into as an alternative for metal-ceramic and ceramic-ceramic joining. This modification of TLP bonding uses a multilayer metal structure composed of a thin insert outer layer of lower melting temperature with a thick core of a refractory ductile metal [30]. The processing temperature is chosen so that the outer layer melts, while the ductile core layer remains and acts to aid the CTE mismatch.

During processing a liquid is formed at the joining temperature either because the melting point of the outer layer has been exceeded or because reaction between the core and outer layer has produced a phase that is molten at this temperature. The liquid wets the solid surfaces and inter-diffuses with the parent material to transform into a more refractory solid material. Homogenisation of the outer layer during joining or subsequent thermal treatment makes it possible to produce joints with operational temperatures near or equal to that used in joining [31].

Paulasto *et al.* [31] looked into joining of silicon nitride to itself by use of CuTi/Pd/CuTi interlayer (950-1050°C, 50 kPa, 10-240 minutes). Their conclusions were in-depth and interesting. In brief, they concluded that for the formation of a useful transient liquid the more successful insert combinations are those where melting takes place due to a reaction between the core and the outer layer, i.e. in systems containing a eutectic valley or a liquidus depression.

Zheng *et al.* [32] reported the joining of silicon nitride to itself by use of a Ti/Cu/Ni multi-interlayer (1050°C, 60 minutes, 0.1 MPa – step 2. 1120°C, 30 minutes, 0.1 MPa). Four point bend testing was carried out to evaluate joint strength. Higher values were obtained (some 60%) by use of the Cu, i.e. Ti/Cu/Ni, as opposed to the Ti/Ni interlayer. This was due to the formation of Ni-Ti compounds, which would appear to be brittle. This demonstrates the importance of studying the interfacial reactions and products, and their drastic effect upon joint integrity.

PTLP bonding was successfully used in the joining of alumina to 304 stainless steel [33]. Two interlayer systems were looked at, the first multilayer was Sn-based solder/$Cu_{50}Ti_{50}$ amorphous Sn-based solder and the second Sn-based solder/NiCrB /Sn-based solder. In both cases the highest shear strength was obtained at 500°C. During all the joining trials (300-600°C) the $Cu_{50}Ti_{50}$ amorphous system gave the highest values. This was due to the formation and width of the reaction layer and microvoids, which had a greater effect on the NiCrB system. A shear strength value of almost 100 MPa for the $Cu_{50}Ti_{50}$ amorphous system is very impressive but this is a low temperature system and cannot be used for higher temperature applications.

TLP bonding has resulted in the successful joining of an aluminium-based MMC (6061) to the ceramic alumina by use of a Cu interlayer [34]. In this comprehensive study, the effects of processing parameters, interlayer foil thickness and particle segregation were all investigated and related to joint integrity and microstructure. Shear strength values of 70 MPa were obtained using the thinnest interlayer foil, 5 µm, (580°C, 20 minutes, 1MPa). The width of the detrimental particle segregation layer increased with hold time and increased interlayer foil thickness.

11

TLP and PTLP bonding can be used to produce ceramic-ceramic and metal-ceramic joints. However, considerably less work has been carried out on both these systems compared to metal-metal and MMC-metal joining. The differences between TLP bonding and brazing are few, with respect to metal-ceramic joining. The major differences being that TLP bonding occurs isothermally. The interlayer melts and solidifies as a result of inter-diffusion with the base material, all at constant temperature. The possibility of formation of brittle phases, which is a common problem with brazing is avoided. However, no reports have been found of metal-silicon nitride joining by use of TLP or PTLP bonding. Following this, PTLP bonding was looked at for the joining of Fecralloy-silicon nitride during the course of this work. This study is presented in Chapter 4.

2.2   *Active Metal Brazing*

The term 'brazing' comes from the original use of brass as the joining material, but nowadays a wide range of alloys are used for the joining of metal-ceramic and ceramic-ceramic.

Brazing possesses a major advantage over conventional welding, as the base materials do not melt. This allows brazing to be applied in the joining of dissimilar materials, which cannot be joined by fusion processes due to metallurgical incompatibilities.

Brazing differs from soldering as the joining interlayer has melting temperatures in excess of 450°C [35].

Joining is achieved in two different ways;

(i).   Indirect brazing – where ceramic surfaces are metallised prior to brazing.

(ii).   Direct brazing – more popular and simple, where the filler alloys contains active elements such as titanium (active metal brazing).

In an ideal brazing process, the interlayer melts and flows over the surfaces. It then proceeds to wet and react with the ceramic and then solidifies to form a permanent bond. The molten interlayer has to have high temperature capillary attraction, otherwise it would just flow out.

2.2.1 Wetting

Successful brazing is highly dependant upon the ability of the molten interlayer to wet adequately the ceramic interface. Thus, the role of wetting behaviour during joining is an important topic upon which successful metal-ceramic joining is reliant.

Non-reactive metals poorly wet most important ceramics. Wetting is improved by the addition of active elements especially titanium, and hence the name active metal brazing. Th's causes a further reduction of the interfacial energy contributed by the negative Gibbs free energy of the chemical reaction between the reactive element and the ceramic and also, by the formation of a reaction product at the liquid-ceramic interface. Extensive studies of wetting behaviour have been made using the sessile drop technique. This has provided a valid means of studying wetting and spreading behaviour and the associated reactions. One parameter attained from the sessile drop experiment is the contact angle θ, which can be related to the surface and interfacial energies of the system by the Young-Dupre equation [36];

$$\gamma_{SV} = \gamma_{SL} + \gamma_{LV} \cos \theta \qquad \textbf{Equation 2.1}$$

Where γ_{SV} = surface energy of the solid

γ_{SL} = interfacial energy of the liquid and solid

γ_{LV} = surface energy of the liquid

θ = contact angle

A representation between the wetting characteristics of a liquid on a solid surface is shown in Fig 2.2. If the angle θ is 90° or below, then the liquid wets the surface, while wetting does not occur above 90°.

For a liquid metal drop in contact with a solid ceramic, Equation 2.1 is re-written as:

$$\gamma_C = \gamma_{CM} + \gamma_M \cos \theta \qquad \textbf{Equation 2.2}$$

Where γ_C = ceramic surface energy

γ_M = metal drop surface energy

γ_{CM} = interfacial energy

13

If the interfacial energy γ_{CM} is larger than the ceramic surface energy γ_C, the liquid will not wet and spread freely as Cos θ will be negative and contact angle θ above 90°.
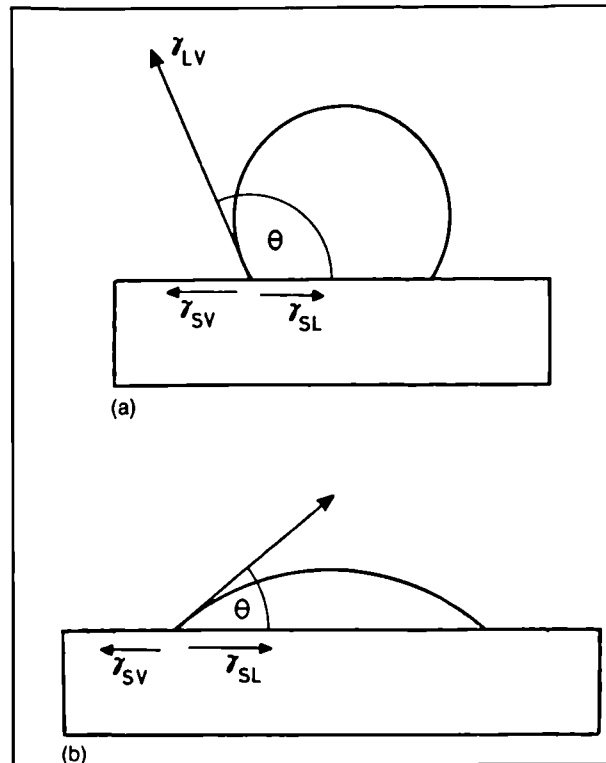
Figure 2.2   Schematic diagrams of wetting characteristics of a liquid on a solid surface: (a) non-wetting (b) wetting

The Young-Dupre equation has its drawbacks, as it does not account for the formation of new phases at the interface. Work by Landry *et al.* [37] concluded that wetting in reactive systems is governed by the final interfacial chemistry at the triple point as opposed to the intensity of interfacial reactions. It was proposed that two types of reaction product were possible, the first was more wettable than the initial substrate and this promoted wetting. The second was a reaction product that was less wettable compared to the initial substrate and this did not promote wetting.

The Young-Dupre equation also assumes a perfectly flat and horizontal reacting interface. In reality, interfacial reactions can result in partial dissolution of the substrate resulting in a non-horizontal surface at the triple point. Thus, the resulting configuration no longer has the horizontal force balanced assumed for the Young-Dupre equation and so determination of the contact angle experimentally is difficult and differs from the theoretically-derived values.

14

Warren *et al.* [38] put forth two extreme cases of dissolutive wetting. In the first case, it is assumed that the dissolution of the ceramic does not significantly change the surface and interfacial energies, σ_{LV} and σ_{SL}. Thus, dissolution modifies only the geometry at the triple point (Fig 2.3a). In the second case, the interfacial energies are modified due to the dissolution of small quanties of tensio-active species in the solid, while the solid/liquid interface is assumed to remain almost flat (equilibrium contact angle θ given by the Young-Dupre equation, Fig 2.3b).
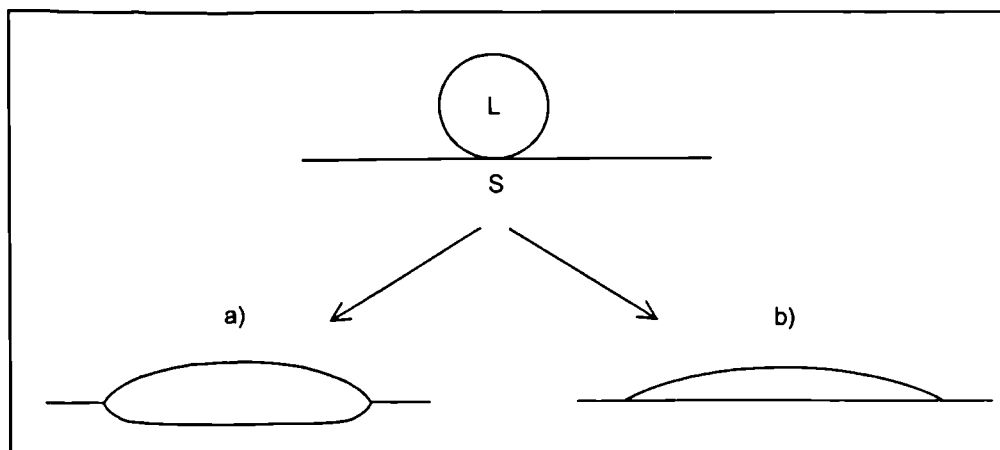

Figure 2.3   Two cases of dissolutive wetting. (a) Dissolution of the solid modifies the geometry at the triple line (b) A slight dissolution is enough to modify the surface energies of the system while the S/L interface remains planar [24]

Most of the models that describe the wetting and spreading behaviour are thermodynamic. Some models take into account the formation of a reaction product layer and so the Young-Dupre equation is modified by the addition of a free energy of reaction terms [39].

Other models predict the wetting or non-wetting behaviour based on the work of adhesion or the change in the surface energy of the system [40]. In the latter, wettability is only a function of the free energy change related to the surface reaction and no contact angle is predicted. In all of the models, only the initial and final geometries of the drop were considered and it was assumed that the reaction product formation was complete at the ceramic/liquid interface.

With ceramic-ceramic joining the braze must wet and satisfy the Young-Dupre equation. This is not the case with metal-ceramic joining, as the sum of the contact angles assumed by the ceramic and metal must be less than 180° [41]. This low requirement is because it is sufficient for the total energy of a liquid to advance while in contact with both component surfaces to be

negative. Thus, the energy change caused by the small advance δx, shown in Fig 2.4 is δF, where;

$$\delta F = \delta x \left(\sigma_{SL} - \sigma_{SV}\right)_{Metal} + \delta x \left(\sigma_{SL} - \sigma_{SV}\right)_{Ceramic} \qquad \text{Equation 2.3}$$

Introducing the equilibrium contact angle of the liquid on the solid metal, θ_Y^{Met}, and on the ceramic, θ_Y^{Cer}, and taking into account the equilibrium condition $\dfrac{d(\delta F)}{d(\delta x)} = 0$, leads to the conclusion that

$$\theta_Y^{Met} + \theta_Y^{Cer} = 180° \qquad \text{Equation 2.4}$$

Thus, the condition for the liquid to advance is $\theta_Y^{Cer} < (180°-\theta_Y^{Met})$. For metal surfaces θ_Y^{Met} is usually lower than $50°$, and the penetration requirement $\theta_Y^{Cer} < 130°$ is satisfied by most ceramics [41]. It should be noted that while the condition $\theta_Y^{Cer} < 90°$ is not necessary for the creation of a ceramic-metal joint, it is highly desirable.

Without adequate wetting, formation of a sound bond is not assured and microvoids may be present.
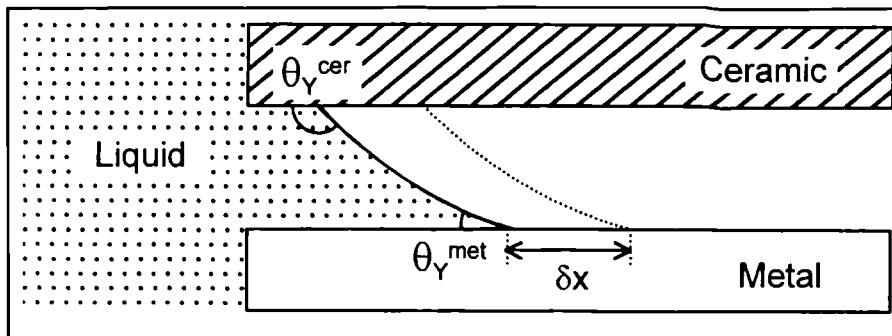
Figure 2.4   Schematic of infiltration of a liquid into a gap between metal and ceramic [41]

2.2.2   *Interfacial Reactions*

One finds that considerable attention has been paid to the ceramic alumina, where extensive wetting studies have been carried out. The main reason for this is that via active metal brazing, alumina has been joined to metal and found use in the automotive (eg. spark plugs) and electrical industries (light bulb) for instance.

16

The most popular and thoroughly investigated brazing interlayer systems are based on the Ag-Cu-Ti. The concentration of Ti has been reduced from about 10 wt% to 1-2 wt% by varying the Ag/Cu ratio or by use of Sn or In which increase the thermodynamic activity of Ti. High concentrations of Ti were not beneficial to wetting/joining as the maximum solubility of titanium in the liquid eutectic is about 2 wt% and also Ti intemetallics are brittle (low Ti improves ductility of the joint). The interfacial reactions between silicon nitride and liquid metal can be classed into two reaction types [42];

The first is;

$$\text{Silicon Nitride} + \text{Metal} \Rightarrow \text{Metal Silicide} + \text{Free Nitrogen} \qquad \textbf{Equation 2.5}$$

The free nitrogen may react with the metal to form a metal nitride or be released from the system as nitrogen gas. Sometimes it remains as nitrogen gas or solute and this can be detrimental to joining as pores are formed at/close to the joint interface. In the temperature range in which the free energy change is negative, the reaction proceeds to the right hand side of the equation.

If the formation of a metal nitride becomes the rate-determining step then the following reaction will proceed;

$$\text{Silicon Nitride} + \text{Metal} \Rightarrow \text{Metal Nitride} + \text{Free Silicon} \qquad \textbf{Equation 2.6}$$
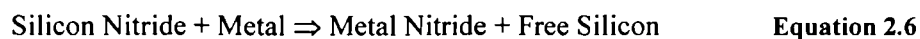
The free energy change of this reaction can be obtained from Ellingham diagrams. The released free silicon may also react with the metal forming a metal silicide.

However, the minimum temperatures for both reactions of Equations 2.5 and 2.6 are important and cannot be deduced from the free-energy changes alone because at low temperatures the diffusion and reaction rates are slow. Also, the formation of nitrides also depends on the partial pressure of nitrogen during joining.

With reaction bonded silicon nitride the presence of oxides/oxynitrides and surface free silica will also play a role, reacting to form metal silicides. The oxide/oxynitride layer is a physical barrier on the silicon nitride and is only removed in vacuum at high temperatures. This is demonstrated in Fig 2.5, which shows the variation in contact angle with temperature for

aluminium on silicon nitride [43]. A transition from non-wetting to wetting ($\theta < 90°$) is observed in the 950-1000°C range. At low temperatures large contact angles are observed and this is due to the oxide/oxynitride surface layer on the silicon nitride and alumina (Al_2O_3) layer on the aluminium. At 1100°C low contact angles are observed and this is due to direct contact between the aluminium and silicon nitride, where the reaction proceeds to form aluminium nitride.
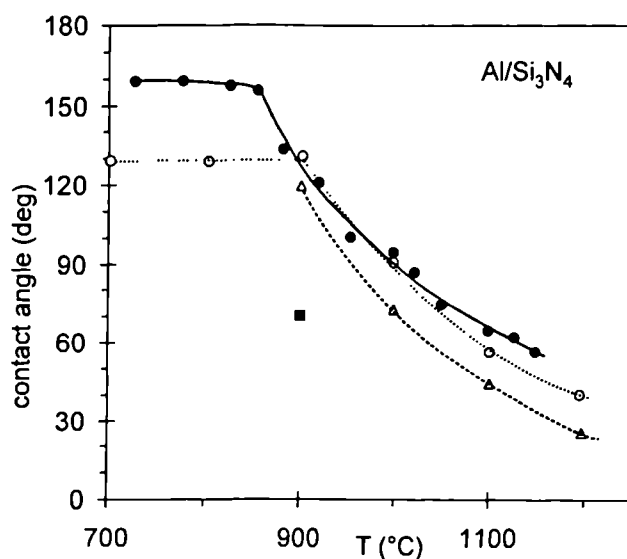

Figure 2.5   **Contact angle vs temperature for Al on silicon nitride [43]**

Not all commercially active metal brazes are based on the Ag-Cu system. Ni-Cr brazes (Ni-19Cr-10Si and Ni-14Cr-10P) were looked at for possible high temperature use in the joining of silicon nitride [44]. However, no commercial use has been found as the Ni-Cr-Si braze forms excessive amounts of silicides and the Ni-Cr-P does not wet adequately.

In recent years, work on wettability and interfacial reactions has been more focused on active-elemental effects and joining [45,46,47,48] and trying to understand the mechanisms of the reactions [49,50,51]. It was found that the addition of Cr to liquid copper up to its solubility limit promoted wetting on silicon nitride [52]. Improved wetting with higher Cr content was achieved by the addition of Ni to the Cu-Cr alloys. The undesirable formation of a brittle interfacial reaction layer was suppressed by the addition of Si to the Cr containing brazing interlayer alloy.

Similar results were observed using silicon carbide, where Si was added to the Cu-Cr braze alloy to suppress the formation of the Cr_3Cr_2 and Cu/Cu duplex phases [53].

18

Zhou *et al.* [54] found that the volume change of the ceramic substrate during reaction played a key role in the effect of the chemical reaction on wetting. If the volume of the ceramic substrate decreases after the reaction, the wettability is not improved by the chemical reaction. However, if the volume of the ceramic substrate increases after the reaction, the wettability is improved by the chemical reaction. This is an interesting concept and is based upon work carried out on alumina and not silicon nitride. However, this concept could be applicable to most ceramics, including silicon nitride. When the ceramic shrinks, a crack or cavity is induced some 90° to the interface and this becomes a physical barrier to the spreading and wetting of the molten interlayer.

It would be correct to say that the exact mechanisms of reaction bonding and the effects of the chemical reactions on wetting are still not known and fully understood. This must change if the full potential of ceramics are utilized in structures by use of metal-ceramic joining.

2.2.3   *Joining using active metal brazing*

Inconnel 718 alloy was joined to silicon nitride by use of a Ag-27Cu-3Ti interlayer (790-900°C, 7-49 minutes) [55]. Shear testing gave moderately low values in the 46-70 MPa range. These values were attributed to the formation of a Ti-Cu-Ni alloy layer between the interlayer and Inconnel 718. With increasing joining temperature the growth of the Ti-Cu-Ni alloy layer was much greater than that of the reaction product layer. So the diffusion rate of titanium into the base metal was much greater than the reaction rate with silicon nitride at the high temperature.

Similar work looked into the joining of Inconnel 600 to silicon nitride by use of an Ag-27Cu-2Ti interlayer (800-900°C, 5-20 minutes, 3-13 MPa) [56]. Shear strength measurements were not carried out, rather four-point bend tests, which were very modest. One is led to believe that this is a flawed joining system, as a very low cooling rate of only 1 K/minute produces joints, at the specified temperature of 830°C. Processing above this temperature causes failure due to excessive thermal stresses and a lower processing temperature is insufficient for joining. If this metal and ceramic had to be joined for commercial reasons, a different joining interlayer system would undoubtly be used.

19

A great deal of attention is rightly paid to the processing parameters during joining (dwell time, pressure, temperature and composition variations). In the joining of pure Cu to silicon nitride via an Ag-35.25Cu-1.75Ti braze, the effects of the surface smoothness of the Cu and application of load were investigated in relation to shear strength [56]. Low shear strength values in the 14-34 MPa were range obtained and these values are due to the residual thermal stresses induced during processing. This is caused by the large difference in CTE between the Cu, 17×10^{-6} K^{-1}, and silicon nitride, 3×10^{-6} K^{-1}. It was found that the smoother the Cu interface, the higher the shear strength value. This is because there is greater contact between molten the interlayer and metal, and microvoids are avoided.

The application of a small load also increased the shear strength, which decreased with higher loads. It was put forth that the small load causes ejection of some Ag-rich liquid that results in a more ductile, stronger brazed joint structure. While that is true, a small load also assists in the breaking down of the surface oxide layer and in establishing contact and avoidance of microvoids.

An interesting report [58] suggests that in the joining of silicon nitride to Invar by use of an Al interlayer, the Al does not wet the silicon nitride but can bond well to it (700-950°C, 0-0.15 MPa, 2-30 minutes, Ar/N$_2$/O$_2$ atmosphere). This was based on the findings that there was no reaction layer present at the Al/silicon nitride interface.

Opinion is varied about the presence of a reaction layer product. Some authors [59] believe them to be very detrimental to joint strength and their absence is preferred. Others [60] attribute interfacial failure in their work due to the thinness of the reaction layer product.

The Japanese automotive industry has successfully incorporated ceramic components into their engines. Silicon nitride is used in glow plugs, precombustion chambers, rocker arms, turbocharger rotors and tappets [61]. Researchers at the R & D centre, NGK Spark plug company Japan, successfully joined silicon nitride to a steel shaft (Ni-Cr-Mo steel) via an Ag-Cu-In-Ti brazing interlayer (exact composition is a commercial secret) [61]. This had an excellent average shear strength of 250 MPa and survived the service-like conditions in a diesel engine. For comparison silicon nitride was joined to another steel shaft (carbon steel) this time employing a PTLP method, where a sandwich like interlayer was used, Ag-Cu-In-Ti braze/Cu/Ag-Cu-In-Ti braze. It was hoped that the ductile Cu would remain and increase mechanical properties by reducing the residual thermal stresses. However, this method

produced joints with average shear strength values of 100 MPa. It was difficult to make any direct comparisons between this and the previous method as steel shafts of a different composition were used.

There has been considerable effort into finding alternate brazes, mainly due to cost. The large quantity of silver in the Ag-Cu-Ti braze is expensive especially for production on a large commercial scale. A Cu-Ni-Ti-B brazing alloy was proposed as a possible contender to the conventional Ag-Cu-Ti braze [62]. The study was not particularly in depth and there was no follow up work. However, it was shown that interlayer foil thickness had a role in joining and when it was increased from 20 to 80 μm the 3-point bend strength increased dramatically. Further increase in foil thickness was detrimental to the bend strength.

Heim *et al.* looked into the use of Cu-Ga amalgams for metal-ceramic joining [63]. Stainless steel was joined to silicon nitride and the optimum joints were produced in an argon atmosphere with considerable pressure (450 MPa) at 900°C. The biggest drawback of this technique is that samples were under pressure and temperature for a period of ten hours. Also, considerable amounts of Ga were reported to be lost in the process.

Ni-Hf alloys for possible joining interlayer applications have been looked at due to their excellent oxidation resistance and high melting temperature [64]. Ni-Hf-Cr, Ni-Hf-Co and Ni-Hf-Cr-Co have all been studied and used in joining. However, these interlayer systems are very susceptible to the formation of unwanted brittle phases and to combat this problem makes the process uneconomic. Another disadvantage, which results from the high content of metalloids is the high inclination of these elements to diffuse into the base metal. At high temperatures this causes the development of borides in the base metal near the joint. The development of chromium borides causes a decrease in the corrosion resistance.

Although alumina is the most commonly used structural ceramic, another oxide that is gaining in importance is zirconia [65]. Zirconia exhibits high strength and fracture toughness, particularly at temperatures below 300°C and it is also a good ionic conductor at high temperatures. Zirconia can be found in applications ranging from wire drawing dies, cutting and machining tools, to oxygen sensors and fuel cells [65].

Upon cooling from high temperatures, zirconia undergoes a tetragonal-monoclinic transformation, involving a 3-5% volume increase. This can be sufficient to induce cracking

and so additives are used to prevent this transformation. Better mechanical properties, compared with fully stabilised zirconia (FSZ) are achieved with partially stabilised zirconia (PSZ), where precipitates of very small (50-100 nm) particles of the metastable tetragonal phase are induced into the cubic matrix by thermal treatment. The resultant properties are a result of transformation toughening, where the volume change of the tetragonal-to-monoclinic transformation improves both toughness and strength. PSZ finds use in wire drawing dies and cutting tools, while FSZ is used in sensors and fuel cells.

PSZ was joined to itself, to 316 stainless steel and to pure Ti by the use of different composition variants of the Ag-Cu-Ti braze (850-1000°C, 5-30 minutes) [65]. Joint strengths were measured using a four-point bend test and the PSZ-Ti joint gave the highest value while PSZ-316 stainless steel gave the lowest value. At/close to the joint region the PSZ de-colourised and this was due to the Ti reacting with Zirconia causing an oxygen-depleted region [65].

Zirconia was joined to 1Cr-18Ni-9Ti stainless steel (800-1050°C, 0-60 minutes, 40 kPa) [66] and to itself (same processing parameters) [67]. Ziconia was joined to the stainless steel via an Ag-38Cu-3Ti braze. The highest shear strength was 150 MPa and this was highly dependant upon interlayer thickness, brazing temperature, dwell time and reaction layer thickness. A shear strength value of 170 MPa was achieved in the zirconia-zirconia joint. It was shown that the shear strength was controlled by interfacial morphologies. It is interesting that pure zirconia is used in both cases and that good shear strength values were obtained. It is felt that thermal cycling would weaken the joints considerably due to the polymorphic transformation and CTE mismatch.

Diverting from the conventional Ag-Cu-Ti brazes, zirconia was joined to forgeable cast iron (3 wt% C) by use of Cu-Ga-Ti and Cu-Sn-Pb-Ti interlayers (950-1150°C, 10 minutes, 1-3 MPa) [68]. Excellent shear strength values were obtained, 277 MPa for the Cu-Ga-Ti and 136 MPa for the Cu-Sn-Pb-Ti. One of the main reasons for these high values is due to the almost identical CTE values for metal and ceramic. This was selected on purpose.

As was mentioned earlier, alumina (Al_2O_3) is the most widely studied and used engineering ceramic. Conventionally it has been joined to metals via the Ag-Cu-Ti braze for low/moderate temperature use. There has been an effort to raise service temperature and joint strength.

Employing a technique very similar to PTLP bonding, stainless steel (1Cr-18Ni-9Ti) was joined to alumina via a Ag38-Cu5-Ti/Mo or Cu/Ag38-Cu-5Ti interlayer (850°C, 30 minutes) [69]. The Mo insert gave higher shear strength values (about 150 MPa) compared with the Cu insert (about 100 MPa). It was suggested that there must be other factors introduced by the Cu that lower joint strength.

Alumina has been joined to itself via a Cu/Nb/Cu interlayer (1150-1400°C, 2.2 MPa, 30-329 minutes) [70]. Four point bend tests showed that the joints retained strength at high temperature. The high temperature and long dwell time make the process unviable. Modifying the conventional Ag-Cu-Ti braze, Ag-Cu-Zr was used to join alumina with Ni-Cr steel and also Cu (750-950°C, 30 minutes) [71]. Zr was selected as the active element as it showed a stronger work of adhesion on alumina ceramics and more negative ΔG of oxide formation than Ti. The alumina-steel joints had an average shear strength in the 112.3-130.5 MPa range. These values were highly dependant upon interfacial morphology and one predominant factor could not be established. The alumina-Cu joints gave low values by comparason of 94 MPa. The Cu was expected to relax the thermal stress by plastic deformation, due to the low yield strength of Cu. At the brazing temperature, the excessive inter-diffusion and reaction between the Cu and Zr from the braze and the Cu substrate caused the braze/Cu substrate interface to move towards the alumina. Thus, the joint gap decreased leading to a larger thermal stress being generated compared to the alumina-steel joint. A lower joining temperature was proposed to counteract this problem.

2.2.4   Addressing the thermal stress problem

Residual stresses are generated during processing because of the difference in thermal and/or elastic properties of the joined materials. Metals tend to be softer than ceramics and have higher thermal expansion coefficients. So the problematic thermal residual stress depends upon thermal expansion and to a lesser extent elastic mismatch between the metal and ceramic.

Without a doubt, thermal stress is a major obstacle to successful metal-ceramic joining. In order to overcome this, the solution has to consider factors such as will the joint strength be effected and so on. In order to address this problem, it is very important that it is studied in-depth first. Finite element analysis (FEA) is a valid technique used to estimate thermal stresses developed in metal-ceramic joints.

In a recent study [72], FEA was used to look into thermal stresses developed in silicon nitride bodies joined by metallic interlayers. Those chosen were Ni, Al and Si and this was due to their elastic and elastic-plastic behaviour. Many conclusions were put forth from this study. The stress distribution for any combination of metal and ceramic showed the following features. Non-zero stresses were confined to a narrow region, including the interlayer, the interfaces and an adjacent part of the adherents, within a distance about three times the thickness of the interlayer. The stresses parallel to the interface were tensile in metals and compressive in ceramics showing a jump at the interface. In both metal interlayer and ceramic adherent the stresses reduced to zero towards the free edge. Stresses normal to the interface were near zero throughout the body except for a local near-surface region of the metal interlayer, where tensile stresses developed in the ceramic and compressive in the metal. Maximum tension in ceramics occured near the free edge of the interface, where the stresses were singular. This tensile stress developed in the ceramic adherent may be the most important factor effecting joint failure.

Besides thermal and elastic mismatches, the size of the joint and metal plasticity are important factors which additionally influence tensile thermal stress build ups in the ceramic. Thermal residual stress was found to decrease with interlayer thickness and with sample size. The disadvantage of mere FEA calculations is that the results for points very close to the free edge, where the stresses are singular are not accurate. Thus, it advantageous to combine an analytical description with additional FEA calculations. This was carried out for various metal-ceramic combinations [73]. Numerous equations were put forth relating various factors such as interlayer thickness and stress intensity. Also, the stresses near the free edge of the interface in the ceramic were dependant on the material parameters of all three components (metal, ceramic and interlayer).

Moving onto practical solutions to overcome this problem, a wide variety of methods have been developed to overcome the CTE mismatch and these include soft metal interlayer, composite interlayers (particulate and fibrous), laminate interlayer (soft metal with a low expansion hard metal) and microcracked interlayers [74].

Fernie *et al.* [75,76] successfully showed that mechanically flexible interlayer systems could be used to absorb the strains induced due to the CTE mismatch. Soft metal interlayers such as Al and Cu can reduce the residual stresses by their elastic, plastic and creep deformation. However, a single layer does not remove the residual stress efficiently for silicon nitride-metal

systems. They would also not resist thermal cycling. A laminate interlayer system of a hard/soft/hard metal could accommodate rigorous thermal cycling. Composite interlayers such as functionally graded materials (FGM's) are another effective method of accommodating thermal mismatch, but problems are encountered in the strength and reliability of the interlayer itself.

Another solution is the use of a powder metallurgy route to produce an interlayer. Fecralloy was successfully joined to calcia stabilized zirconia (CSZ) (1000°C, 5 hours) using a mixture of Fe, Cr and Al powder as a brazing filler using a screen printing/powder metallurgy method [77]. Mechanical testing was not carried out, but the joint withstood thermal cycling in air at 850°C. Although the results are encouraging, the approximately 15-20% porosity in the interlayer could weaken the joint strength.

2.3   *Joining via Combustion Reactions*

Combustion synthesis (also termed reaction synthesis) is a process used to form ceramics, intermetallics and their composites at operating temperatures much lower than their melting points and in very short processing times via exothermic reactions [78].

Work by Miyamoto *et al.* [79] showed that metal-ceramic joining was possible using combustion synthesis by placing a thin layer of powder reactant between the metal and ceramic and applying pressure during processing.

This technique was used to produce weak silicon carbide-silicon carbide joints [80]. Using tape casting, a Ti-C-Ni mixture was used to join silicon carbide-silicon carbide by the formation of a TiC-Ni interlayer (1125°C, 5-20 MPa, Ar). The advantages of using combustion synthesis as a fabrication process include low processing temperatures and short processing times; no need of specialised equipment (low set up costs); the formation of pure products due to the evaporation of low boiling point impurities; and near-net shaping. The biggest disadvantages are the excessive porosity and lack of process control [78].

While considerable research effort has investigated the use of combustion synthesis to produce bulk intermetallic compounds [81], little or no work has considered them as metal-ceramic

joining interlayers. While the exact reasons are unknown, excessive porosity, limited process control and poor joint strength are the most likely reasons. This technique does offer the possibility of high temperature and oxidation-resistant interlayers and during the course of this work, nickel aluminide (NiAl) was investigated [82] as a possible interlayer and the results are presented in Chapter 5.

2.3.1   *Combustion Synthesis of NiAl*

The Ni-Al binary system [83], as shown in Fig 2.6, is composed of five ordered intermetallic phases. Single phase NiAl has very attractive properties, namely its high melting point (1683°C), excellent oxidation resistance, low density and good thermal conductivity.

The fabrication of NiAl from its constituent elemental powders has been carried out by numerous techniques [84,85,86,87]. Of most interest is combustion synthesis, where the mixed elemental powders are heated to a temperature where they react exothermically to form the intermetallic. Figure 2.6 shows a schematic of this process. Usually, the reaction occurs on the first formation of liquid, normally a eutectic liquid at the interface between contacting particles. The formation of NiAl is an exothermic process and the reaction becomes self-sustaining. Many have termed this process combustion synthesis or self-propagating high temperature (SHS) synthesis, [88,89,90]. At a particular temperature, a spontaneous combustion reaction occurs, only for a few seconds at most, and there are two basic modes of combustion reaction differing by their modes of ignition. In the propagating reaction mode, the powder reactants are ignited locally at one end of the sample using an external heat source and the combustion wave propagates through the sample converting it into product. The second method is thermal explosion, where the sample is heated at a constant heating rate in a furnace, until the reaction is iniated uniformly throughout the sample at the ignition temperature, T_{ig}. During the reaction the combustion temperature, T_c, reaches a very high temperature in a short period of time
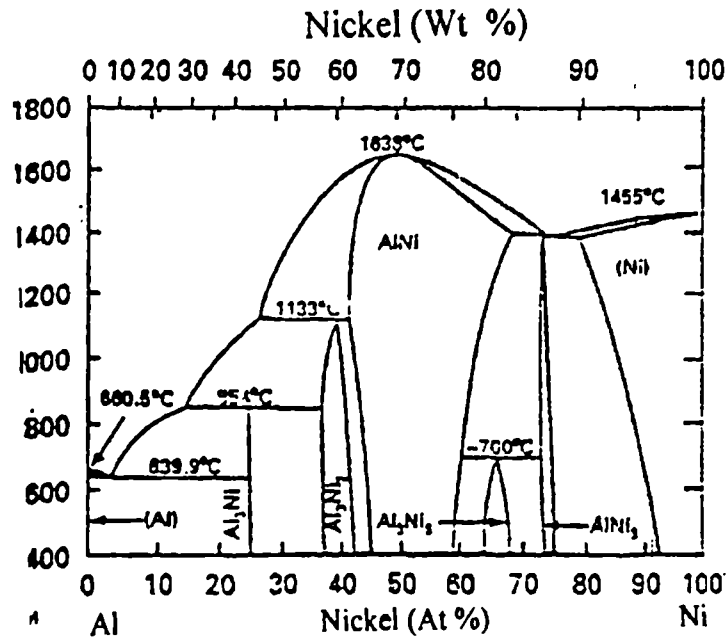
Figure 2.6   Phase diagram for the Ni-Al system [83]
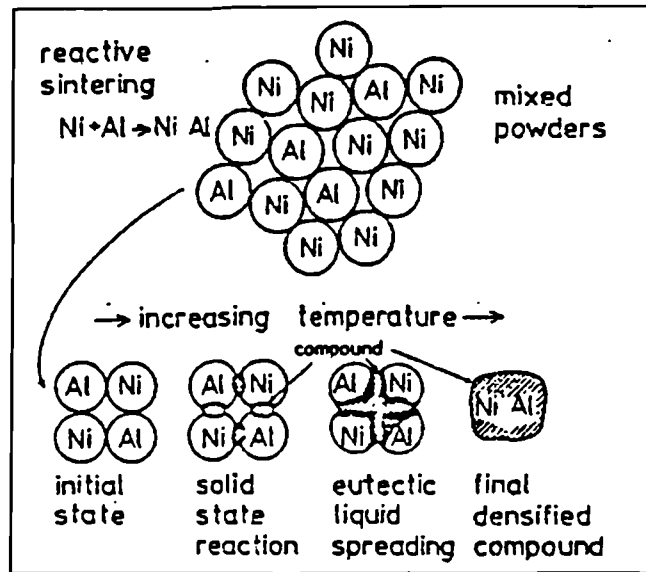

Figure 2.7   A sketch of the reactive synthesis process for Ni-Al mixed elemental poweders

Extensive studies of the reaction using differential thermal analysis (DTA) have shown that the reaction can proceed at temperatures below the eutectic temperature of 640°C [78]. This was attributed to solid-state inter-diffusion that occurs between Al and Ni particles at temperatures below the eutectic temperature. Mainly Al-rich compounds are formed and these reactions are exothermic, heating the sample to the eutectic temperature and iniating the reaction.

Nardou *et al.* [84] reported that a pre-combustion stage exists for high heating rates of 20 K/minute or above. This occurred at around 600°C and was due to the formation of NiAl layers, which effectively raised the temperature of the compact to the eutectic temperature. However, when the volume fraction of Al is large, such as in NiAl, the formation of these Al-rich intermetallic phases by solid-state reactions acts as a buffer that dilutes the exothermic reactions that normally cause melting.

The processing atmosphere plays an important role, mainly upon the final density. Vacuum is preferred as it reduces heat loss to the surroundings and maintains the combustion temperature for slightly longer times. Internal porosity is also evacuated leading to higher density. When inert gases such as argon are used, heat is carried away from the reacting compact by the atmosphere. Also, inert gas can be trapped inside the pores hindering further densification.

While there are no reports of successful metal-ceramic joining via a combustion synthesis route using NiAl as the joining interlayer, Matsuura *et al.* have joined NiAl to metal by various methods. In the first method a 5mm compact of Ni and Al powder was placed on a 15mm block of ultra-low carbon steel (627-1200°C, 150 MPa) and joining was achieved [91,92]. A Ni-Al compact of 5mm or less did not result in joining due to heat loss absorption by the steel block. Joint strength was evaluated by tensile testing and values of 150 MPa were achieved. The second method is that of reactive casting, where this has been used to produce ingot NiAl [93,94] and to join to steel [95,96]. In the joining process, molten Al and then molten Ni were poured onto a steel block (750°C). The heat of the exothermic reaction is transferred to the steel block and the surface steel melts. Iron from the melted steel dissolves in the molten NiAl and an intermetallic compound of NiAl-Fe pseudo-binary system is produced. Four-point bend testing was carried out and very good values were obtained.

2.4   *Other Joining Options*

2.4.1   *Mechanical Joining*

This method of joining is based upon localised point attachment processes, where a nail, rivet or bolt provides the joint. These joints depend upon residual tensile stresses in the attachment to hold the components in compression. Joining is achieved completely through mechanical forces from either physical interface (or inter-locking) friction, or both and there is no

chemical/molecular bonding forces. One of the biggest advantages of this process is the ease of assembly and disassembly, particularly for maintenance. The heat resistant undercarriage tiles of the space shuttle are mechanically clamped on and this process is best suited for the space shuttle, as they can be easily put on/off after missions for inspection and replacement.

Another advantage is that the chemical composition or microstructure is not altered. Despite these important advantages, mechanical joining does introduce severe stress concentrations at the joint interface. This often results in premature failure if incorrectly designed [1-5].

2.4.2   *Adhesive Bonding*

In adhesive bonding materials are joined with the aid of a substance capable of holding them together by surface attachment attraction forces. Adhesives are polymeric compounds and are usually applied at room temperature and may harden either at room temperature or after some treatment. The hardening of the adhesive bond is referred to as curing. The main advantage of using adhesive bonding is that it is easy to apply and produce a strong bond within minutes. However, the main disadvantage is that the joints cannot be used above 300°C, due to their low polymeric melting/ degradation temperatures.

To achieve satisfactory strength the polymer molecules must be chemically bonded to the substrate. It is found that steric hinderance between the polymer molecules results in only a small occupancy of the substrate. Strong chemical bonding to the surface generally requires ionic or covalent bonding. Chemically inert surfaces cannot be bonded. Adhesive bonds tend to be sensitive to environmental factors such as sunlight and moisture.

Wide ranges of adhesives are now commercially available. The epoxy resins are among the most successful thermosetting adhesives, but they are degraded by moisture and have poor adhesion to metal and plastics.

Polyurethane's are available in a wide range of grades and are extremely versatile and their low temperature strength and toughness are generally better than that of expoxy, though their precursors can be toxic.

Acrylics and cyanoacrylics are effective over a wide range of temperatures and can be used for bonding metal, plastic and rubber.

Adhesive bonding can be a viable joining process for metal-ceramic joining, provided the joints are not exposed to elevated temperatures and environmental factors [1-5].

2.4.3   Soldering

This is a subdivision of welding and even brazing. Like brazing it requires an interlayer that melts and substrates that do not. It differs from brazing in that the interlayer melting point is below 450°C.

Solder systems are all based on the low melting temperature, high atomic weight metals found towards the end of the periodic table. The Pb-Sn system is the classic example and it melts at about 200°C, demonstrating their low temperature drawbacks. Other disadvantages of the Pb-Sn system are the high costs of the constituents and their low creep strength of the alloys.

The toxicity of Pb and the need to find a more corrosion resistant solder alloy system has led to the development of the tin-gold system with a melting point of about 220°C [1-5].

2.5   Joining using New Techniques

Joining is also possible using 'less conventional' and new techniques. One of these is the Joule heating method, where silicon carbide-silicon carbide joining has been achieved by use of an interlayer compact consisting of silicon metal, carbon and silicon carbide powder [97]. Electrodes are connected to either side of the silicon carbide joint and an electric current is passed through the material to cause resistive or Joule heating. Joints of moderate strength are possible, however, an overall porosity of 30-50% remains a problem.

NASA has also taken a serious look into joining. They have developed a technique called the Arc Join T, which is affordable and robust in the joining of ceramic-ceramic [98,99]. The joining steps include the application of a carbonaceous mixture on the joining interface (110-120°C, 10-15 minutes, air). This step fastens the pieces together. Silicon or a silicon alloy in tape, paste or slurry form is applied to the joint area and heated to 1250-1425°C for 10-15 minutes, depending on the type of infiltrate. The molten silicon/silicon alloy reacts with the carbon to form silicon carbide with contractible amounts of silicon and other phases as determined by the alloy composition. Controlling the properties of the carbonaceous paste and

the applied fixture force can readily control joint thickness in this process. This technique is capable of producing joints with tailorable thickness and composition, with the heat treatment being carried out in air.

The formation of joints by this technique is attractive since the thermomechanical properties of the joint interlayer can be tailored to be very close to that of the ceramic base material, such as silicon carbide.

2.5.1   *Functionally Graded Materials (FGMs)*

The concept of functionally graded materials (FGM) was first proposed in 1984 by a Japanese scientist as a mean of preparing thermal barrier materials for heat shielding structural materials for the future space programme [100]. The continuous changes in the composition, microstructure, porosity, etc of these materials results in gradients in properties such as mechanical strength and thermal expansion.

In 1992 an international feasibility study was carried out on FGMs [100]. The results showed that FGMs would remarkably increase the efficiency of photoelectric, thermoelectric. and nuclear energy conversions.

It was realised that they also offered the possibility of bridging the CTE gap between metal and ceramic, by use as an interlayer. However, to date their have been no reports of successful metal-ceramic joining by use of an FGM interlayer. This is due to immense difficulties encountered in trying to fabricate a dense and crack free FGM. To complicate this further the FGM has to have similar values of CTE to bridge the gap between metal and ceramic and also be able to wet and react in order to adhere to the metal and ceramic.

Novel work by Glaeser *et al.* [101,102] has looked in to ceramic-ceramic joining by use of FGMs. In a deviation from the standard processing techniques employed for FGM, the FGM was designed to facilitate processing by forming a thin layer of transient liquid phase (TLP). This allows joining by a process that resembles brazing, but allows the formation of refractory joints at reduced processing temperatures. By this technique, strong alumina-alumina, silicon carbide-silicon carbide and silicon nitride-silicon nitride joints were produced that gave high values on four point bend tests. The silicon nitride was joined by using a Ni-Cu-Au-Ti metallic foil interlayer, at 950C and slow cool to room temperature (2 K/minute).

31

FGMs have also been looked at as thermal barrier coatings (TBC). Conventional TBC revealed a severe problem of low durability during thermal cycling and this was attributed to poor bond strength between coating and substrate, low erosion/corrosion resistance and spallation of coatings. The use of an FGM coating is believed to eliminate these problems. Techniques such as plasma spraying [103] and directed vapour deposition [104] have been used to apply such coatings.

Other work on the diverse fields of FGMs has also been concentrated on forming intemetallics-ceramic FGMs, such as Fe_3Al-x vol% Al_2O_3[105]. Iron aluminde, like most intemetallics, is prone to environmental degradation and alloying with metallic elements such as Cr failed to give consistent results. So the addition of a small vol % Al_2O_3 was investigated

2.6   Summary

This chapter has outlined the most applicable metal-ceramic joining techniques, highlighting recent advances and techniques.

The two major categories that have to be considered when joining metal-ceramic are; interfacial bonding and thermal residual stress (due to CTE mismatch).

Many metallic elements react with silicon nitride forming compounds with good interfacial bonding. This has been exploited by numerous techniques, the most popular of which is active metal brazing and to a lesser extent diffusion bonding. While metal-ceramic joining has found some commercial use, especially in the automotive industry, further work is needed to learn and understand metal-ceramic joining if ceramics are to find increasing commercial usage.

Whilst integral metal-ceramic joints have been achieved, they are with limitations. Most metal-ceramic joints produced are small (upto 15 mm in diameter) and to join a large sized metal-ceramic component is a major problem because of the large residual stresses. Also, these joints have a moderately low service temperature (500°C) and, thus, the components incorporating them may not utilize the high temperature properties of silicon nitride.

The various joining techniques have their advantages and disadvantages. The simple and popular active metal brazing can produce excellent metal-ceramic joints, however, wetting and joining are not synonymous. Careful selection of brazing interlayer and processing conditions are important. The relatively low melting temperature of the joining interlayer and thus moderate service temperatures typically governs joints produced by this technique.

Diffusion bonding is another viable technique in competition with active metal brazing. As a solid phase reaction takes place, in principle it is suitable for higher temperature applications compared with active metal brazing joints. The processing conditions can be troublesome, namely immaculate surface preparation, high temperatures and pressures. However, good joining is not possible with ceramic nitrides and carbides due to large CTE differences.

Metal-ceramic joining by use of FGM's is very promising in theory, as they can counteract the CTE mismatch and have high melting points/good oxidation resistance. Work in this area is still in its infancy and it will be a long time before integral metal-ceramic joints can be produced by this technique for commercial applications.

Generally, there is a lack of research effort and funding into improving existing techniques or developing new metal-ceramic joining techniques with improved properties/performance.

It is hoped that this work will contribute to the somewhat grey area of metal-ceramic joining.

3. Experimental

3.1 Introduction

This chapter describes the sample preparation and joining techniques, along with the characterization and testing of joined samples.

Joining was carried out under various conditions and if the result was good joining between the metal and ceramic, the joint would be transversely cross-sectioned. Initially this would be examined by optical light microscopy followed by scanning electron microscopy (SEM). Using energy dispersive x-ray analysis (EDX), compositional analysis and profiling was carried out to identify any new phases present and elemental distribution.

Mechanical testing was carried out to assess the integrity of the joint and to serve as a means of quantitative comparison. Microhardness profiling was one technique used to determine if the joining procedure had any detrimental effects upon the mechanical properties of the metal and as a quantitative comparison.

With regards to the measurement of joint strength there is a lack of international testing standards for metal-ceramic joints. Concern has been voiced about this serious issue by various authors [75] but no standard has been set. So one finds that joint strength is quantified by various test methods according to the author's discretion. This is especially problematic when comparing joint strengths tested by different means. Here shear testing was chosen as it is reliable and has been used by other authors. It gives a fairly accurate value reflecting interfacial joint strength. Tensile testing was not carried out as the results tend to be misleading, recording high tensile strength values even if a small area of the metal and ceramic have joined successfully (poor interfacial joining).

Bend testing (either 3 or 4-point) is another viable technique that is used, especially if the joints are intended for structural applications. The test samples have to be of a particular length (at least 50mm) to get reasonably accurate values. Due to the size constraints of the sample holder and vacuum furnace, such dimensions were not feasible in the present study.

34

Rigorous thermal cycling in air till joint failure was carried out to assess joint performance under possible service like conditions. Failed samples would then be examined using microscopy, EDX and X-ray diffraction (XRD).

Thermal analysis was carried out using differential thermal analysis (DTA), thermogravimetric analysis (TGA) and dilotometery.

3.2 *Materials Used for Joining*

The reaction bonded silicon nitride (RBSN) used was purchased from Morgan-Matroc Ltd UK in sheet form (100mm x 100mm x 8mm). In order to produce RBSN (brand name 'Nitrasil'), the manufacturers uses a silicon powder compact made by pressing, slip casting or injection moulding is pre-sintered in argon at 1200°C. The compact is then reacted in nitrogen gas for a period lasting between 2-12 days at temperatures between 1250-1450°C. In the initial silicon powder compact, the silicon particles have a thick layer of silica (SiO_2) and the manufacturers reduce this by use of catalyst such as iron or iron oxide and H_2 in the atmosphere. With RBSN small amounts of free Si remain on the surface. The reaction bonded production route is more cost effective than hot-pressing. Very complex and accurate shapes can be produced, which retain their shape during firing. RBSN tends to be 15-20% porous, which can be advantageous as it is easier to machine than other silicon nitrides. However, a disadvantage is that bend strength (100-300 MPa) is relatively low compared with HPSN. Strength can be raised to near that of HPSN by a further post-reaction sintering stage. The properties of RBSN are given in Table 3.1. A SEM micrograph of the as-received silicon nitride is shown in Fig 3.1. The material consists of large acicular β-Si_3N_4 grains and small equiaxial α-Si_3N_4 grains. Some pores are also visible.

Goodfellows Cambridge Ltd UK supplied the Fecralloy in rolled sheet form (100mm x 100mm x 5mm). The chemical composition (wt%) is 72.3Fe, 22.0Cr, 5.0Al, 0.3Si, 0.02C, 0.2Mn, 0.1Y, 0.1Zr. The properties of Fecralloy are given in Table 1.

Fecralloy is an 'alumina forming' alloy and considered as one of the best metallic materials for high temperature applications [106]. However, it still has service problems and this is due to a lack of sufficient understanding of the mechanisms through which the material looses its

thermochemical and thermomechanical stability at high temperature in an aggressive environment under mechanical loading [107].

It can be produced by three routes; conventional melting, mechanical alloying and powder metallurgy. Surprisingly little is known about the composition and microstructure of this alloy. Most studies tend to concentrate on the scale growth and effects of temperature/oxidation. The addition of reactive trace elements has led to the formation of a stable alumina oxide spinnel that does not suffer from spallation at 1200°C under thermal cycling [108].

Pure Cu foil (12.5µm, 25µm and 50µm) and Ti foil (12.5µm and 20µm), 99.99% purity, Aldrich Chemicals USA were used.

Ni powder from Aldrich Chemical USA with an average particle size of 15µm and 30µm with a purity of 99.99% and an Al powder also from Aldrich with an average particle size of 10µm and a purity of 99.99% were used.
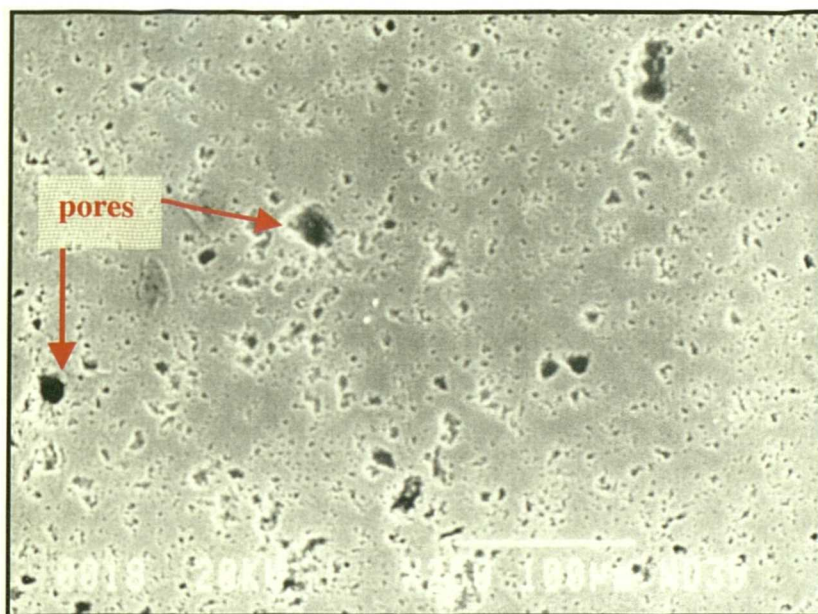
Figure 3.1.   **SEM micrograph of as-received silicon nitride showing slight porosity, large acicular**

β-Si₃N₄ grains and small equiaxial α-Si₃N₄ grains.

Property	RB Silicon Nitride	Fecralloy
Apparent porosity	15-23%	0
Density	2.4 gcm^{-3}	7.2 gcm^{-3}
Thermal conductivity at 20°C	10-16 Wm^{-1}K^{-1}	16 Wm^{-1}K^{-1}
Thermal expansivity, 20-1000°C	3.3 x 10^{-6} K^{-1}	11.1 K^{-1}
Upper continuous use temperature	1200-1500°C	1100-1300°C
Compressive strength	550-650 MPa	Not given
Hardness (Vickers)	800-1000 kgfmm^{-2}	Not given
Shear strength	190-240 MPa	Not given
Tensile modulus	170-220 GPa	330 GPa

Table 3.1 Properties of Fecralloy and silicon nitride (courtesy of Morgan-Matroc Ltd and Goodfellow UK.

3.3   Joining Procedure

3.3.1   High Temperature Vacuum Furnace

Joining was carried out in a purpose built vacuum furnace as shown in the schematic of Fig 3.2. The mild steel vacuum chamber was water cooled and mounted vertically on top of a mobile vacuum-pumping unit. It has a removable chamber lid, thus, allowing the sample holder to be placed inside the furnace unit. Correct alignment must be ensured upon closing, as a moveable stainless steel ramp and bellow unit have been machined and attached to the lid. Weights are placed on the upper ramp plate allowing pressure to be applied on the joining sample. The lower ramp is permantly fixed and protrudes into the furnace chamber upon which the sample holder rests.

The pumping unit is a fully valved system comprising of a Speedivac model 403 diffusion pump with a model 7L4 baffle valve. A Speedivac series 1SC150 rotary pump is used for roughing and backing purposes ("Speedivac" is manufactured by Edwards high vacuum ltd, Crawley UK).

An Edwards penning gauge head is mounted on the baffle valve and an Edward's pirani M6 gauge head is mounted in the backing line. A vacuum of 5×10^{-4} torr was possible. Pressure indication for the vacuum system and the backing line is produced by an Edwards pirani-penning gauge unit.

The power supply transformer, which has an output of 90 Amps at 25 Volts, is housed in a castor-mounted cabinet, which also contains the vacuum gauge control unit. The power output is controlled by a variac dial, which is protected by an overload cut-out device. An ammeter (0-100 A range) and voltmeter (0-30 V range) are fitted into the housing cabinet.

An Eurotherm 840 control unit with a contact switch controls the furnace. This controls heating/cooling rate, dwell temperature and time, by controlling power output to the furnace. This was fitted into the power transformer unit, as the variac dial gave no real control over the furnace.
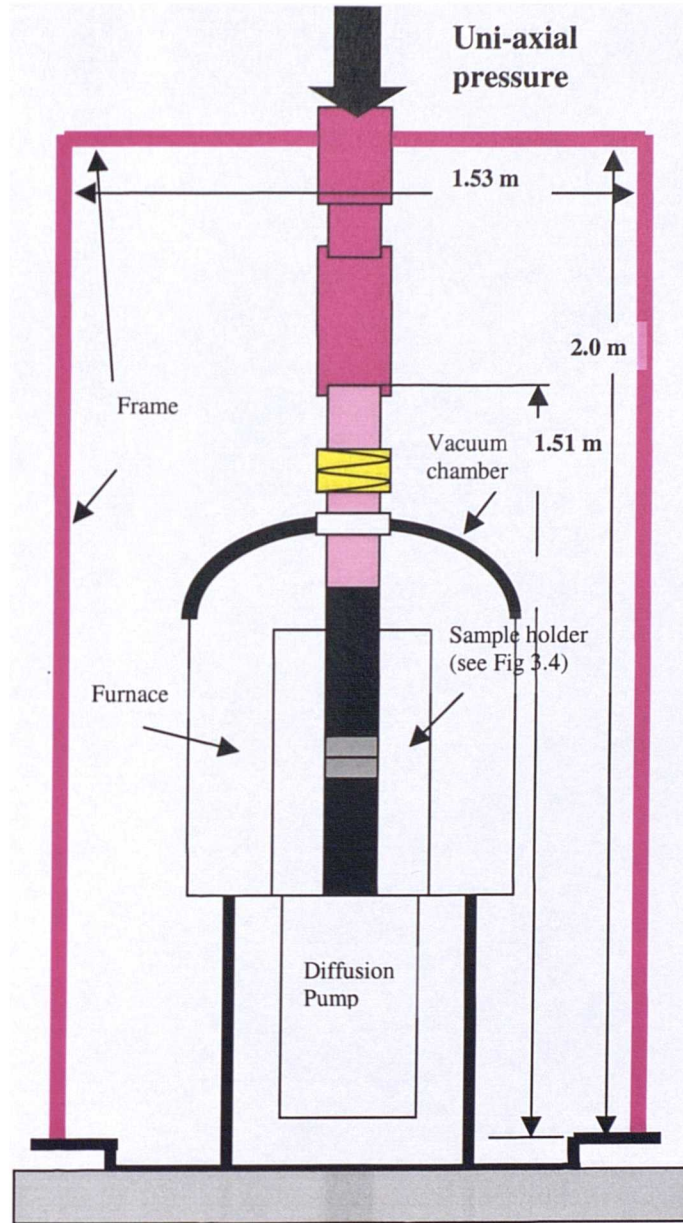
Fig 3.2   Schematic of vacuum furnace (not to scale)

uni-axial pressure

Fecralloy sample

Cu interlayer foil
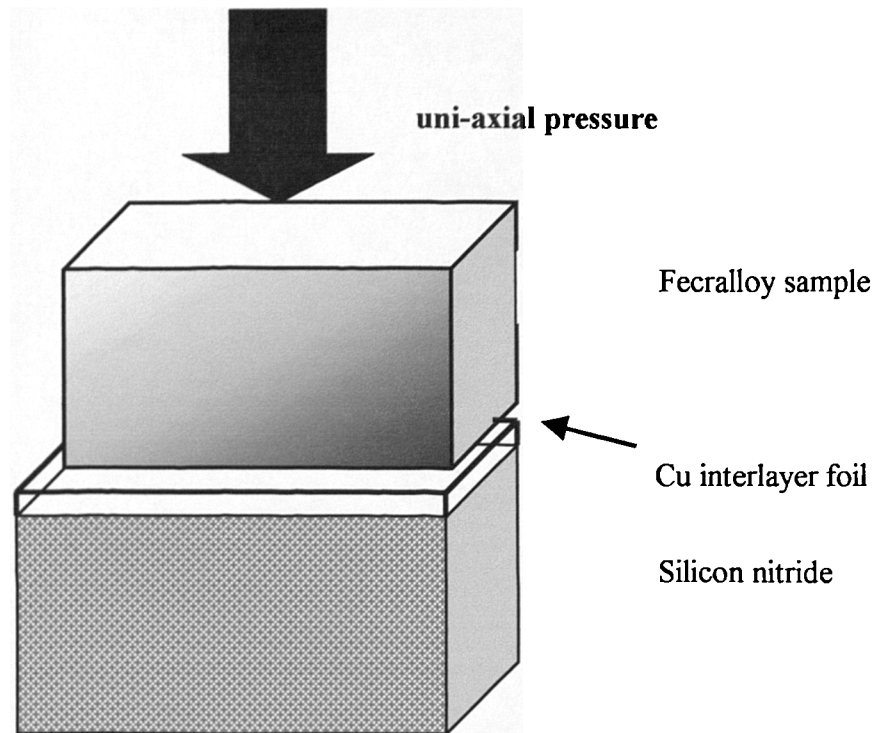
Silicon nitride

Fig 3.3　　　Schematic of joining sample configuration (not to scale)

3.3.2　Sample Preparation and Joining Technique

The silicon nitride and Fecralloy substrates used were all cut using a low speed diamond wheel into samples measuring 10mm x 10mm x 4mm. The joining surface was manually ground to a planar 1200 grit finish. It was then be polished to a 1μm finish using 6μm and then 1μm diamond paste. The samples were then be cleaned ultrasonically in acetone and stored in acetone until use.

3.3.2.1　Joining using metallic foils

• 10mm x 10mm squares of the Cu foil were cut, cleaned ultrasonically in acetone and stored under vacuum till use.

• The Cu foil was sandwiched between the polished sides of the metal and ceramic in a butt joint configuration, as shown in Fig 3.3. This was all held together using sellotape that would harmlessly burn off during heating.

• The butt joint configuration was placed into the graphite sample holder (secured by double sided tape). As graphite conducts heat, the sample would be heated thermally.

• The desired pressure was applied via the bellows unit, where 'dead' weights are placed, as shown in Fig 3.2.

• The sample holder was then placed into the vacuum furnace and turning on the rotary pump started the process of 'roughing'

• The diffusion pump heater was turned on to heat the diffusion pump oil.

• After 30 minutes the vacuum pressure reaches close to 1 x 10^{-4} torr and the rotary valve was closed. The diffusion pump was turned on and baffle valve opened.

• After 10-15 minutes the vacuum pressure reaches close to 5 x 10^{-4} torr and the heating process can begin.

• The Eurotherm 840 control unit is programmed with the desired heating/cooling schedule.

• For the joining trials the temperature range was 850-1140°C, dwell time 0-60 minutes and applied uni-axial pressure 0-9.5 MPa.

• The optimum heating and cooling rate was found to be 5 K/minute. A higher cooling rate could cause cracking after processing, or a weak joint due to the excessive thermal stresses.

• At room temperature the butt joint configuration would be removed and examined.
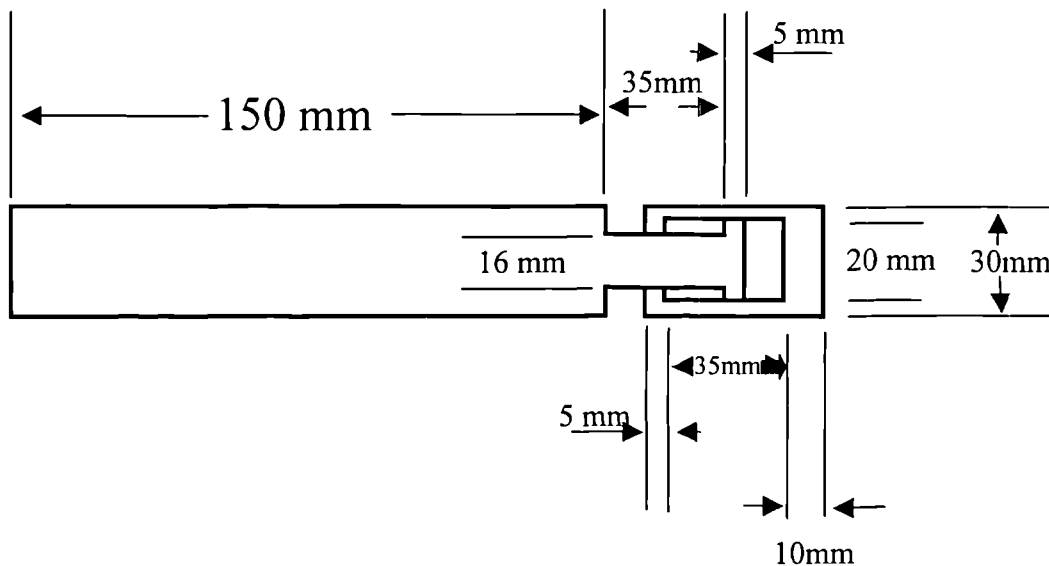
Figure 3.4   Cross-sectional schematic of graphite sample holder

Joining of Fecralloy-silicon nitride was attempted using Cu foil. Fecralloy-silicon nitride joining using a Ti/Cu/Ti multi-interlayer and its variations was also investigated.

41

Primary focus was on the effects of processing parameters (temperature, dwell time and pressure) upon the microstructure-property-performance of the resulting joint. The effect of varying Cu foil thickness was touched upon with the Fecralloy-silicon nitride joints.

3.3.2.2   *Joining via a powder metallurgy route*

Two different powder metallurgy routes looked at Fecralloy-silicon nitride joining via a NiAl interlayer. The first involved applying the Ni-Al powder mixture in paste form and the second as a cold pressed compact.

The initial step for both routes was the dry mixing of the Ni-Al powder mixture (1:1 molar ratio) for ten hours in a Turbula^{Tm} mixer.

Paste route:

• Ni-Al paste of moderate viscosity was made by the addition of blythe binder (50wt% mixture of the solvent terpineol and 50wt% of the binder ethyl cellulose).

• The thoroughly mixed paste was then applied to the polished silicon nitride interface. To ensure quality control for the same thickness/quantity of paste to be applied for each trial, the silicon nitride was put into a die cast (square measuring 10mm x 10mm x 8mm cut into plate sheet).

• After paste application a drying period of three hours in air was carried out.

• Initial trials conclusively showed that binder burn off is a pre-requisite for good joining (large voids and unreacted particles compared with those with binder burn off). TGA was used to determine binder burn off temperature and Fig 3.5 shows the TGA plot. The graphs show that almost 90wt% of the binder is burnt off at 170°C. Hence, binder burn off was carried out at 200°C for two hours.

• The same procedures outlined in 3.3.2.1 were employed with regards to sample loading via graphite holder and vacuum furnace operation.

• Trials were carried out in an argon atmosphere and repeated under vacuum for 5-15 minute dwell times at temperatures of 800-1000°C under pressures of 0-45 MPa.

The effects of processing atmosphere were investigated in addition to processing parameters upon the microstructure-property-performance of the joints were investigated.

Cold pressed compacts:

• Cold pressing (900 MPa) the Ni-Al powder into 10mm x 10mm compacts of thickness 2mm was carried out using a hydraulic press.

• The cold pressed compact was inserted between the polished sides of the metal and ceramic, in a butt joint configuration.

• The same procedures outlined in 3.3.2.1 were employed with regards to sample loading via graphite holder and vacuum furnace operation.

• Joining trials were carried out between 800-1000°C, dwell times 5-15 minutes and pressure 0-45 MPa.
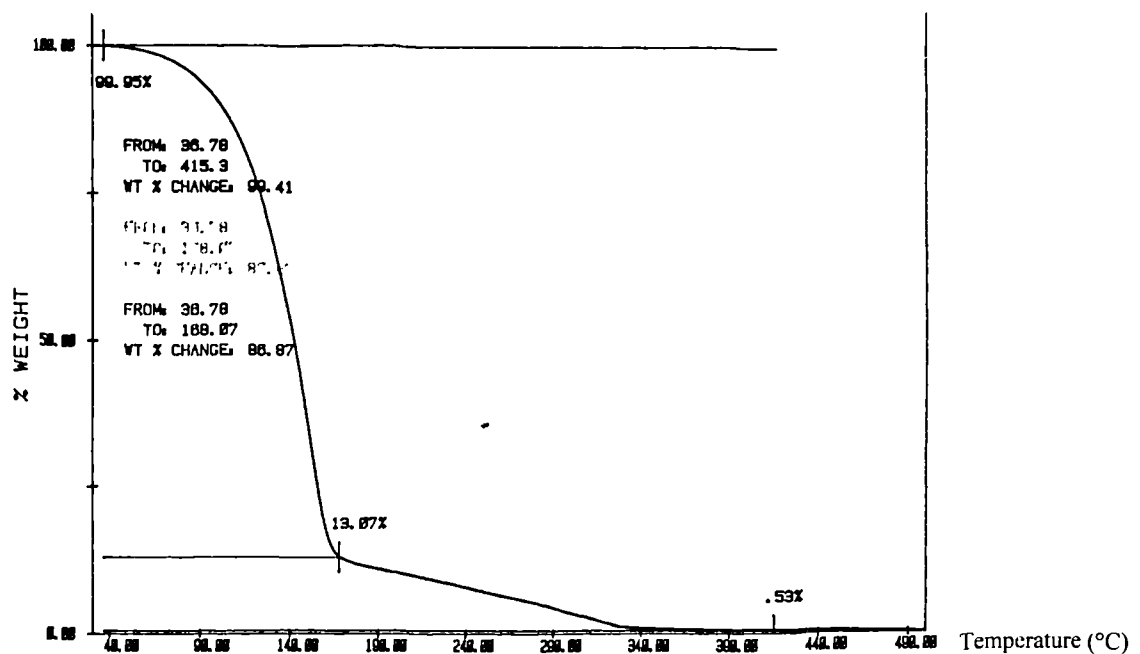
Figure 3.5   **TGA plot determining the binder burn off temperature**

3.4   Metallographic Examination

3.4.1   Optical Light Microscopy

In order to understand and improve metal-ceramic joining, it is very important to analyse and characterize the joining interface. Relationships or trends can be drawn from the interfacial microstructure with regards to processing parameters and joint integrity (mechanical performance). Hence, the requirement to transversely cross-section the joint.

43

All the joined samples would be cross-sectioned transversely using a low speed diamond wheel. The cross-sectioned sample was then mounted in cold acrylic resin and the joint interface manually ground using 320, 800, 1200 and 2400 SiC grit papers, to remove any scratches and to produce a planar surface. Polishing continued by use of $6\mu m$ and $1\mu m$ diamond paste. The sample was then cleaned ultrasonically and rinsed in acetone and blow dried. This was the methodology used for all the joined samples.

Incident reflected light microscopy (Leitz) was the initial method of optical analysis and joint characterization. Chemical etching of the metal side of the joint was generally not carried out, as the formation of new phases/precipitates were easily visible.

3.4.2 Electron Microscopy

3.4.2.1 Scanning Electron Microscopy (SEM)

A SEM is a microscope that uses electrons rather than light to form an image. The main advantage over light microscopy is the large depth of field, which allows a large amount of the sample to be in focus at one time and produce a high-resolution image.

A JEOL 840A SEM was used to analyse the interfacial microstructure. The samples used for the optical microscope were vacuum coated with a thin layer of gold (to make the sample conductive) and attached to a SEM mount using carbon tape. All image and analysis work was carried out using secondary electron imaging/analysis.

3.4.2.2 Energy dispersive x-ray analysis (EDX)

EDX analysis was used to identify and display elemental concentrations (ZAF corrected) across the cross-sectioned sample.

Elemental composition variation is an important analytical means of assessing and characterizing the joint interface. It helps in the understanding of the joining process and also has an important influence on the mechanical properties of the joint.

Qualitative elemental variation profiling (line scan) was carried out across the metal-ceramic interfacial region.

X-ray mapping was used to map and display the elemental distribution across the metal-ceramic joint interface.

3.4.3   X-ray Diffraction (XRD)

XRD is a versatile, non-destructive analytical technique for the identification and quantitative determination of the various phases present in powdered and solid samples.

Identification is achieved by comparing the x-ray diffraction pattern from the sample with an internationally recognised database containing reference patterns for more than 70,000 phases.

A Philips PW1140 diffractometer was used during the course of this work

3.5   Mechanical Testing

3.5.1   Shear Testing

All joined samples were machined down to 5mm x 5mm x 8mm shear test samples. In order to ensure greater accuracy three samples were tested for each joining condition.

A designed fixture was used such that sample movement was prevented during testing and that shear force was applied to the bond line and either side of bond line (see Fig 3.7). A computer assisted Instron tensile testing machine was used with a cross-head speed of 0.5 mm/minute.
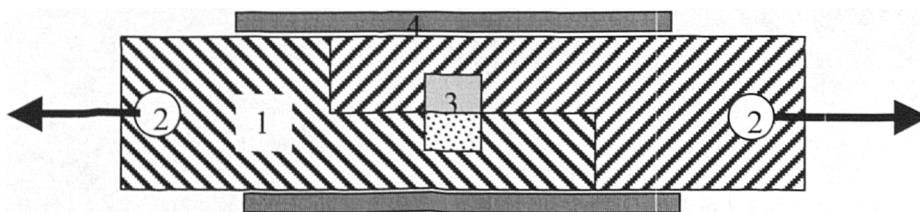
Figure 3.7   (1) Schematic of shear test jig, (2) direction of pulling pins, (3) joint sample and (4) Instron holder.

3.5.2   Thermal Cycling

This was carried out on all joined samples to assess the effects of thermal shock upon joint integrity in possible service like conditions. The joined sample were placed in an air furnace and heated to 850°C with a dwell time of four hours (high heating and cooling rate, 50/50 K/minute). Upon cooling the sample was then inspected and if still intact the rigorous thermal cycling would be repeated until joint failure.

3.5.3   Microhardness

Microhardness is the resistance to plastic deformation of a material and is a parameter to assess the behaviour of the material. With small metal samples such as those used in our work, the standard Vickers indenter is not practical as the indent is about 3mm (sample is 10mm x 4mm) and so a micro-indenter was used.

A Leitz miniload hardness indenter was used (Vickers diamond pyramid indenter). The indents were very fine and had to be measured using the built in microscope. Measurements were made at the bond line and every 50μm into the metal until 500μm away from the bond line. To ensure accuracy, at each measurement three readings were taken and an average value recorded.

As-received Fecralloy had an average microhardness of 245 H_v (±3 H_v). However, it was found that heating a test piece to 1100°C for 30 minutes under vacuum caused this average value to drop to 237 H_v (±3.5 H_v). This is caused by the process of annealing, which reduces a metals tensile strength but increases its ductility.

If a metal is reheated to a sufficiently high temperature for a long enough time, the cold worked metal structure will go through the stages of recovery followed by recrystallisation and finally grain growth Thus, heating Fecralloy at 1100°C for 30 minutes causes the alloy to go through the above stages.

3.6 Thermal Analysis

3.6.1 Differential Thermal Analysis (DTA)

DTA measures the difference in temperature between a sample and a reference, which are exposed to the same heating schedule via symmetric placement with respect to the furnace. The reference material is usually alumina in powder form, with about the same thermal mass as the sample. The temperature difference between the sample and reference is measured by a differential K-type thermocouple. One junction is in contact with the underside of the sample crucible and the other is in contact with the underside of the reference crucible. The voltage measures temperature across the appropriate terminal.

DTA was used to characterize the as-compacted Ni-Al powder mixture in nitrogen atmosphere (vacuum not possible) at varying heating rates of 5, 10, 15 and 20 K/minute. The trials were then repeated using large Ni particle size.

3.6.2 Thermogravimetric Analysis (TGA)

TGA studies the weight changes of a sample as a function of temperature. It is particularly useful for transformations involving the absorption or evolution of gases from a sample. The weight balance is highly sensitive with resolutions down to $1\mu g$.

TGA was used to measure the effects of oxidation on the Ni-Al powder and NiAl interlayer in air and nitrogen atmospheres.

3.6.3 Dilotometery

This is used to measure the change in length of a sample as a function of temperature. It was used to experimentally confirm the CTE and to calculate the stress/strain at temperature of the various metal and ceramics used.

Fig 3.8 shows the heating and cooling curves for silicon nitride and Fecralloy. In all cases the CTE is dependant upon temperature, increasing to about 900-1000°C at which the maximum value is reached.
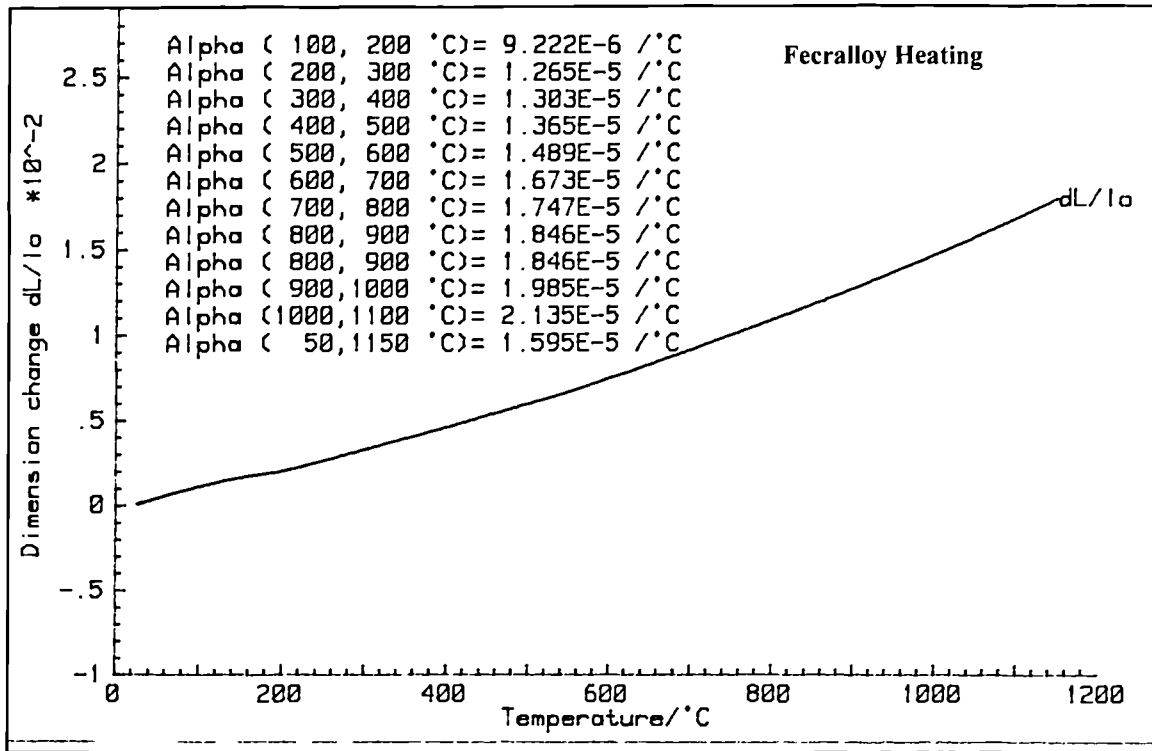
RBSN Heating

Alpha (200, 300 °C)= 2.380E-6 /°C
Alpha (300, 400 °C)= 1.764E-6 /°C
Alpha (400, 500 °C)= 1.104E-6 /°C
Alpha (500, 600 °C)= 3.759E-6 /°C
Alpha (600, 700 °C)= 4.030E-6 /°C
Alpha (700, 800 °C)= 3.794E-6 /°C
Alpha (800, 900 °C)= 3.869E-6 /°C
Alpha (900,1000 °C)= 4.591E-6 /°C
Alpha (1000,1100 °C)= 4.727E-6 /°C
Alpha (191,1150 °C)= 3.364E-6 /°C

RBSN Cooling

Alpha (100, 200 °C)= 2.259E-6 /°C
Alpha (200, 300 °C)= 2.931E-6 /°C
Alpha (300, 400 °C)= 2.673E-6 /°C
Alpha (400, 500 °C)= 3.274E-6 /°C
Alpha (500, 600 °C)= 3.920E-6 /°C
Alpha (600, 700 °C)= 4.330E-6 /°C
Alpha (700, 800 °C)= 4.431E-6 /°C
Alpha (800, 900 °C)= 4.147E-6 /°C
Alpha (900,1000 °C)= 5.150E-6 /°C
Alpha (1000,1100 °C)= 5.663E-6 /°C
Alpha (50,1150 °C)= 3.880E-6 /°C

49

Alpha (100, 200 °C)= 9.222E-6 /°C
Alpha (200, 300 °C)= 1.265E-5 /°C
Alpha (300, 400 °C)= 1.303E-5 /°C
Alpha (400, 500 °C)= 1.365E-5 /°C
Alpha (500, 600 °C)= 1.489E-5 /°C
Alpha (600, 700 °C)= 1.673E-5 /°C
Alpha (700, 800 °C)= 1.747E-5 /°C
Alpha (800, 900 °C)= 1.846E-5 /°C
Alpha (800, 900 °C)= 1.846E-5 /°C
Alpha (900,1000 °C)= 1.985E-5 /°C
Alpha (1000,1100 °C)= 2.135E-5 /°C
Alpha (50,1150 °C)= 1.595E-5 /°C

Fecralloy Heating

dL/lo

Dimension change dL/lo *10^-2

Temperature/°C

Alpha (200, 300 °C)= 1.225E-5 /°C
Alpha (300, 400 °C)= 1.195E-5 /°C
Alpha (400, 500 °C)= 1.288E-5 /°C
Alpha (500, 600 °C)= 1.278E-5 /°C
Alpha (600, 700 °C)= 1.594E-5 /°C
Alpha (700, 800 °C)= 1.673E-5 /°C
Alpha (800, 900 °C)= 1.792E-5 /°C
Alpha (900,1000 °C)= 1.920E-5 /°C
Alpha (1000,1100 °C)= 2.139E-5 /°C
Alpha (200,1150 °C)= 1.586E-5 /°C

Fecralloy Cooling

dL/lo   Cv.

COOLING

Dimension change dL/lo *10^-2

Temperature/°C

Figure 3.8   **Dilotometry plots for heating/cooling cycles of materials used.**

50

4. *Joining by use of Metallic Foil*

4.1 *Introduction: Use of pure Cu foil*

The joining of Fecralloy-silicon nitride was investigated by use of thin Cu foil (12.5μm) and also by thicker foils (25μm and 50μm). A thin foil was chosen due to Cu's poor oxidation resistance and poor wettability on silicon nitride. A thin foil would not remain after high temperature processing and so avoid the mentioned problems.

The mechanism of joining is studied and a sequential model outlining the joining process is put forth. The effects of processing parameters are looked into and the microstructure-property-performance relationships of the joints presented. A theoretically derived value for melt-back distance is compared to microhardness profiles and this relationship is looked at.

4.2 *Results and Discussion*

4.2.1 *Interfacial Microstructure*

Characterization of a joined metal-ceramic interface is vital as it reveals many important factors. The interfacial microstructure can be directly related to the joint integrity and this can be used to vary processing parameters, for instance, to improve the joint integrity.

EDX elemental line scans were chosen to characterise accurately the metal-ceramic interface, as shown in the plots below the respective micrographs. To a lesser extent EDX elemental mapping was used to visually demonstrate the elemental migration and presence of a thin reaction product layer at the ceramic interface.

Micrographs of successful and failed Fecralloy-silicon nitride joints are shown in Fig 4.1-4.8. With the joined samples good interfacial bonding is apparent in all cases, with no remaining Cu foil or visible reaction product layer on the ceramic interface. The joints formed by the

51

application of a low pressure (1.5 MPa, Fig 4.1 and 4.2) have considerable open porosity at/close joint interface and surrounding areas of the ceramic, no infiltration zone of liquid metal into silicon nitride, no visible reaction product layer at the silicon nitride interface and no diffusion zone at the Fecralloy interface.

At 1100°C, 1.5 MPa (Fig 4.1) there are virtually no precipitates on the metal side, and an increases in temperature to 1140°C, 1.5 MPa (Fig 4.2) results in the formation of numerous precipitates. The EDX elemental map of Fig 4.5 shows the presence of these precipitates, in particular the needle like precipitates, along with the elemental distribution. Our results suggest that the needles like precipitates are chromium nitride (Cr_2N), while the smaller and numerous precipitates are iron silicide (Fe_3Si).

A slight increase in pressure to 3.5 MPa at 1100°C, 30 minutes (Fig 4.3) does not greatly affect the joint morphology compared with Fig 4.1. However, the catastrophic effects of a higher cooling rate are demonstrated in Fig 4.4, where interfacial cracking is apparent. The most likely reason for this is the residual stresses build up due to CTE mismatch.

When the applied pressure is increased (Fig's 4.7 and 4.8) there is an infiltration zone of liquid metal into the silicon nitride and this closes porosity in the silicon nitride interfacial region and there is a Si and N diffusion zone in the Fecralloy interfacial region. The joints formed using greater applied pressure (Fig 4.7 and 4.8) all have a diffusion and infiltration zone. Our results show the first diffusion zone at the Fecralloy interface is that of Si, where precipitates of Fe_3Si are present. The second is that of N; where the needle like Cr_2N precipitates exist. The chemical composition of the infiltrated liquid metal was found to be similar to that of the parent metal in addition to small amounts of Cu, Si and N (<10 wt%). The size of the diffusion and infiltration zones is affected by an increase in temperature as opposed to pressure or time. This is because they are thermally assisted processes.

These results establish that a thin reaction product layer exists at the silicon nitride joint interface for all of the joined samples (average thickness of 8μm). experimental analysis carried out to identify this suggest that the reaction product layer is aluminium nitride, AlN.
That Cu, Si and N have diffused into the Fecralloy, while Fe, Cr, Al and Cu infiltrate the silicon nitride. The results suggest that there is a required temperature, dwell time and applied pressure to form a good joint. These are discussed in section 4.2.3.

The use of a thicker Cu foil did not result in joining, as can be seen in Fig 4.6. The foil remained after processing adhering to the Fecralloy only. The rough silicon nitride interface indicates that there was reactive wetting, but this was not enough for good interfacial bonding and a strong joint. EDX analysis found that only small amounts of Cu were present up to 12μm into the silicon nitride. High levels of Si were present in the Cu interlayer forming mostly copper silicide (CuSi). Cu had diffused into the Fecralloy and only small amounts of Fe, Cr and Al into Cu interlayer.

The morphology of the metal-ceramic interface depends upon the type of interaction that has occurred. If only physical interaction has occurred, the structure of the metal and ceramic is unchanged. However, if a chemical reaction occurs, the morphology is effected depending upon whether solid-solid or solid-liquid reactions occur and if new interfacial phases are formed. Formation of new interfacial phases not only alters the microstructure but also the physical and mechanical properties. These interfacial phases or reaction product layer are a consequence of the reactions needed to cause wetting of the ceramic. One can consider the reaction product layer as chemical bridges between the metal and ceramic.

A thick reaction product layer weakens the interface due to excessive growth stresses and brittle nature. Opinion is varied about the pressure of a reaction layer product. Some researchers believe they are very detrimental to joint strength [59], while others attribute interfacial failure due to a thin reaction layer product [60]. It is believed that this varies from system to system and generalisation would be difficult. It is interesting to note that the processing variations did not greatly effect the thickness of the AlN reaction product layer in the joined samples. Reaction product thickening occurs during the wetting and spreading process. Data on the spreading kinetics would be useful, as the minimum time for spreading would be extrapolated and used during processing to keep the reaction product thin. Theoretical modelling of the spreading kinetics is very complex and this is due to surface irregularities, surface contaminants/anomalies and interfacial reactions. Lack of thermodynamic data and speed of the spreading kinetics are the major difficulties for experimental data collection.

The first stage of the metal-ceramic joining process is the physical interaction process of wetting. The second stage is that of chemical interaction involving chemical reactions at the interface. The redox and dissolution reactions are the key factor in the joining process and aid wetting by a further decrease in the free energy of the surface. However, these reactions only

proceed if certain conditions are fulfilled. Proper understanding of how and why these reactions proceed requires both thermodynamic and kinetic data for all the phases present in the joint microstructure. With a complex system such as ours, many different reactions are possible and not all the necessary data is available. However, it is important to mention the major reactions that are thought to occur, which are;

$$Si_3Ni_{4\,(s)} \Rightarrow 3\underline{Si} + 2N_{2\,(g)} \qquad \text{Equation 4. 1}$$

where $\underline{Si}$ is the silicon in solid solution with the Fecralloy.

$$\underline{Al} + \tfrac{1}{2}\,N_{2\,(g)} \Rightarrow AlN_{(s)} \qquad \text{Equation 4. 2}$$

$$2\underline{Al} + Si_3N_{4\,(s)} \Rightarrow Al_2S_{3\,(s)} + 2N_{2\,(g)} \qquad \text{Equation 4. 3}$$
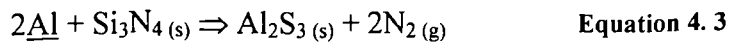
where $\underline{Al}$ is aluminium as a constituent of Fecralloy or in solution.

$$2\underline{Cr} + \tfrac{1}{2}\,N_{2\,(g)} \Rightarrow Cr_2N_{(s)} \qquad \text{Equation 4. 4}$$

$$9\underline{Cr} + Si_3N_{4\,(s)} \Rightarrow Cr_3Si_{(s)} + N_{2\,(g)} \qquad \text{Equation 4. 5}$$
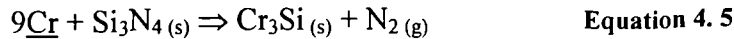
where $\underline{Cr}$ is chromium dissolved in Fecralloy or in solution.

$$9\underline{Fe} + Si_3N_{4\,(s)} \Rightarrow 3Fe_3Si_{(s)} + 2N_{2\,(g)} \qquad \text{Equation 4. 6}$$
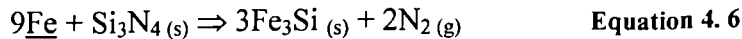
where $\underline{Fe}$ is iron as a constituent of Fecralloy or in solution.

$$3Cu_{(s)} + Si_3N_{4\,(s)} \Rightarrow 3CuS_{(s)} + 2N_{2\,(g)} \qquad \text{Equation 4. 7}$$

$$3Si \Rightarrow 3[Si]_{Cu} \qquad \text{Equation 4. 8}$$

$$2N_2 \Rightarrow 4[N]_{Cu} \qquad \text{Equation 4. 9}$$
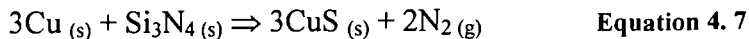
The dissociation of the silicon nitride, as given in Equation 4.1, is the rate-determining step of the joining process. Silicon nitride is the least stable compared to aluminium nitride and boron nitride. Its stability is even lower when in contact with liquid metals that have a high affinity for Si, such as Cu or Ag. However, the presence of oxide/oxynitride surface barriers prevents direct contact between liquid metal and silicon nitride. These surface barriers disappear at high temperatures and pressure permits direct contact.

Under atmospheric conditions (partial nitrogen pressure $\approx 0.8 \times 10^5$ Pa), the Gibbs free energy of Equation 4.1 is positive at 1000°C (40.8 kJmol^{-1}) and will not proceed. Lowering of the nitrogen partial pressure leads to a lowering of the Gibbs free energy. All experiments were

carried out under vacuum with a low nitrogen and oxygen partial pressure. Under these conditions the dissociation of the ceramic given in Equation 4.1 is thermodynamically possible (Gibbs free energy of –36.3 KJmol^{-1}). This tends to be the case with other reactions that have a positive Gibbs free energy under atmospheric conditions.
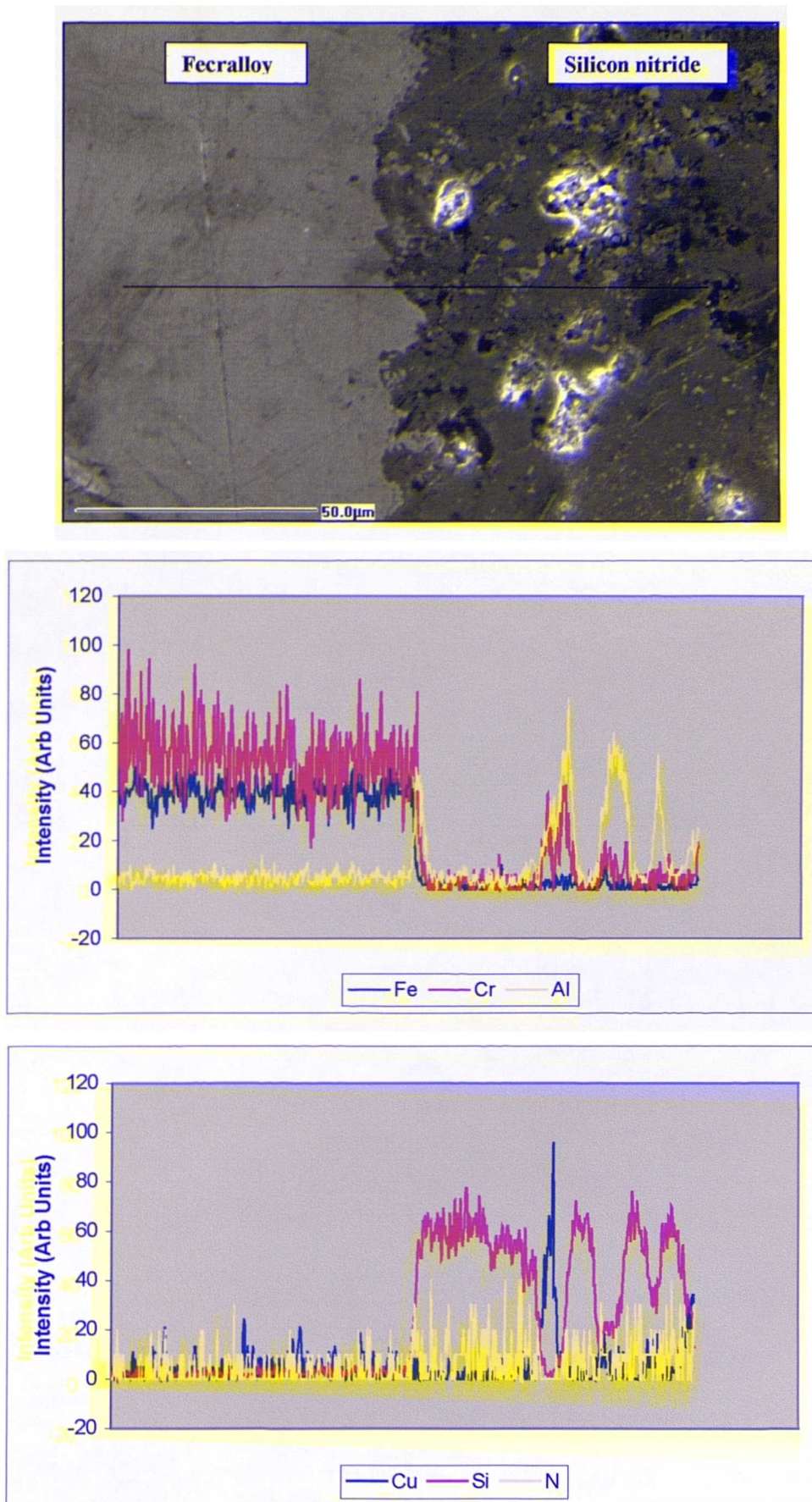
Figure 4.1 **Micrograph and EDX line scan of a Fecralloy-silicon nitride joint (1100°C, 30 minutes, 1.5 MPa). Good interfacial bonding is apparent with signs of reactive wetting (uneven joint interface).**
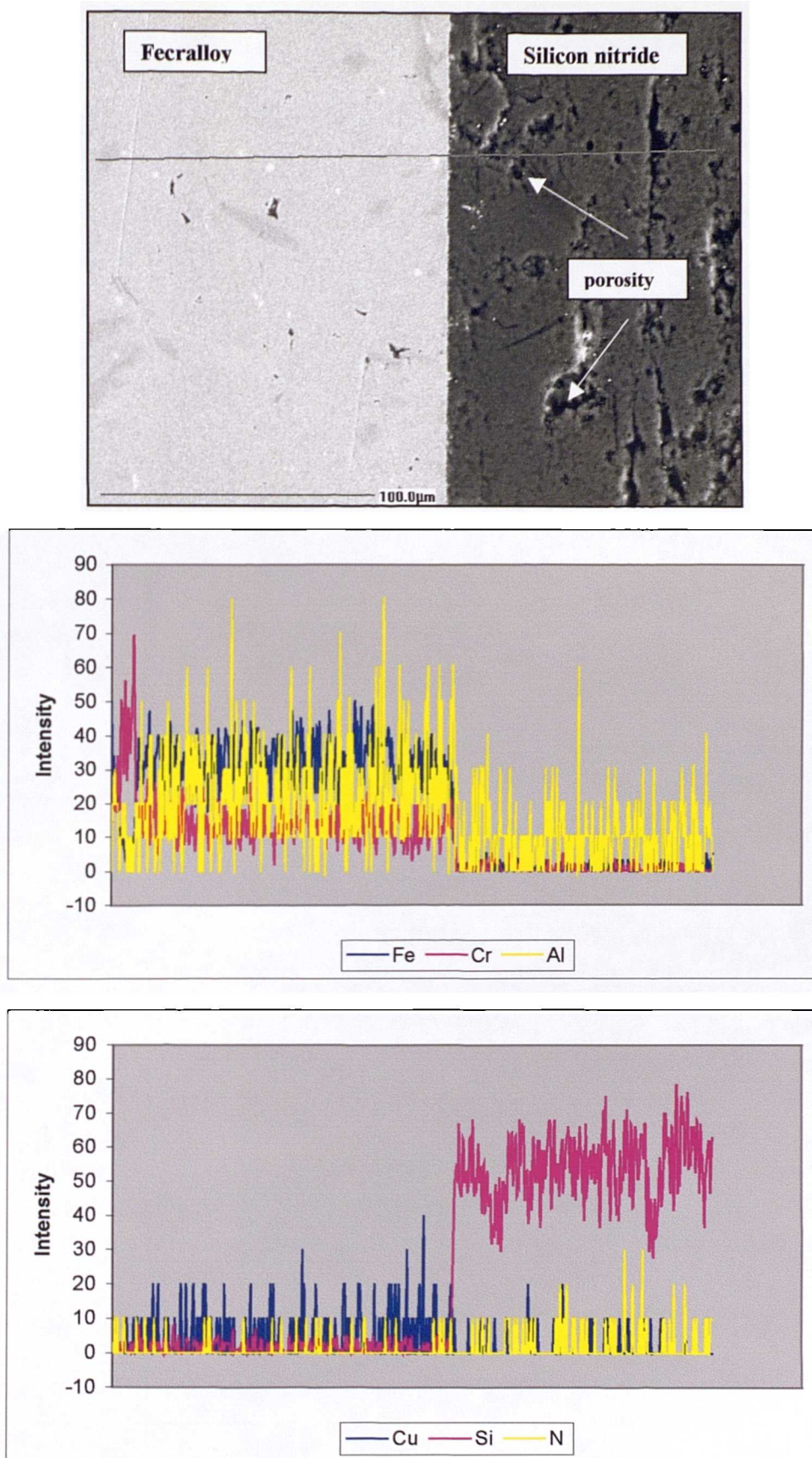
Figure 4.2   Micrograph and EDX line scan of Fecralloy-silicon nitride joint (1140°C, 30 minutes, 1.5 MPa)
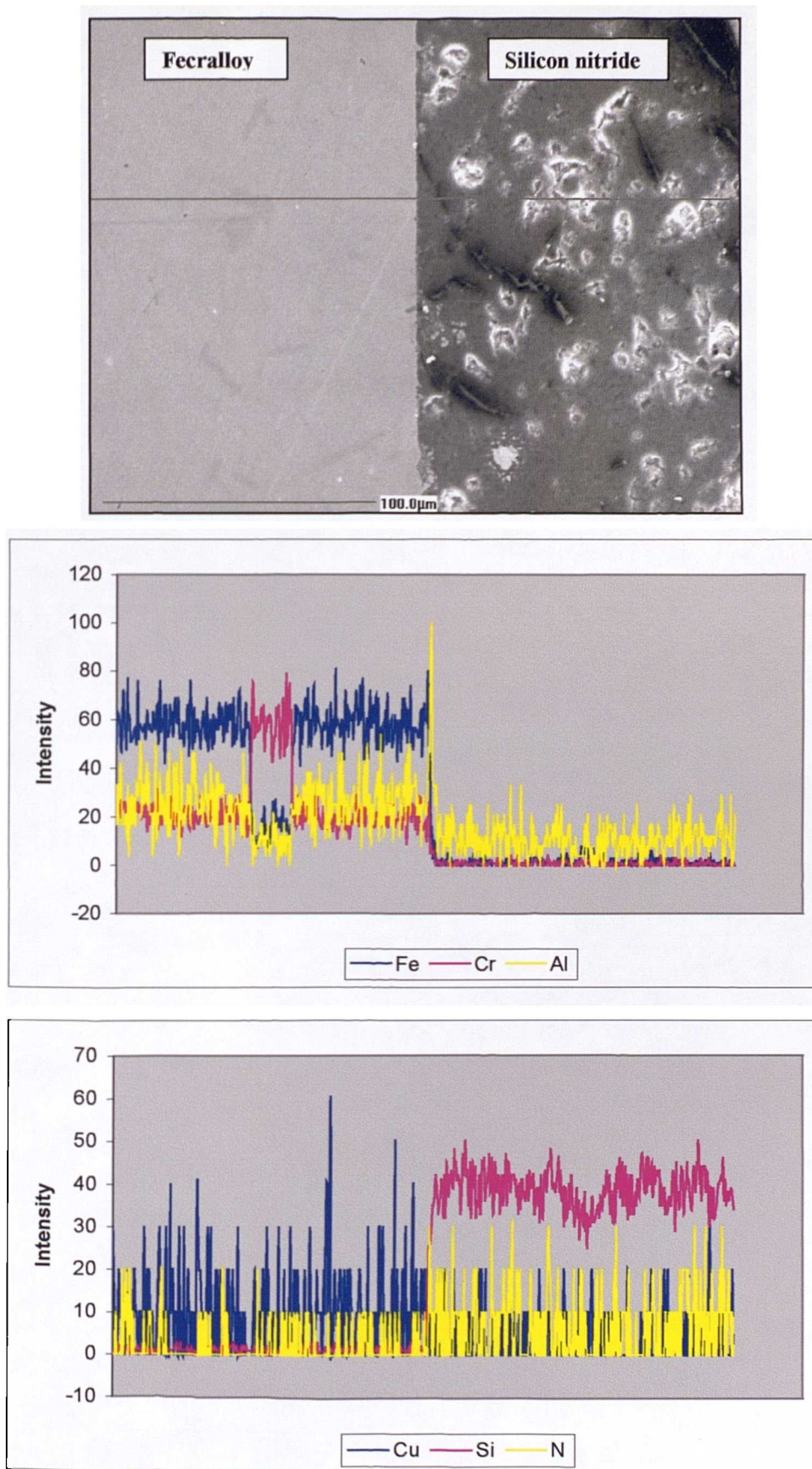
Figure 4.3   Micrograph and EDX line scan of a Fecralloy-silicon nitride joint (1100°C, 30 minutes, 3.5 MPa)
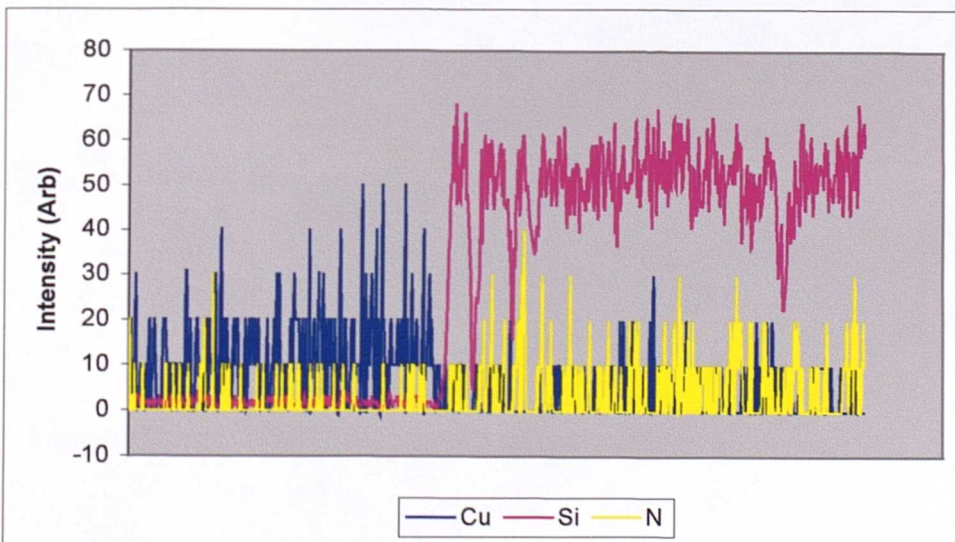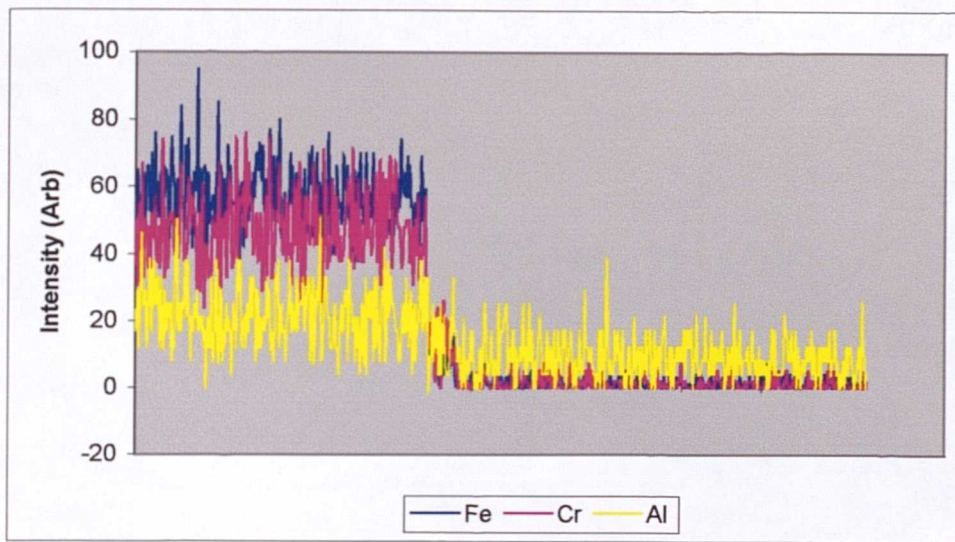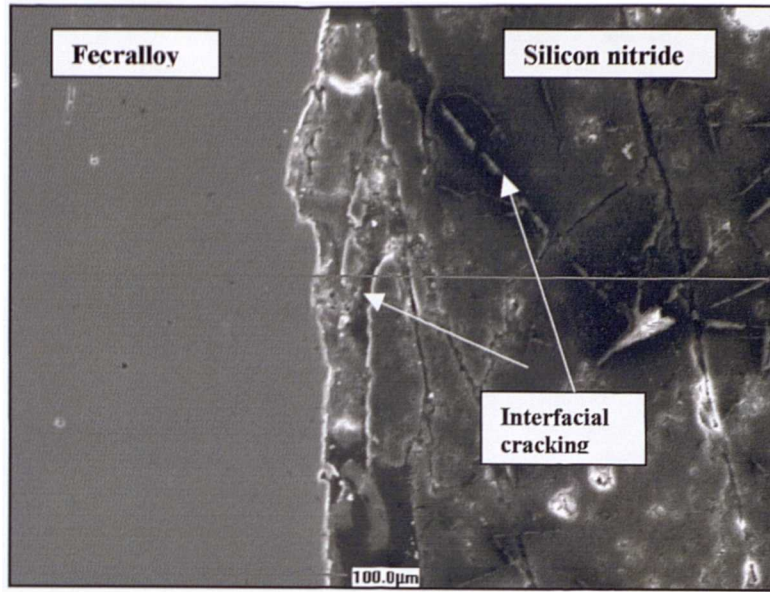
Figure 4.4   Micrograph and EDX line scan of a failed joint due to high cooling rate (1100°C, 30 minutes, 1.5 MPa).
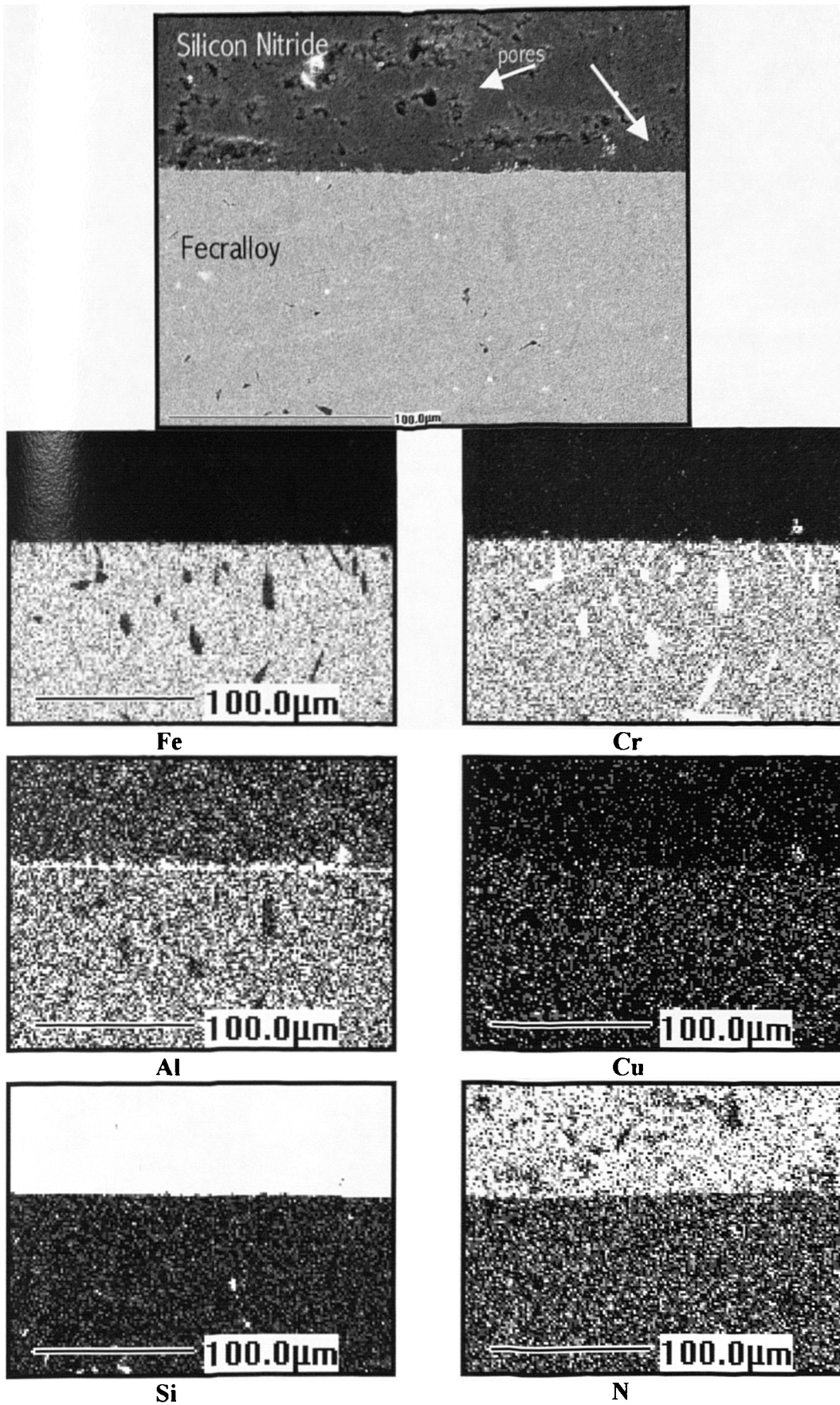
Figure 4.5   EDX elemental map showing presence of AlN reaction product layer and
needle like Cr_2N precipitates (1140°C, 30 minutes, 1.5 MPa).
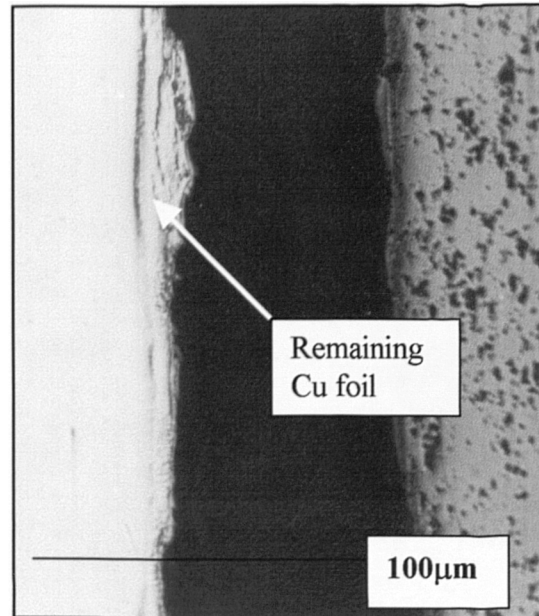
Figure 4.6   Micrograph showing failed Fecralloy-silicon nitride joint using a thicker Cu foil (1100°C, 30 minutes, 1.5 MPa).
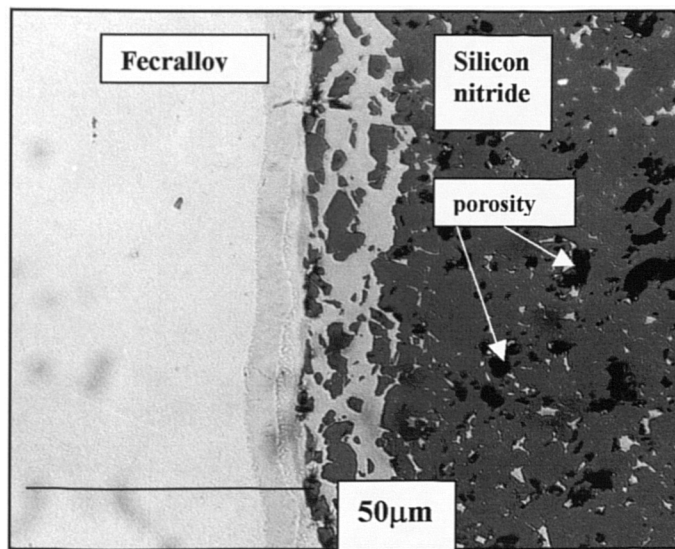
Figure 4.7a   Micrograph of Fecralloy-silicon nitride joint (1100°C, 30 minutes, 5.5 MPa)
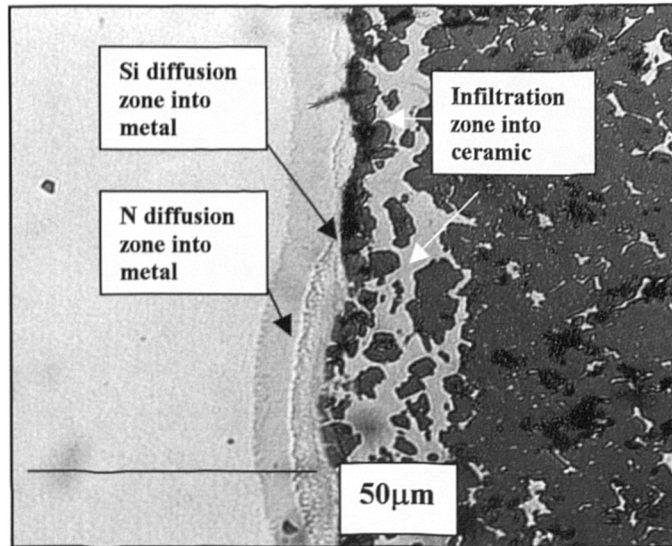
Figure 4.7b   Micrograph of Fecralloy-silicon nitride joint (1100°C, 30 minutes, 7.5 MPa)
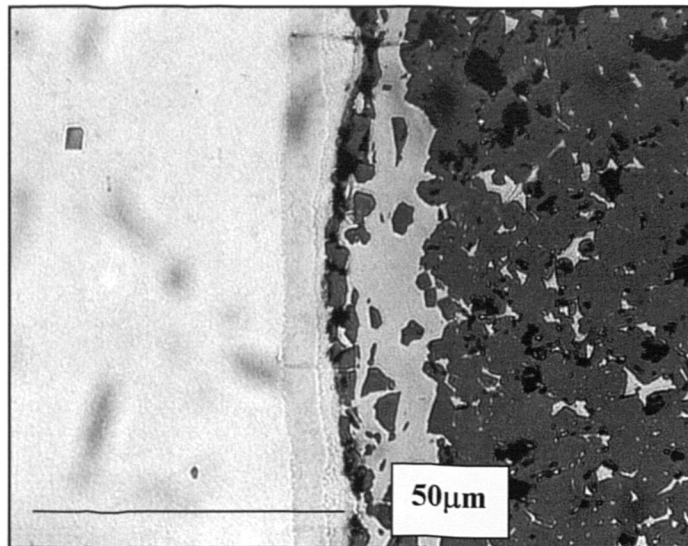
Figure 4.7c   Micrograph of Fecralloy-silicon nitride joint (1100°C, 30 minutes, 9.5 MPa)
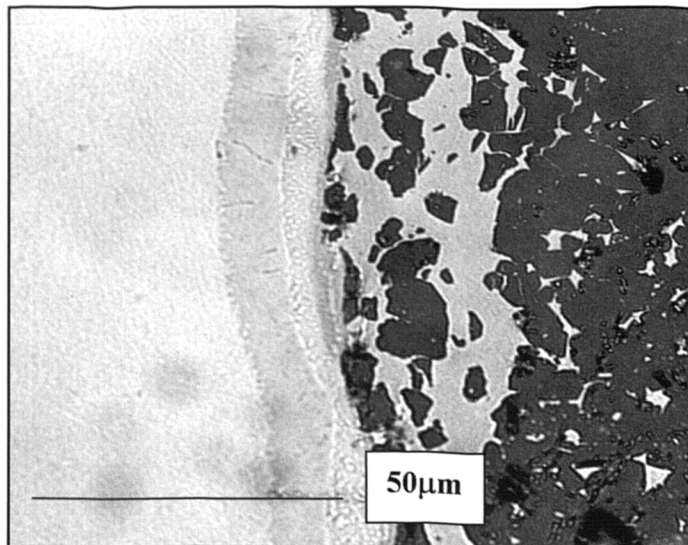
Figure 4.8a   Micrograph of Fecralloy-silicon nitride joint (1140°C, 30 minutes, 5.5 MPa)
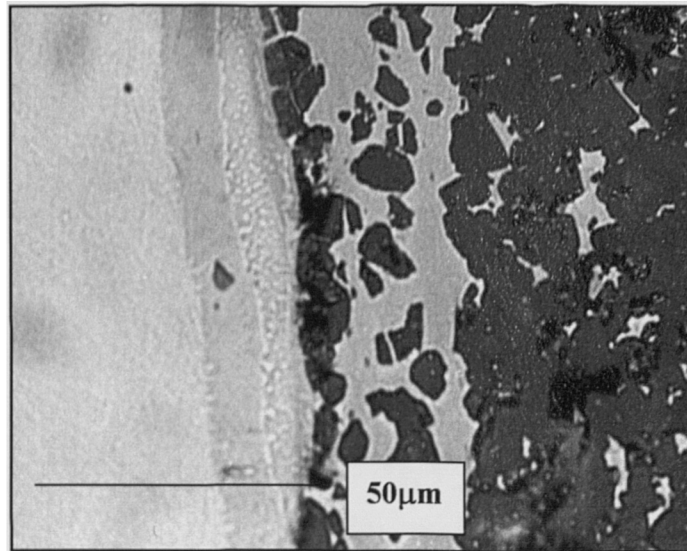
Figure 4.8b   Micrograph of Fecralloy-silicon nitride joint (1140°C, 30 minutes, 7.5 MPa)
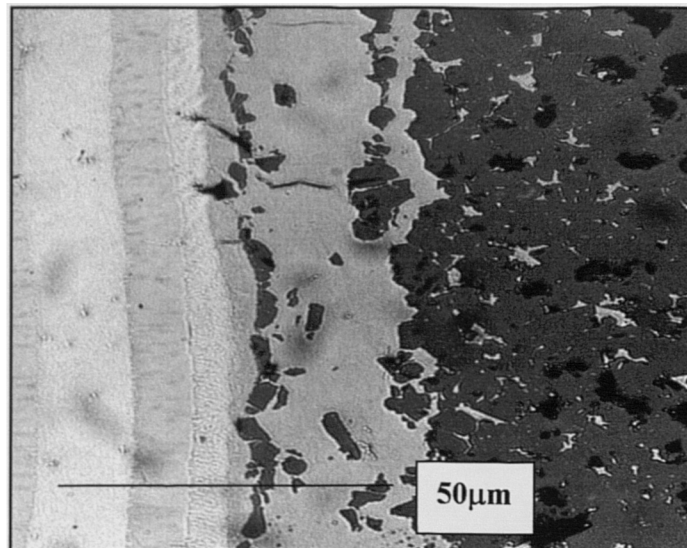
Figure 4.8c   Micrograph of Fecralloy-silicon nitride joint (1140°C, 30 minutes, 9.5 MPa)

4.2.2   *Effects of Processing Conditions*

The primary variables in the joining process are pressure, temperature, time and interlayer thickness. These variables are not independent from each other and the effect of each variable is discussed outlining the important considerations associated with each variable.

4.2.2.1   *Pressure*

In order to determine the optimal process conditions, the influence of applied bonding pressure on joint integrity was studied. Experiments were carried out with different pressures varying

between 0 and 9.5 MPa. Fig 4.9 shows a plot of average shear strength (±5) versus bonding pressure at 1100°C and 1140°C.

It is clear that the applied pressure affects joint strength. At high temperature and applied pressure the yield point of Fecralloy is lowered. The applied pressure causes partial deformation of the Fecralloy at the joining interface, which is sufficient to bring the Fecralloy into full contact with the silicon nitride on an atomic scale. Once full contact is made, further increase of pressure aids the diffusion/infiltration process that is occurring at the interface. The liquid metal that infiltrates the silicon nitride holds the substrate together by mechanical interlocking. It follows that the more liquid metal that infiltrates the silicon nitride, the stronger the joint. Of course there must be an applied pressure after which detrimental effects occur such as bulk deformation of the metal, expulsion of the liquid metal, etc. This was not identified in the present work.

The applied pressure also helps to break up surface oxides present at the joining interface. Fecralloy has a protective iron-chromium-aluminium oxide spinnel and a silicon oxide layer covers silicon nitride. These oxide layers present a barrier for the diffusion/infiltration process, giving rise to an incubation period for the interfacial reactions to begin. Quantitative data about the applied pressure required to promote the removal of these oxide layers is not available.
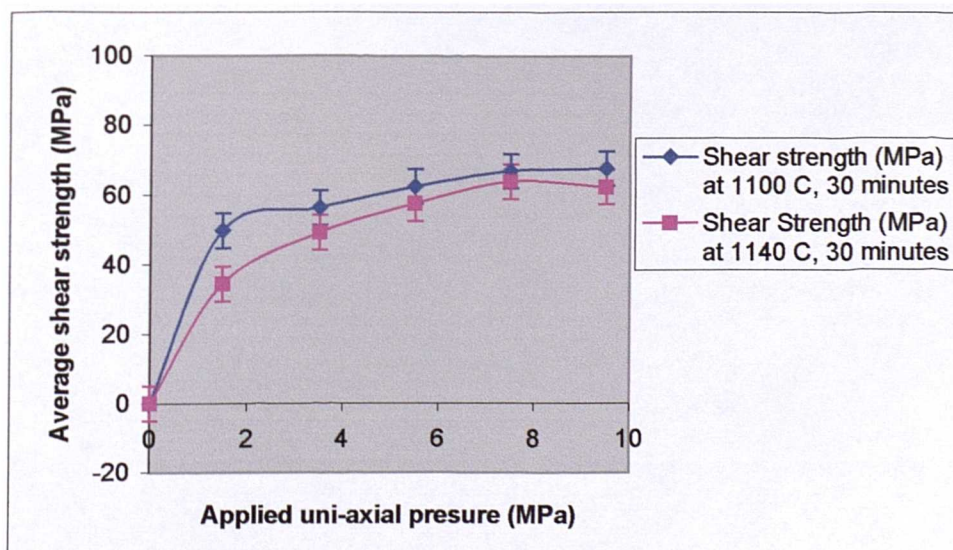
Figure 4.9   Graph showing dependence of average shear strength of joints with applied pressure.

4.2.2.2 Temperature

This is an important variable and the dependence of strength on temperature can be explained by considering the behaviour of the materials in the vicinity of both the metal and ceramic interface. Temperature increases interaction across the metal-ceramic interface by increasing the mobility of the atoms and also the mobility of dislocations in the metal during joining.

Diffusion and infiltration are thermally-assisted processes and so an increase in temperature is followed by an increase in their respective rates. Joining is only possible above 1100°C and this is due to the eutectic temperature being reached and initiating the joining process outlined in section 4.2.4.

Increasing temperature can cause a non-wetting-to-wetting transition for liquid metals in contact with ceramics, usually at 1100°C. This was found to be the case for an Al drop on silicon nitride [41]. At low temperatures, large non-wetting angles were observed as both Al and silicon nitride had surface oxide layers. At higher temperatures (1100°C) contact angles of 90° were observed and believed to be due to the breaking down of surface oxide layers and lowering of free surface energy.

4.2.2.3 Time

The dwell time at temperatures of 1100°C or above effects the interfacial reactions and size of diffusion/infiltration zones. At 1100°C and 1140°C we see the same pattern where there is a minimum time to initiate the reactions in order to produce a joint (10 minutes), an optimum time that produces joints of maximum strength (30 minutes) and a detrimental time that produces weak joints/no joints (60 minutes). From this it is apparent that there is a minimum time to initiate the joining process and this is due to the breaking up of surface oxides and wetting of ceramic interface. There is an optimum time, where sufficient wetting/interfacial reactions have occurred that produce a thin reaction product layer and elemental diffusion/infiltration to produce a good joint. Then there is a detrimental excess time, where the reactions proceed to form brittle products, usually silicides that cause a weak joint.

The elemental migration via diffusion and infiltration and also the diffusion/infiltration zone size is effected by time. With increased time the interfacial reactions occur generating increased concentration of by-products such as Si or N, and so these diffuse into the metal causing increased concentration and larger zone size.

4.2.2.4   *Interlayer Thickness*

A number of experiments were carried out to determine the influence of interlayer thickness on the joint strength. It was found that when the Cu foil thickness was increased to 25μm and 50μm, the joints broke under handling after processing (see Fig 4.6). Failure was always at the ceramic-interlayer interface. The reason for this is believed to be due to the formation of brittle phases at the ceramic-interlayer interface (*mostly copper silicides*).

Temperature (°C)	Dwell Time (mins)	Applied Pressure (MPa)	Average Shear Strength (MPa)	No. of thermal cycles till joint failure
1000	10	1.5	0	0
1000	30	1.5	0	0
1000	60	1.5	0	0
1100	10	0	0	0
1100	30	0	0	0
1100	60	0	0	0
1100	10	1.5	12.7	1
1100	30	1.5	49.6	3
1100	60	1.5	32.3	2
1100	30	3.5	56.1	0
1100	30	5.5	62.3	3
1100	30	7.5	66.8	3
1100	30	9.5	67.5	3
1140	10	0	0	0
1140	30	0	0	0
1140	60	0	0	0
1140	10	1.5	16.1	1
1140	30	1.5	34.3	2
1140	60	1.5	11.8	1
1140	30	3.5	48.9	2
1140	30	5.5	57.4	2
1140	30	7.5	63.8	3
1140	30	9.5	62.2	3

Table 4.1   Results of joining trials and thermal cycling using Cu foil interlayer

4.2.3   *Eutectic Liquid Phase Bonding (ELPB) Sequence*

In this section the mechanism of joining is examined and a sequential model outlining the joining process is put forth. From section 4.2.1, it has been established that joining is possible using a thin Cu interlayer. That a thin reaction product layer is formed at the silicon nitride interface, results suggesting it to be AlN and that Si and N have diffused into the Fecralloy, while Fe, Cr, Al and Cu infiltrate the silicon nitride.

The ability of the pure Cu interlayer to wet adequately the silicon nitride and eventual joining is rather surprising. Pure Cu is not considered to be active enough for wetting and joining of ceramics. This is demonstrated by metal-ceramic joining via an active metal brazing route, where a Cu-Ag-Ti interlayer is used. The Ti is the active element that actually wets the ceramic [3].

In sessile drop experiments of liquid Cu on silicon nitride carried out at 1100°C and 1150°C under vacuum, no evidence of reaction was found with a high contact angle, θ, of 130°. [109,110]. It is important to mention that HIP silicon nitride was used in the sessile experiments, as opposed to reaction bonded. Apart from differing mechanical properties, RBSN is about 15% porous and contains small amounts of free Si on the surface. It is these two factors that are believed to be instrumental in our joining process.

Suganauma *et al.* [9] tried to utilise these two factors when trying to join metals such as Fe and Ni to silicon nitride by a solid–state process (1200°C-1400°C, 100 MPa). Their attempts to produce viable metal-ceramic joints were unsuccessful and they were unable to identify a primary cause for this. This author believes that failure was due to the rapid heating and cooling rates (80 K/minute) which generated large residual thermal stresses that led to joint failure. This work found that a cooling rate above 5 K/minute was more likely to cause a weak/failed joined after processing.

A number of trials were carried out replicating Suganauma and co-workers idea of utilising the free Si without the use of an interlayer. These produced weak joints that broke under handling. However, there was evidence of reactive wetting at the silicon nitride interface, shown by the presence of small pits and crators. It can be argued that the low applied pressure of 50 MPa is arbitrary compared to that of 100 MPa used by Suganauma *et al.* for this solid state joining

process. However, there was great concern that an applied pressure greater than 50 MPa might cause failure of the graphite sample holder. It is strongly believed that increased pressure of 100 150 MPa would result in weak joints only, as the free Si activity is not sufficient to cause sufficient wetting for joining.

The most likely sequence of events occurring during joining are shown schematically in Fig 4.11. At 1100°C, numerous eutectic temperatures are possible which are: Cu-Si=823°C, Fe-Si-1083°C, Cr-Cu-1076°C, Al-Cu=1037°C, Fe-Cu=1083°C [111]. Above 1083°C the pure Cu interlayer completely melts and comes into contact with the Fecralloy and silicon nitride. Reactions with the free Si on the silicon nitride interface start at lower temperatures and at 1100°C a Cu rich-Si solution is formed. This is not active enough to cause the rate determining break up of surface oxides/oxynitrides and dissolution of silicon nitride interface as given in Equation 4.1. Small amounts of this Cu rich–Si solution diffuse into the metal eventually leading to partial melting of the metal interface bringing Fe, Cr and Al into solution.

EDX line scans show that Al was always present in the silicon nitride with the greatest concentration. This in addition to the presence of the AlN reaction product layer indicates that the liquid metal contained mostly Al. Work by Kubo *et al.* [112] showed that silicon nitride could be wetted by a Cu-Al braze. They also used this braze to join silicon nitride to itself (1100°C, 60 minutes) and the highest obtainable shear strength was 186 MPa with an Al-1.7at%Cu braze. Increasing the Cu content of the braze was detrimental to joint strength due to the formation of brittle intermetallic compounds. The liquid mixture in our joining process is reactive enough to initiate the reactive wetting process. While the exact mechanism of reactive wetting is still not fully understood by the scientific community, process parameters such as high temperatures and pressures and vacuum conditions (low O_2 and N_2 partial pressures) all aid the process. Non-planar interfaces, as illustrated in Fig 4.1 and 4.10, indicate extensive reactive wetting and partial dissolution of both interfaces. These non-planar ceramic interfaces illustrate one of the drawbacks of the Young-Dupre equation.

Due to the number of elements involved, numerous reactions are possible, the most likely of which were mentioned in section 4.2.1. For simplicity, three generalised equations describing the interfacial reactions can be given as:

Liquid metal mixture$_{(l)}$ + Silicon nitride$_{(s)}$ $\Rightarrow$ metal nitride + free Si   **Equation 4.10**
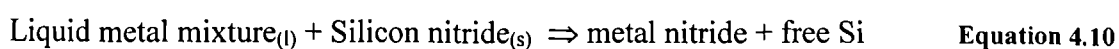
Liquid metal mixture$_{(l)}$ + Silicon nitride$_{(s)}$ $\Rightarrow$ metal silicide + nitrogen   **Equation 4.11**

Silicon nitride $\Rightarrow$ 3Si + 2N$_{2(g)}$ **Equation 4.12**

The main by-products of the reactions are Si and N, which diffuse into the Fecralloy forming mainly Fe$_3$Si and Cr$_2$N. Diffusion of the N into the metal is one route, while the other is that it remains in the silicon nitride. This is undesirable as it causes bubbles and pores at the interface, as can be seen in some of the micrographs.

The liquid metal mixture reactively infiltrates the silicon nitride and this process is greatly assisted and influenced by pressure. Two types of pressure act on the liquid metal, the first is the applied uni-axial pressure and the second is the capillary pressure. The capillary pressure is defined as the pressure difference across the liquid–vapour interface in a pore [113]. Under vacuum conditions, the gas present in a pore is removed and so an increase in applied pressure increases the capillary pressure and more of the pore space is filled with liquid. This explains why the width of the infiltrated metal in the ceramic increases with pressure and that up to the maximum test pressure of 9.5 MPa, there is no liquid expulsion (drawn into silicon nitride by increased capillary pressure).

Infiltration is also affected by other factors such as temperature and porosity characteristics (size, shape and amount of porosity). In order to infiltrate the silicon nitride, the contact angle of the liquid in the pores has to be below 90°. In other words, the liquid metal has to adequately wet the silicon nitride, where the rate–determining step (reactive infiltration kinetics) is the reaction between the liquid metal and silicon nitride. Infiltration will only occur above a critical temperature and low partial pressure of oxygen. Oxygen tends to lower the surface energy of liquid metal, while the effect of N$_2$ is not as drastic.

The chemical composition of the infiltrated metal is almost the same as the parent metal. It is this infiltrated metal that holds the joint by mechanical interlocking.
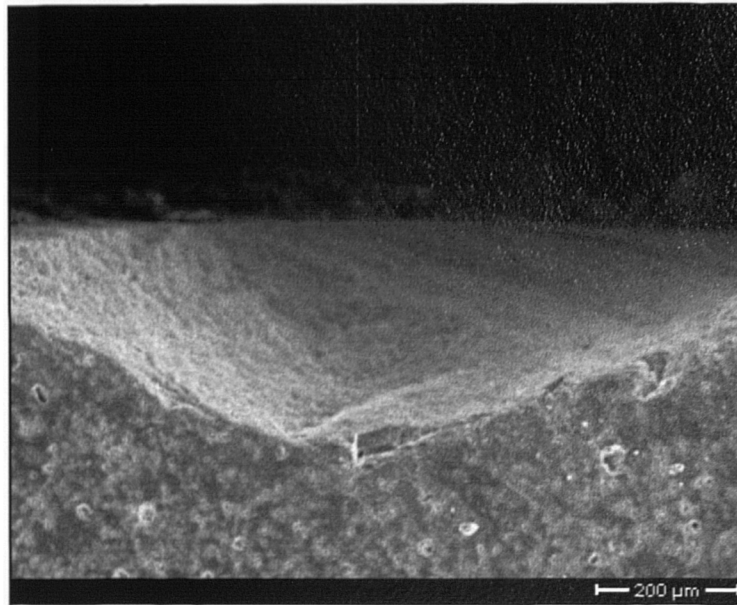
Figure 4.10   Micrograph showing a 'crator' on the silicon nitride surface, which is due to excessive reactive wetting.

Eutetic Liquid Bonding Sequence

Stage 1: At room temperature.
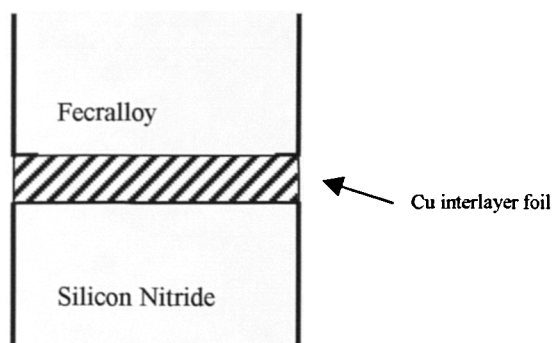
*Stage 2:* At 1100°C: Cu foil melts and forms Cu rich-Si solution with free Si on ceramic surface.

70
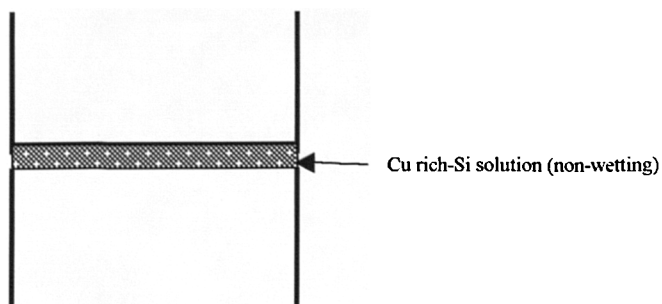
Stage 3: At 1100°C: Cu rich-Si solution causes partial melting of Fecralloy interface, bringing Fe,Cr and Al into solution.

Partial melting of Fecralloy interface, bringing small amounts of Fe Cr & Al into solution with the Cu rich-Si solution forming a liquid metal mixture (wettable)
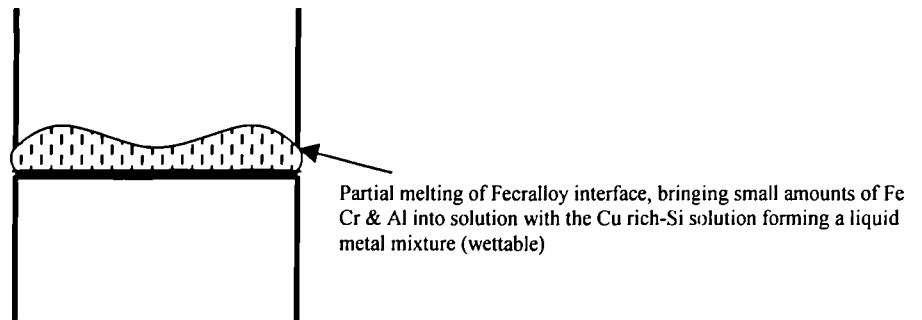
Stage 4: At 1100°C: The ceramic interface is shown where reactive dissolution wetting is occurring by liquid metal mixture, where metal nitride and/or metal silicides are being formed with Si and N_2 as by products. A slight dissolution is enough to modify the surface energies of the system while the interface remains almost planar.

Silicon nitride

Liquid metal mixture causes a slight dissolution of silicon nitride interface by reactive dissolution wetting
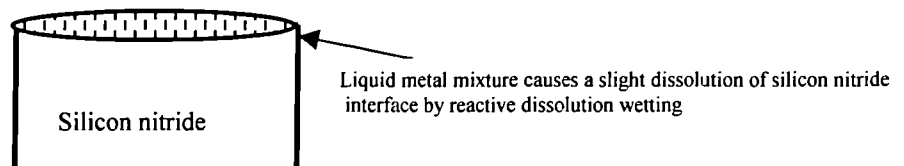
Stage 5: At 1100°C: Elements Fe,Cr,Al and Cu reactively infiltrate the ceramic, while elements Si, N and Cu diffuse into the Fecralloy.

Si   N   Cu

Fe   Cr   Al   Cu
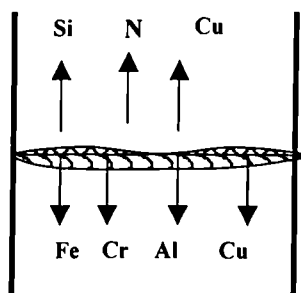
Stage 6: Room temperature: Joint is formed with good interfacial bonding and no remaining Cu interlayer.
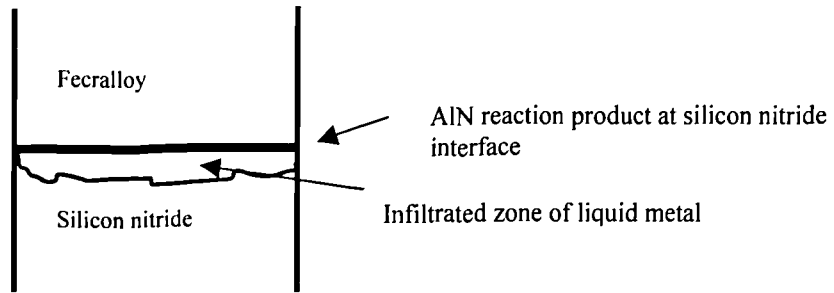
Figure 4.11   Schematic of proposed ELPB sequence (not to scale)

4.2.4   Mechanical Testing

4.2.4.1   Shear Testing

Table 4.1 presents the data for the average shear strength of the joined samples. Shear strength ranged from 11.8-67.5 MPa and are modest compared to those of metal-metal and ceramic-ceramic joining. Metal-ceramic joints tend to have inherently low shear strength values. The two main reasons for this are the residual thermal stress due to the CTE mismatch and formation of brittle phases at the joint interface. Our shear strength values compare well to other metal-silicon nitride joints. Using an active metal braze, Lee [55] presented shear strength values of 46.1-70.4 MPa for Inconnel 718-silicon nitride joints. Work by Vegater [114] produced Zirconia-silicon nitride joints using a Ni interlayer that has a maximum shear strength of 57 MPa.

The modest shear strength values obtained in this work can be attributed to the mentioned reasons along with the presence of interfacial defects such as cracks and pores. Processing conditions do affect the shear strength of the joint and the results reveal the following trends.

1. At a given joining time and pressure, the shear strength increases with joining temperature, reaching a maximum and then decreasing with further temperature increase.

2. At a given joining temperature and pressure, the shear strength increases with joining time, reaching a maximum and then decreasing with further dwell time increase.

3. At a given joining time and temperature, the shear strength increases with pressure. This work did not establish the maximum pressure after which shear strength decreases.

These results establish that the optimum processing conditions to produce a Fecralloy-silicon nitride joint with the highest shear strength is 1100°C, 9.5 MPa and 30 minutes. Dwell times greater than 30 minutes and temperatures greater than 1100°C, make the formation of brittle silicides at the ceramic interface likely and lower shear strength.

Yvon *et al.* [115] studied the residual stresses in various metal-ceramic joints using an x-ray diffraction technique and compared these with analytical calculations of the residual stress. They put forth a figure of 700 MPa for a directly joined 316 SS-silicon nitride joint. This value is believed to be similar for Fecralloy-silicon nitride joints. While the exact figure of residual stress is unsure, it is clear that it is considerably high. This explains why metal-ceramic joints tend to have low shear strength values.

Analysis of the broken shear test samples always had a granular fracture surface, with failure always occurring in the ceramic side. A small section of ceramic would still remains firmly attached to the metal interface.

4.2.4.2   Thermal Cycling

Total reliance upon joint strength measurements to characterize the mechanical behaviour of a metal-ceramic joint in service like conditions is incorrect. As mentioned in the previous section failure is mainly attributed to residual thermal stress and formation of brittle interfacial phases. Interfacial defects such as cracks and pores and the local variation of stresses governed by the geometry of the joint, the elastic and plastic properties of the metal/ceramic and loading conditions all influence joint failure.

It is therefore important to characterize mechanical behaviour of the joint under service like conditions. One option is to measure joint strength at temperature and this always shows that joint strength decreases with temperature [45]. The main reason for this tends to be the low melting temperature of the active metal braze and an annealing effect at lower temperatures. Another option is thermal cycling, which was used in this work. This gives an indication to the durability of the joint to thermal shock. Provided all the test conditions are kept the same, the results are reliable enough to serve as a means of comparison.

The temperature of 850°C was chosen as it higher than the service temperature of most active metal braze joints. From Table 4.1 it can be said that the thermal cycling results are quite

ncouraging. They can be directly related to the shear strength values, as the stronger joints end to be able to withstand more thermal cycles.

t is the residual stress factor that comes into play leading to joint failure during thermal ycling. The stresses parallel to the interface are tensile in metals and compressive in ceramics howing a jump at the interface. Maximum tension in ceramics occurs near the free edge of the nterface, where the stresses were singular. It is this tensile stress developed in the ceramic dherent that is thought to be the most important factor effecting joint failure. Fig 4.12 shows a iicrograph of a sample that failed after thermal cycling. Extensive cracking in the ceramic vhere the cracks initiate and propagate from the side can be seen. Failure was due to the xcessive thermal stresses in the joint.
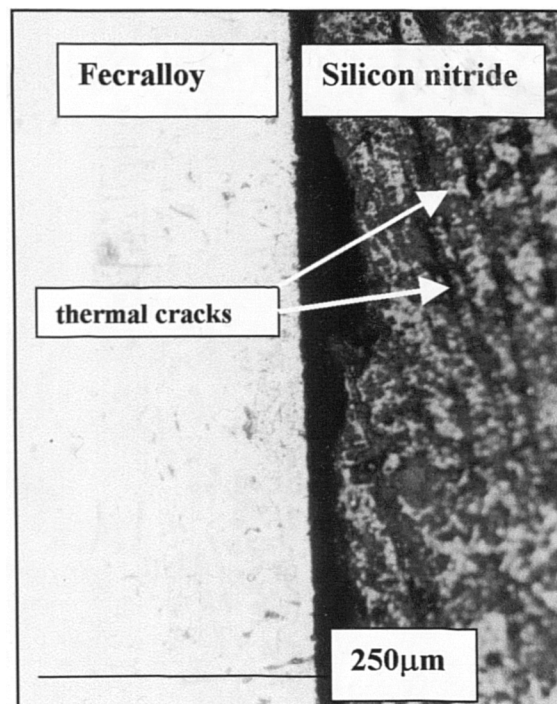
Figure 4.12   **Micrograph of a failed sample during thermal cycling.**

4.2.5   *Microhardness profiling and melt-back distance*

Microhardness profiling was carried out to see if the joining process had any detrimental effects upon the Fecralloy and to see if homogenisation had occurred after joining. As previously mentioned in section 3.5.3, as-received Fecralloy was found to have an average

microhardness of 245 Hv. Heat treatment under vacuum (1100°C, 30 minutes) lowers this value to 237 Hv due to the process of annealing.

It should be noted that the average change in microhardness (from as-received condition) is plotted with distance away from joint interface. This gives a better indication of how the microhardness for Fecralloy varies from joint interface and any effects of process conditions. The general trend for all the microhardness profiles shown in Fig 4.13 is that at the Fecralloy interface the average microhardness is high and this levels off with distance from the Fecralloy interface. This is due to the presence of precipitates at the Fecralloy interface, mostly Fe_3Si. Factors that cause increased diffusion into the Fecralloy, such as an increase in temperature or pressure have higher interfacial microhardness. This is due to the increased concentration of precipitates at or close to the metal interface.

All the profiles show that homogenisation is not occurring, as the precipitates tend to concentrate around the joint interface. Increased dwell time has little effect on this and tends to be detrimental to joint integrity.

Melt-back distance is the width of metal that melted forming a solution at the joining interface. Tuah-Poku et al. [23] found that there was good agreement between experimentally observed and theoretically derived melt-back distance values in the TLP bonding process of two metallic substrates. It was emphasised that many important considerations were neglected in the equation. The validity of the experimentally derived values is questionable, as this was measured optically by observing changes in microstructure in cross-sectioned samples.

The relationship between a theoretically derived melt-back distance value and its relation to the mechanical parameter of microhardness was investigated. Any correlation between the two would be of great interest.

The mass conservation equation put forth by Tuah-Poku et al. [23] that can be used to calculate a value for the total melt–back distance is given by;

$$W_m = W_0 \left[\left(1 + \frac{C^B - C^{L\alpha}}{C^{L\alpha}} \right) \frac{P_Y}{P_X} \right]$$ **Equation 4.13**

Where W_m maximum liquid width

W_0 initial interlayer thickness

C^B – initial concentration of melting point depressant in interlayer

$C^{L\alpha}$ = liquids concentration at joining temperature

P_Y – density of interlayer foil

P_X = density of metal

The total melt-back distance for one interface is calculated by,

$$\left(\frac{W_m - W_0}{2}\right)$$ **Equation 4.14**

The reason why melt-back proceeds is to reduce the concentration of Cu in the liquid layer. The interlayer melts forming a liquid that is not in equilibrium with the metal and so the metal dissolves to dilute the liquid. The interlayer atoms diffuse in to the solid metal to form an α-phase at the interface and this causes the partial melting when the interlayer concentration in the α-phase adjacent to liquid exceeds $C^{\alpha L}$. In this process, solid-state diffusion, D_S of the interlayer in to the metal is important.

Along side this process, the metal solution mixes with the liquid interlayer and this process is controlled by the liquid phase diffusion, D_L. The liquid layer continues to widen until the concentration profile within the liquid flattens to the equilibrium value $C^{L\alpha}$. At $C^{L\alpha}$ the liquid layer has reached its maximum width. The effective diffusion coefficient is most likely to be related to a combination of D_L and D_S, but the exact relationship is unknown. In this parallel process, the rate-controlling step is always determined by the faster diffusing element. It was suggested that D_L should be the more dominant process in this stage.

As Al was found to have the greatest concentration in the silicon nitride and is believed to be the major constituent of the wettable liquid metal, we consider the Fe-Cu binary phase diagram in order to obtain a value for $C^{L\alpha}$. Using Equations 4.13 and 4.14, with values of C^B=1 (pure interlayer) and $C^{L\alpha}$=0.10, the total melt-back distance was calculated as 155μm and 71μm at the Fecralloy interface. While the value of 71μm is feasible, it is very difficult to relate this to the microhardness profiles. The profiles show the microhardness values normalising approximately 300μm away from the interface. The steady decrease in microhardness is due to a decrease in concentration of precipitates.

Both Equations 4.13 and 4.14 fail to consider the effects of microstructural features such as grain boundaries and precipitates that effect microhardness. The effects of processing conditions such as pressure are also ignored, which cause increased interfacial melting (melt-back) shown by the large infiltrated zones in the silicon nitride. The equations also do not account for the liquid metal reactively infiltrating the silicon nitride (lost from Fecralloy interface). From all of this it can be concluded that Equations 4.13 and 4.14 are flawed and while it might be possible to obtain a theoretically derived value for melt-back distance this cannot be confirmed experimentally using microhardness profiling.
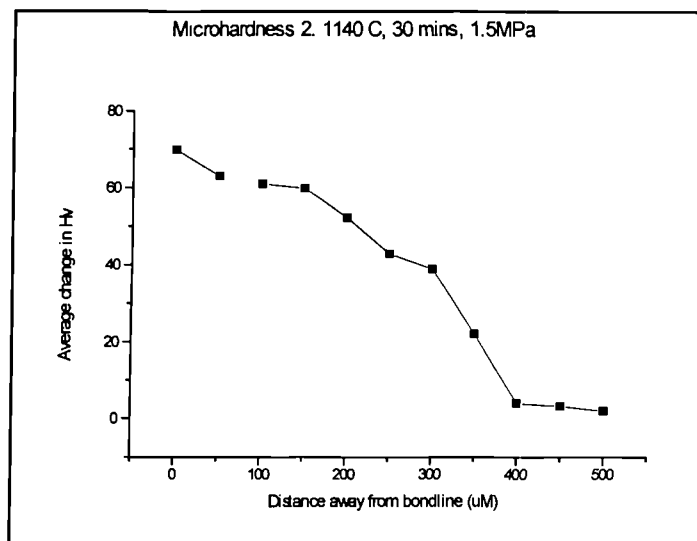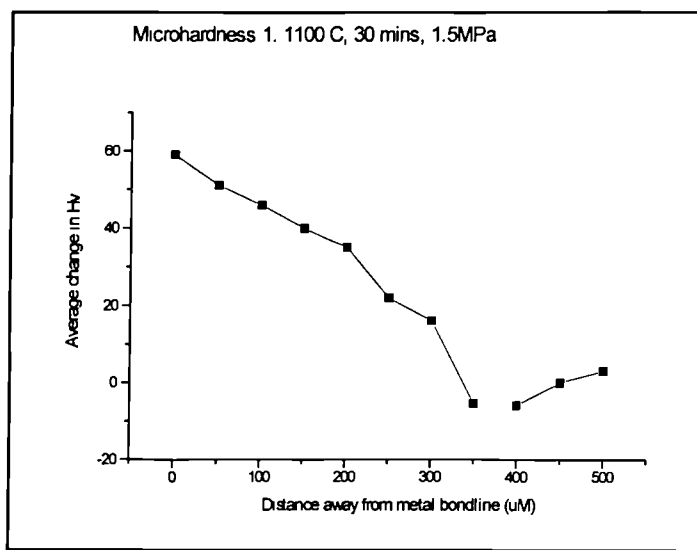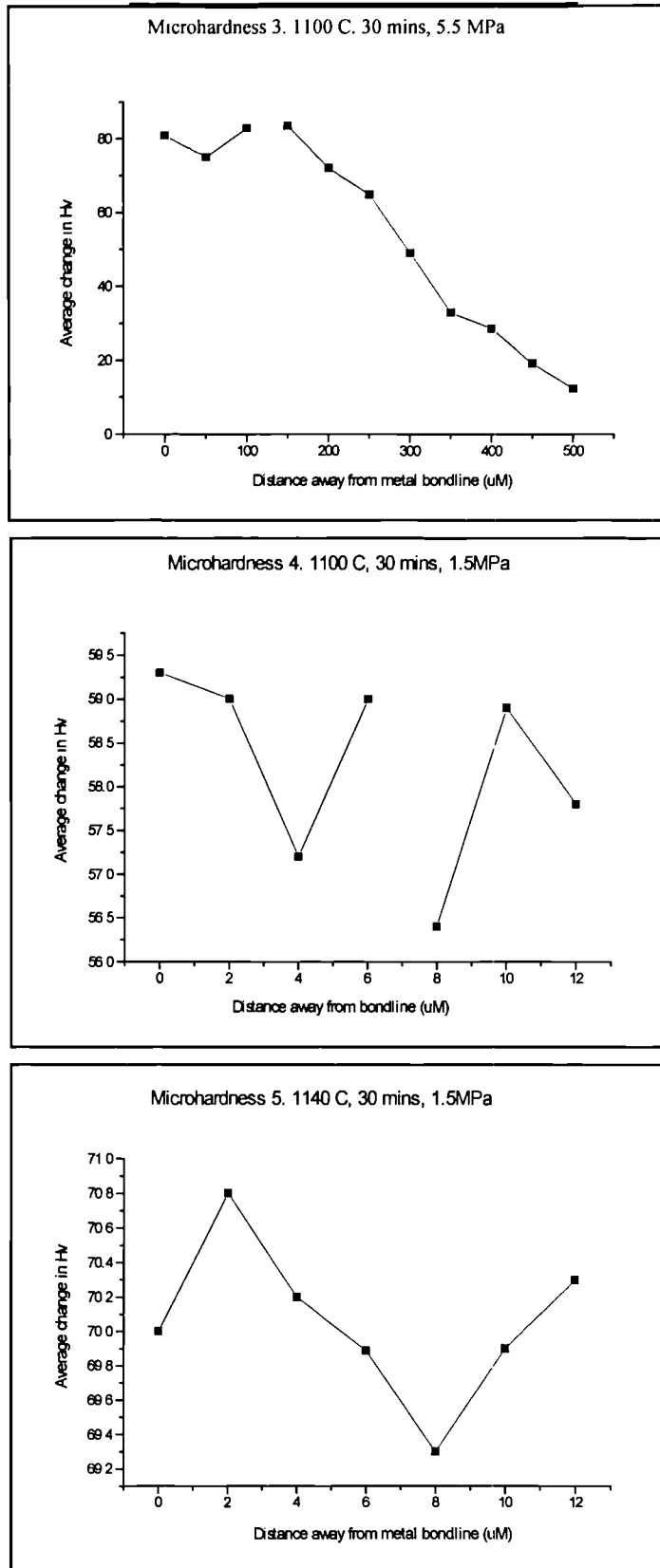
Figure 4.13   **Microhardness profiles of Fecralloy from joined samples.**

4.3   Introduction: Use of Ti/Cu/Ti multi-interlayer

PTLP bonding has been explored for ceramic-ceramic and metal-ceramic joining in recent years [115]. This process offers the possibility of producing an interlayer with a high melting temperature and hence a joint that can possibly withstand high temperatures. Iino [116] used this process to join silicon nitride with Ni using a Ti foil. Zheng *et al.* [117] further increased the strength of this joint (four-point bend test) by the insertion of a Cu foil between the Ni metal and Ti foil.

The joining of Fecralloy-silicon nitride was investigated by use of a Ti/Cu/Ti multi-interlayer and its variations. The Ti/Cu/Ti system was selected as it has a eutectic point and a reaction between the inner insert (Cu) and outer inserts (Ti) would occur with the formation of a transient liquid. At 1050°C the liquid phase formed at the Ti/Cu interface would disappear as the Cu diffused into the Ti. If the Cu concentration in the Ti is below 30wt%, this interlayer has a melting temperature of approximately 1200°C, producing a high temperature ductile interlayer. This system of a remaining ductile interlayer would be compared to that of the previous section where the Cu interlayer does not remain.

4.3.1   Results and Discussion

4.3.1.1   Microstructure of Interface

Table 4.2 presents the results of the joining trials using the multi-interlayer systems. Although varying processing conditions were used, joining was not possible at all as weak joints were produced that broke under handling.

Fig's 4.14 and 4.15 show the trials carried out at 1050°C and 1100°C. From the Cu–Ti phase diagram [111] it is established that a eutectic reaction occurs at 1050°C, while at 1100°C, the Cu foil completely melts. The rough silicon nitride surface indicates that reactive wetting

occurred during processing. EDX analysis of the interlayer found it to be mostly TiCu and Ti$_2$Cu$_3$ both of which had dissolved Si. There were also small areas where pure Cu or Ti existed. EDX analysis of the silicon nitride interface determined the presence of two products. The first was TiN, from the reaction of Ti with the silicon nitride. The second product contained Ti, Cu and Si with small amounts of N. This is believed to be a Ti–Cu Si–N compound and its presence along with that of TiN was also confirmed by Carim [118] in the joining of silicon nitride to itself using a Ti-Ag-Cu braze. From this it is apparent that reactive wetting and dissolution of the ceramic occurs, with small amounts of reactive infiltration into the silicon nitride (Ti, Cu) and diffusion into the Fecralloy(Ti, Cu, Si and N). Joint failure can be attributed to the two reaction products that form in all the joints with varied processing conditions. This can be due to their brittle nature or excessive residual stresses that accompany the volume change with the formation of the reaction product.

In order to overcome this problem and achieve joining two different methods were tried. The first used a thinner Ti foil (12.5μm), as the thickness of the Ti foil determines the amount of liquid present. Weak joints were produced that broke under handling. EDX analysis identified the presence of the Ti–Cu–Si–N compound, which is believed to cause failure. However, it should be noted that though these joints also broke under handling, considerably more force was required with the Ti/Cu/Ti joints. From this it is apparent that as little Ti as possible should be used due to the formation of the brittle compound.

The second approach was a reversal of the multilayer, in that a Cu/Ti/Cu multilayer was used. (12.5μm/20μm/12.5μm). Once again joining was not possible as the joints broke under handling but showed signs of reactive wetting at the silicon nitride interface, as shown in Fig 4.17. At the processing temperatures of 1050°C or 1100°C, the Cu foil would react with the free Si on the silicon nitride surface forming a Cu–Si liquid and would also react with the Ti foil forming a transient liquid. It is believed that a Ti–Cu–Si liquid was present at the silicon nitride interface, which is responsible for the extensive reactive wetting (cratoring). Again the Ti–Cu–Si-N compound was present at the silicon nitride interface. One can conclusively attribute the presence of this compound to failure highlighting the difficulties of metal-ceramic joining.

Multi-layer system	Temperature (°C)	Dwell Time (mins)	Applied Pressure (MPa)
Ti/Cu/Ti	950	30	2
	1000	30	1.5
	1000	30	3.5
	1000	60	1.5
	1100	10	1.5
	1100	30	3.5
	1100	30	5.5
	1100	60	3.5
	1140	30	1.5
Cu/Ti/Cu	1000	30	1.5
	1100	30	1.5

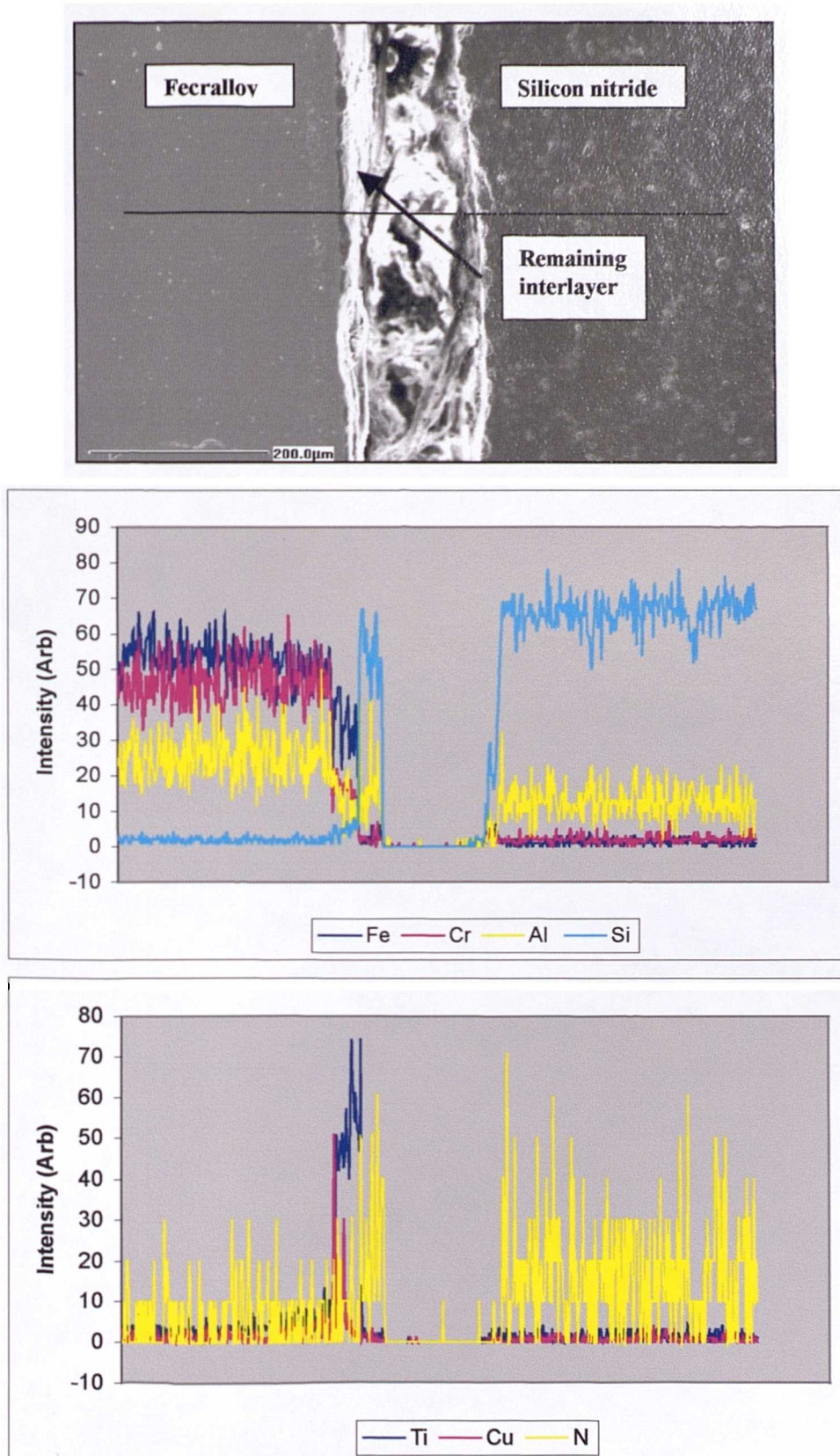**Table 4.2**   **Results of the joining trials using multi-interlayer foil system (no joining)**

Figure 4.14   Micrograph and EDX line scan of failed Fecralloy-silicon nitride joint using Ti/Cu/Ti interlayer (1100°C, 30 minutes, 1.5 MPa).
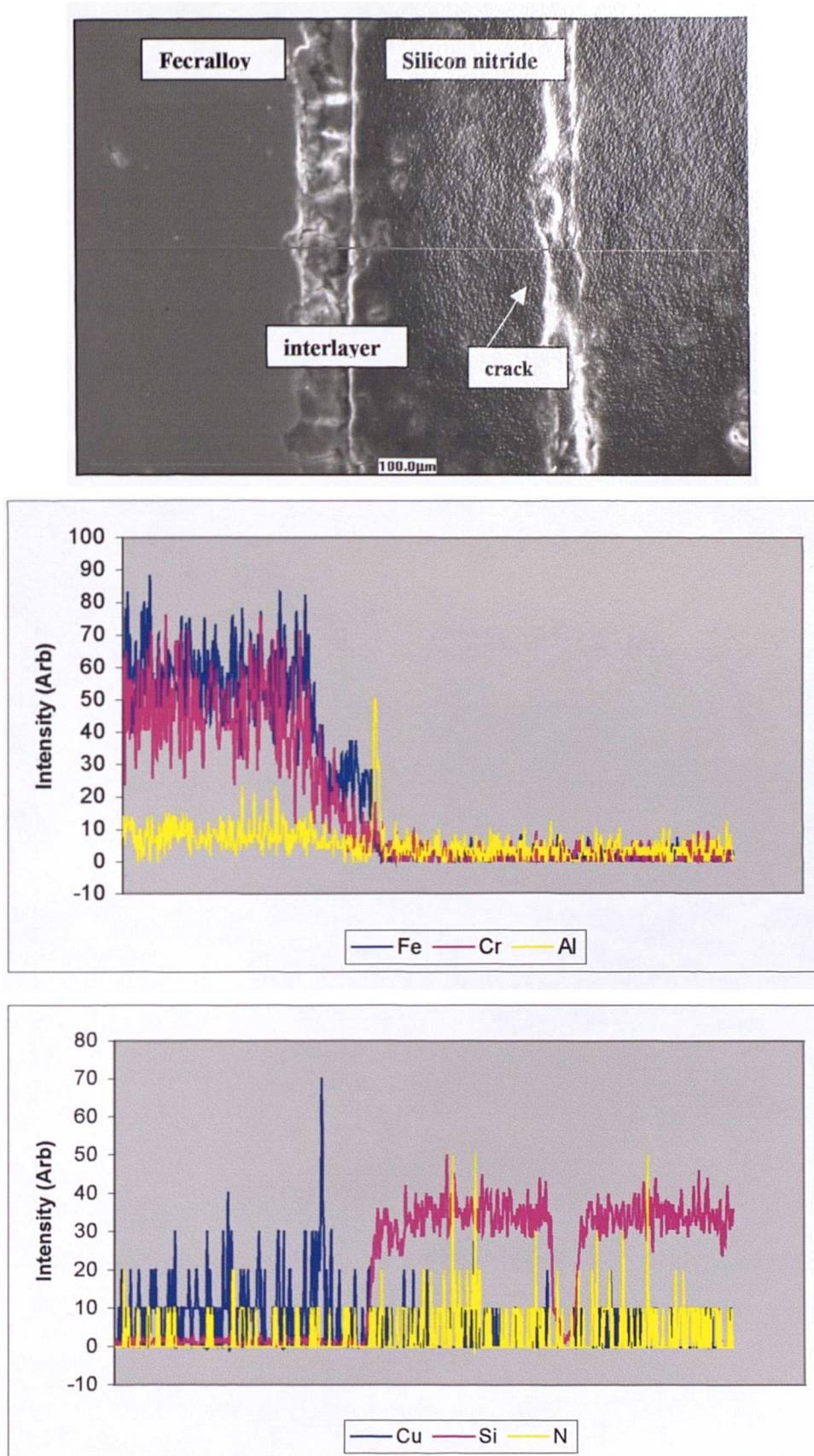
Figure 4.15   **Micrograph and EDX line scan of failed Fecralloy-silicon nitride joint using Ti/Cu/Ti interlayer (1140°C, 30 minutes, 1.5 MPa).**
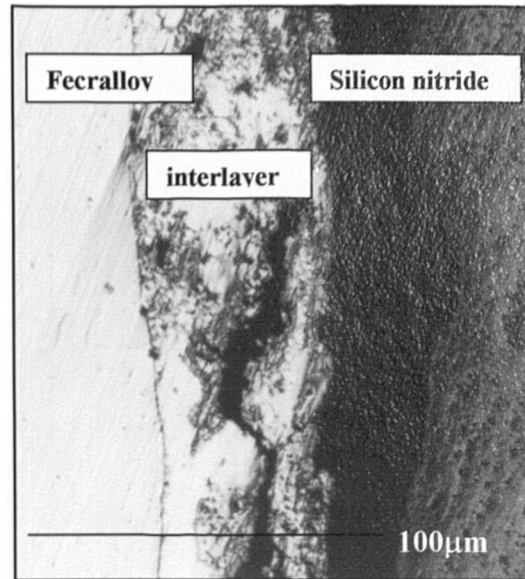
Figure 4.16   **Micrograph showing failed Fecralloy-silicon nitride joint using Cu/Ti/Cu multi-interlayer (1100°C, 30 minutes,1.5 MPa).**

4.4   Summary

It has been possible to join the high temperature Fecralloy with silicon nitride using a thin Cu interlayer foil. Good interfacial bonding is achieved and mechanical interlocking forces hold the joints together that exhibit the highest shear strength. Joining occurs by the process of ELPB that results in a thin reaction product layer at the silicon nitride interface (results suggest AlN), diffusion of Cu, Si and N into the Fecralloy and infiltration of Fe, Cr, Al and Cu into the silicon nitride. The free surface Si and porosity of the silicon nitride along with the various eutectic temperatures above 1100°C are all instrumental in the joining process.

No correlation could be established between the theoretically derived value for melt-back distance and the microhardness profiles. This is primarily due to the shortcomings of the theoretical model.

The shear strength values are very modest but compare well to others metal-ceramic joints, where the CTE mismatch is also large. The thermal stresses that are induced in the silicon nitride during the process cooling are believed to be the main cause of the modest shear strength values and reason for failure during rigorous thermal cycling.

84

To overcome this problem, the use of a remaining and high temperature ductile interlayer was looked in to by use of Ti/Cu/Ti multi-interlayer and its variations. However, joining was not possible and this was attributed to the presence of a Ti–Cu–Si–N brittle compound. Although Ti is an active element aiding the wetting of ceramics, in large concentrations it tends to be detrimental as it can form brittle compounds. This is one of the main reasons why its concentration is low in active metal brazes.

5. Joining by a Powder Metallurgy Route

5.1 Introduction

Nickel aluminide, NiAl, has attracted considerable interest as it offers new opportunities for developing low-density, high strength structural alloys for possible high temperature applications. However, high strength is usually associated with poor room temperature ductility. Intermetallics fall in between metal and ceramics, as they are not as brittle as ceramics because the bonding is predominately metallic.

NiAl has numerous outstanding properties namely low density ($5.9gcm^{-3}$), high melting temperature ($1638°C$), high strength, good corrosion and oxidation resistance, high thermal conductivity and low cost [119]. Its body-centred cubic crystal structure makes plastic deformation easier compared to other intermetallic compounds. A draw back of NiAl tends to be its low ductility at room temperature, which can be improved by reducing grain size or alloying. One of the potential applications of NiAl is as a high-pressure turbine blade material where low-density NiAl turbine blades can reduce the turbine rotor weight by 40% [120].

NiAl was chosen as a viable material to join Fecralloy with silicon nitride due to its outstanding properties and exothermic formation via a powder metallurgy route. The major advantage of a powder metallurgy route is the ability to tailor the interlayer in terms of size and composition, so that it can join materials of different shapes and also the relative low cost. The disadvantages are that the properties of the formed product are greatly influenced by processing conditions and porosity.

The joining of Fecralloy-silicon nitride was investigated primarily by use of cold pressed Ni-Al compacts and the results are presented and discussed. The reaction synthesis of the NiAl was studied using DTA, where the effects of heating rate and Ni particle size were investigated. The reaction kinetics were determined using a kinetic model and its validity investigated. TGA was used to confirm the high temperature oxidation resistance of the NiAl interlayer and to characterise the reactive synthesis process.

86

The joining process has been termed as reaction bonding due to the exothermic synthesis of NiAl from its constituents (termed as reaction synthesis).

The ultimate aim is the successful production of viable Fecralloy-silicon nitride joints by a fully dense NiAl interlayer.

5.2   *Results & Discussion*

5.2.1   *Interfacial Microstructure*

Firstly, let us consider the joints produced using a paste method to apply the interlayer. In Fig 5.1, where a moderately high temperature and pressure were used (1000°C, 15 minutes, 45 MPa), the interlayer is porous and densification has not occurred. Interfacial bonding between interlayer-ceramic was weak, while that between interlayer-metal was better. When the temperature was increased to 1200°C, as shown in Fig 5.2, a densified interlayer is produced with good interfacial bonding between interlayer and metal/ceramic. However, upon cooling cracks were formed in the interlayer close to the interlayer-ceramic interface that caused failure, as can be seen. This is due to residual stresses being introduced into the interlayer at this elevated temperature. The volume changes associated with phase transformation also induce stresses.

Limited reactive wetting is evident at the ceramic interface as shown in Figs 5.3 and 5.4. From these two micrographs the effects of temperature increase from 900°C to 1000°C at 15 minutes, 45 MPa can be observed. Porosity is slightly reduced, but the interlayer remains porous with no densification.

The reaction mechanism is discussed in section 5.4 but good particle contact and compaction is important for the reactive synthesis of NiAl. A liquid phase propagates through the structure leading to densification. However, the use of a binder does not give good particle-particle contact and when the interlayer does burn off, it leaves the interlayer unconnected and reacting particles apart. Thus, localised solid-state reactions occur in pockets that result in no densification and a porous multi-phase interlayer, which is detrimental to the joining process.

Excessive porosity and no densification were apparent with all the joints fabricated by the paste method producing weak joints. Although porosity is associated with the exothermic reaction synthesis of NiAl from its constituents, in this case it is due to the binder. It was concluded that the use of a binder produced weak joints, with little effect by varying the processing conditions and so work then concentrated on using cold pressed Ni-Al compacts.

The micrographs of the joining trials using cold pressed Ni-Al compacts are shown in Figs 5.5-5.11. At 800°C (15 minutes, 45 MPa) weak joints were produced that had large interlayer pores and failure always occurred in the interlayer close to the interlayer-ceramic interface, as shown in Fig 5.5. A considerable portion of the interlayer being attached to the ceramic demonstrates good interfacial bonding between the interlayer-ceramic. The large pores are sites of stress concentrations and from where cracks can initiate and propagate from producing weak joints.

An increase in temperature to 900°C (15 minutes, 45 MPa) results in good joining producing joints that exhibit the highest shear strength. Dense and monophase NiAl is produced with good interfacial bonding and no visible reaction product layer, as shown in Fig 5.6.

The importance of a high processing pressure is demonstrated in Fig 5.7, where pressure was reduced to 30 MPa at 900°C, 15 minutes. Although joining with good interfacial bonding was attained, medium sized pores were present in the interlayer.

When the dwell time was reduced to 5 minutes at 900°C, 45 MPa, good joining was possible but numerous small interlayer pores were formed, as shown in Fig 5.8. All of this demonstrates the effects processing parameters have on the microstructure and ultimately the mechanical properties of the joint.

The EDX line scans confirm the presence of mostly Fe in the interlayer. This is due to a small amount of interfacial melting of the Fecralloy interface due to the large amount of heat released during the exothermic reaction of the NiAl synthesis. Due to the composition of Fecralloy, the melt is Fe rich and this diffuses into the interlayer. According to the Ni-Al-Fe ternary phase diagram [111], the β-NiAl stably co-exists both with α-Fe and γ-Fe. Work by Miracle *et al.* [121] showed that room temperature ductility was dramatically improved by microalloying with either Fe, Ga or Mo. Small additions of Fe (0.1at%) increased room

temperature ductility from 0-2% to 6%, increased fracture toughness and yield strength. Fe has a high solubility in NiAl and can provide significant solid solution strengthening. Thus, the presence of the Fe in the NiAl interlayer was beneficial.

The EDX line scans and EDX elemental map (Fig 5.9) confirm that Si and N have diffused into the interlayer and Fecralloy. This is due to dissolution of the silicon nitride interface by the exothermic reaction and wetting by Al, which has infiltrated the silicon nitride in small amounts. The EDX elemental map does not show the presence of an AlN or any other reaction product layer at the silicon nitride interface.

Interfacial melting of the Fecralloy substrate was also observed in the joining of NiAl to steel by Matsuura *et al.* [92]. In their work molten Al and Ni were poured onto a steel block and once solidified this formed a good joint. It was found that the depth of melted steel increased with the thickness of the NiAl layer and also by heating the steel block

In order to observe the effects of an active element, a number of trails were carried out inserting a thin Ti foil between the interlayer and silicon nitride. From Fig 5.10 it can be seen that apart from the interlayer being porous, the silicon nitride interface is cracked. This is due to the formation of brittle phases (mostly TiN with dissolved Si). The EDX line scan and EDX elemental map (Fig 5.11) confirm that Ti had diffused into the NiAl interlayer as had Fe, Si and Ni and that a TiN reaction product layer is present at the silicon nitride interface. The use of a Ti foil insert was found to be detrimental to the joining process, primarily due to the formation of brittle phases at the silicon nitride interface.
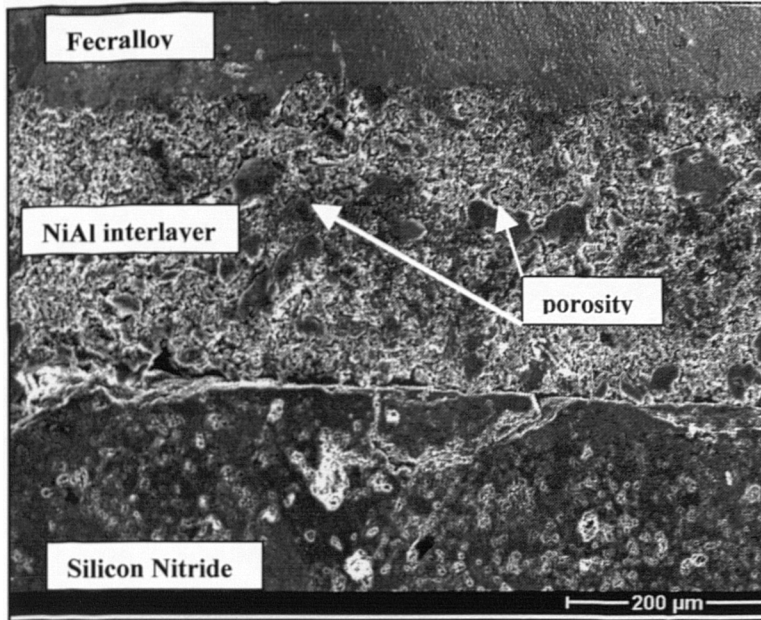
Figure 5.1   Fecralloy-silicon nitride joint formed using paste method (1000°C, 15 minutes, 45 Mpa).
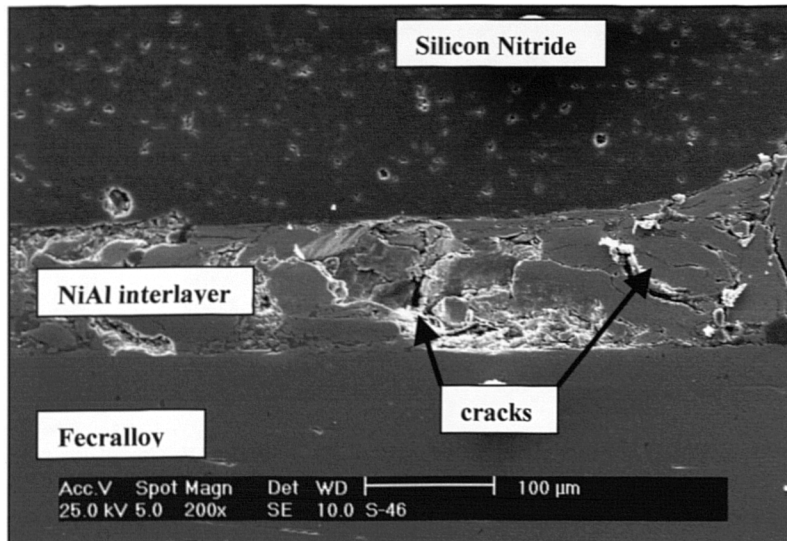
Figure 5.2   Fecralloy-silicon nitride joint formed using paste method (1200°C, 15 minutes, 45 Mpa).
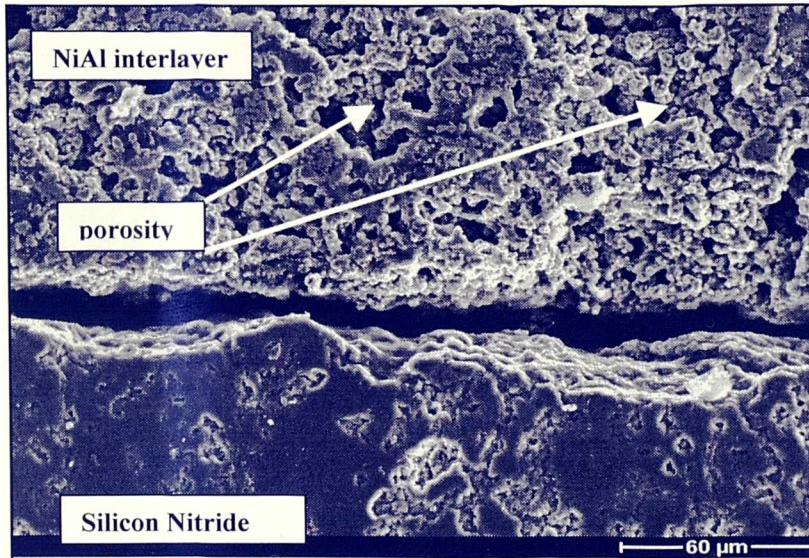
Figure 5.3   Failed interlayer-ceramic interface (900°C, 15 minutes, 45 Mpa).
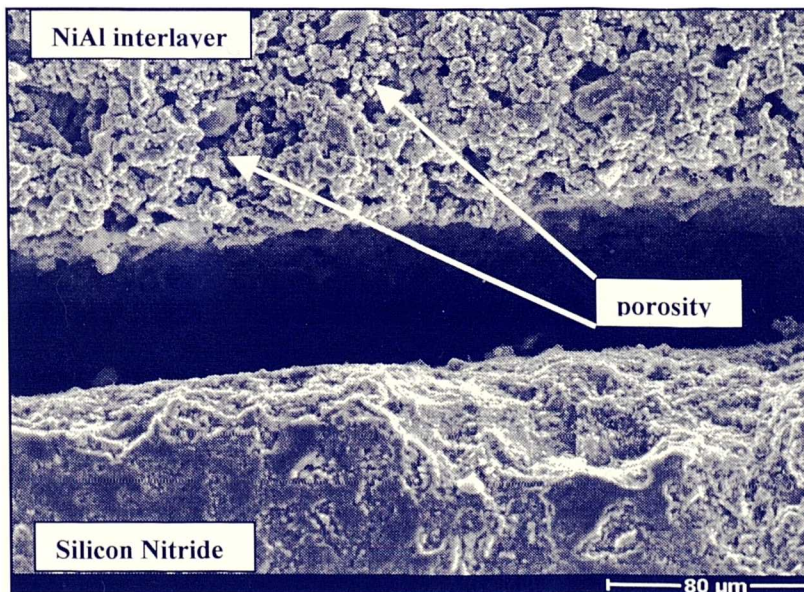
**Figure 5.4**   Failed interlayer-ceramic interface (1000°C, 15 minutes, 45 Mpa).
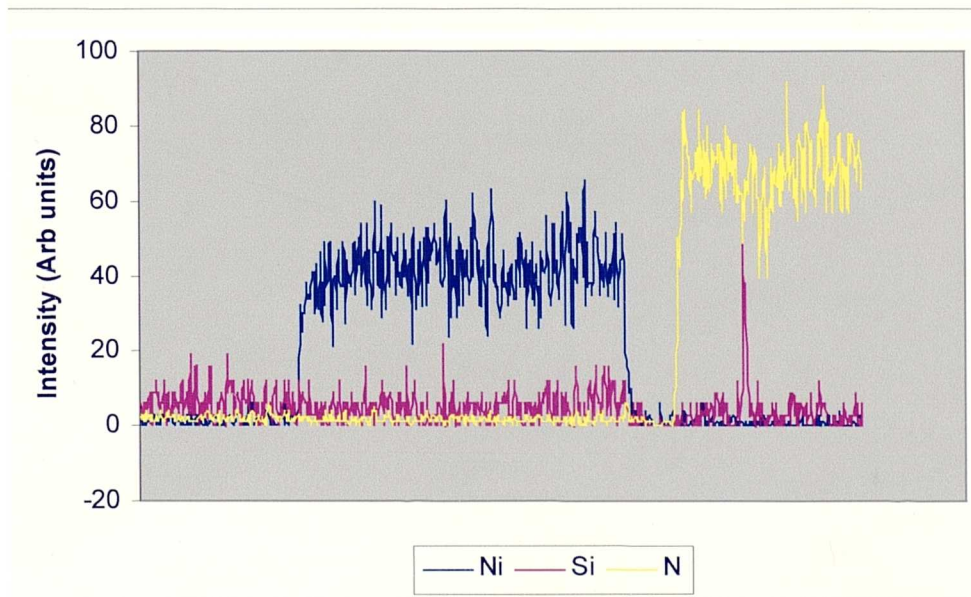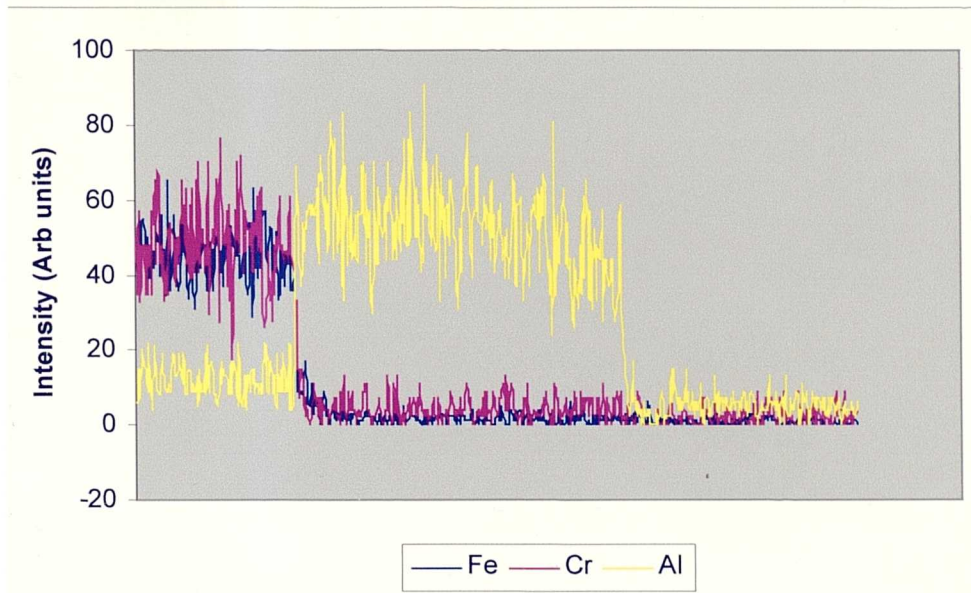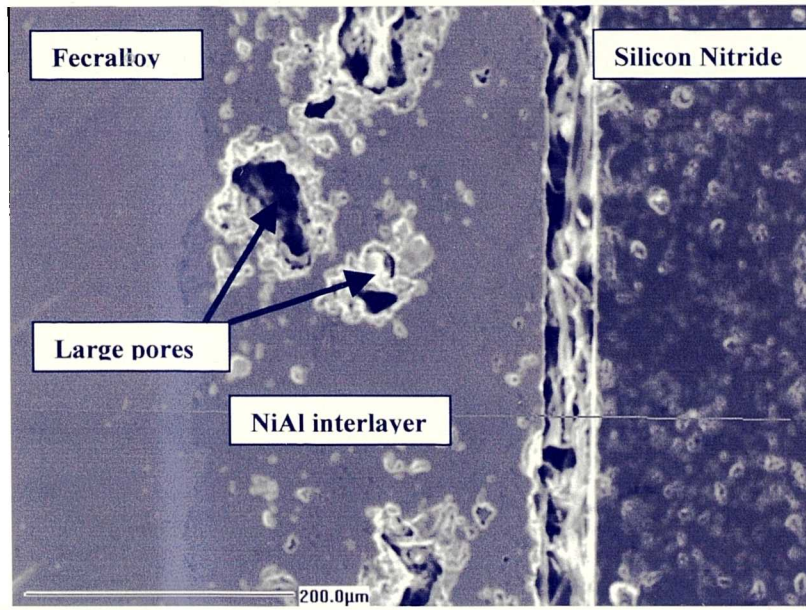
Figure 5.5   Micrograph & EDX line scan of failed Fecralloy-silicon nitride joint (800°C, 15 minutes, 45 MPa).
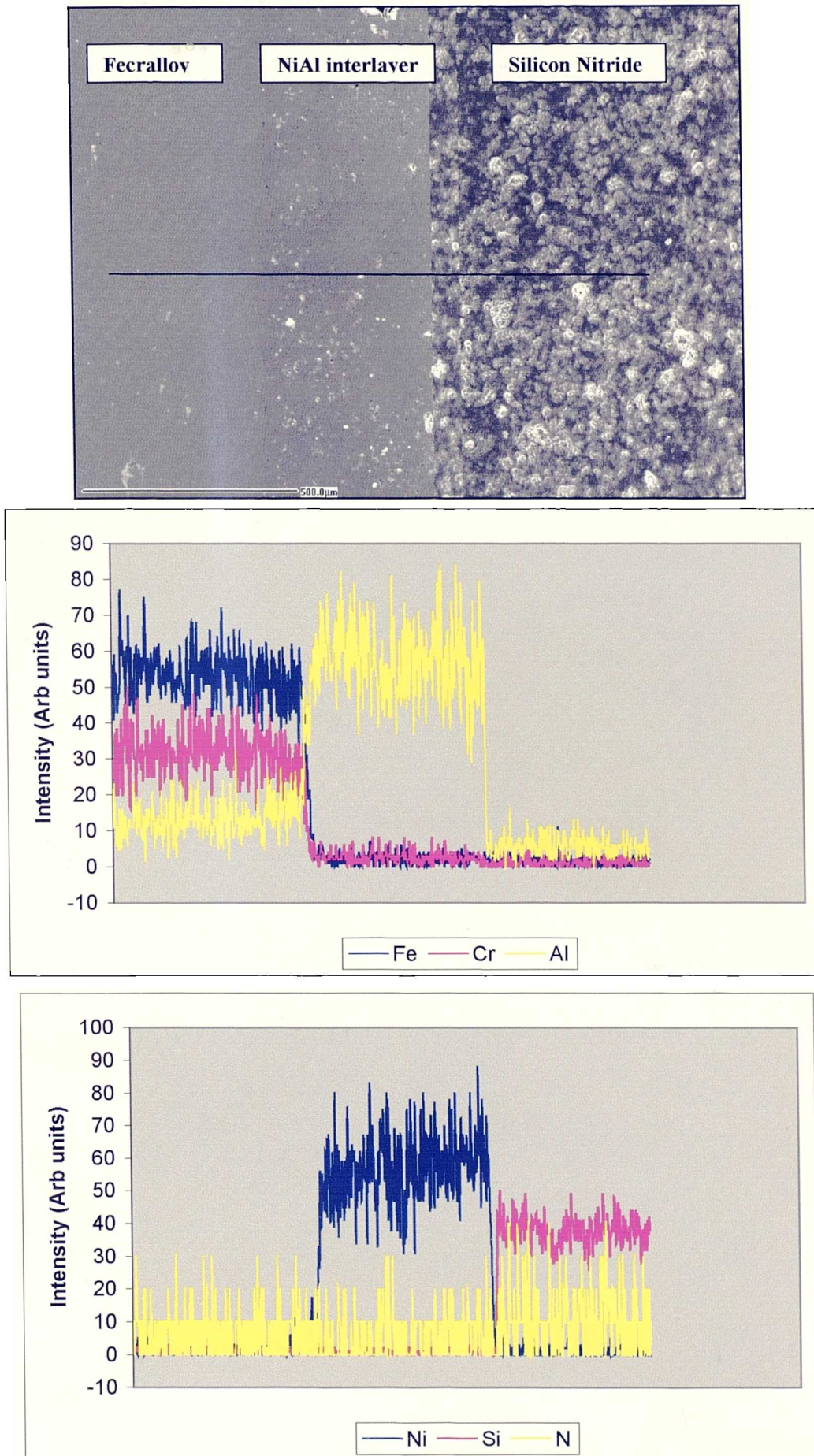
Figure 5.6   Micrograph & EDX line scan for Fecralloy-silicon nitride joint (900°C, 15 minutes, 45 MPa).
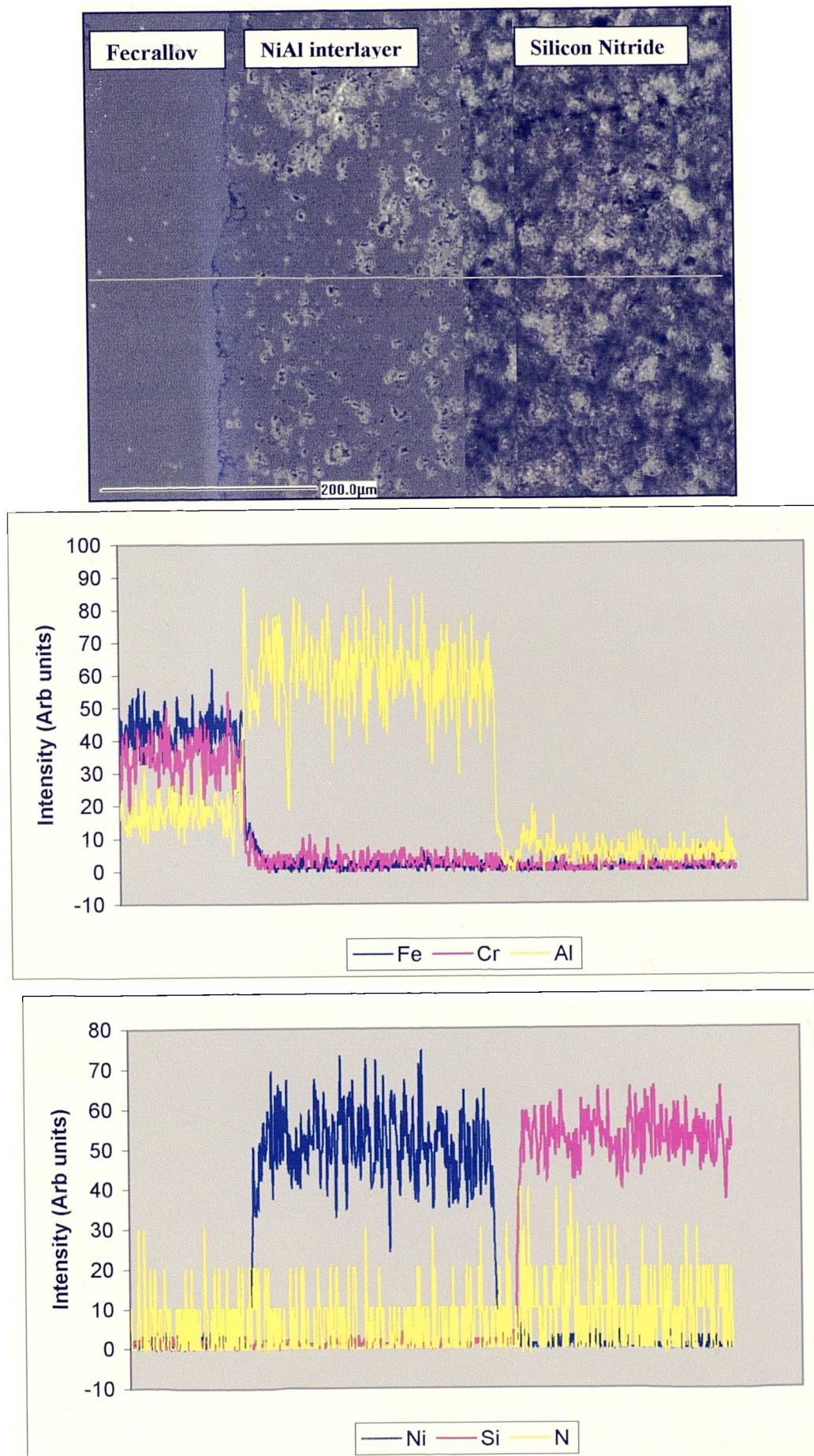
Figure 5.7 **Micrograph &EDX line scan for Fecralloy-silicon nitride joint (900°C, 15 minutes, 30 MPa).**
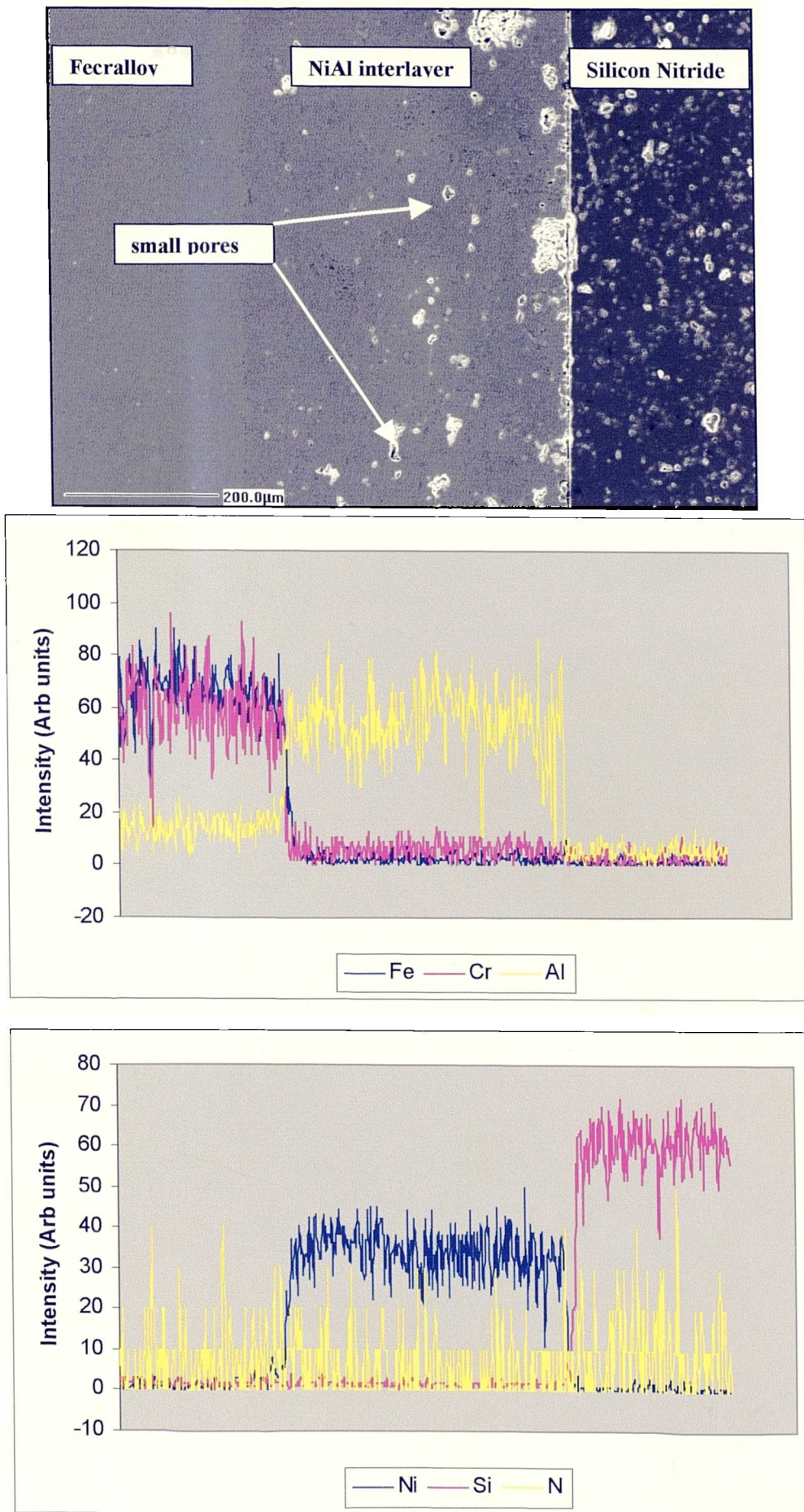
Figure 5.8   Micrograph & EDX line scan for Fecralloy-silicon nitride joint (900°C, 5 minutes, 45 MPa).
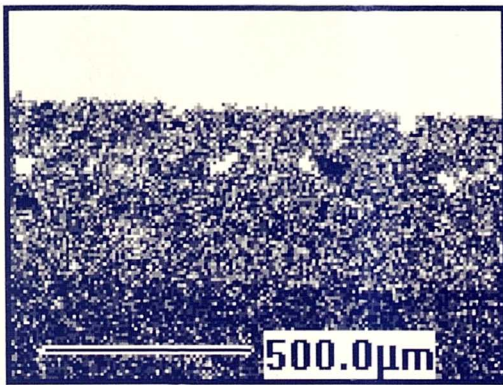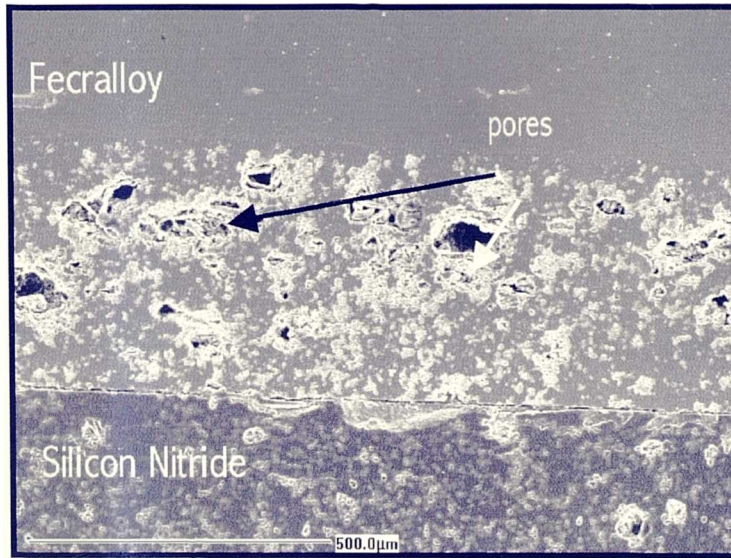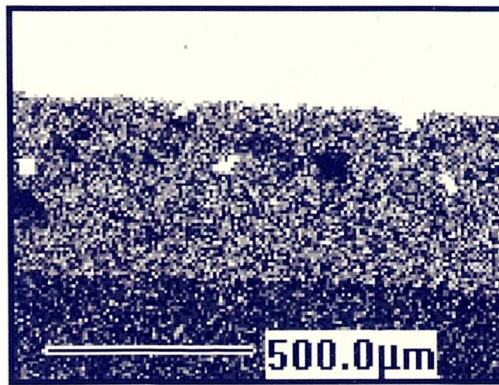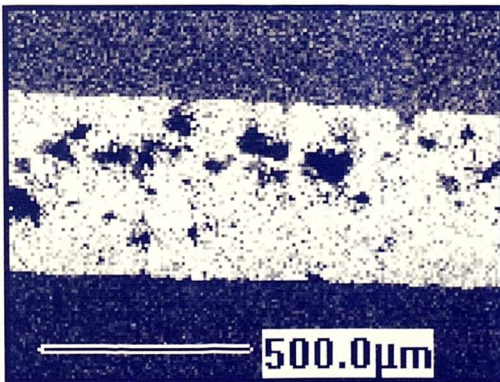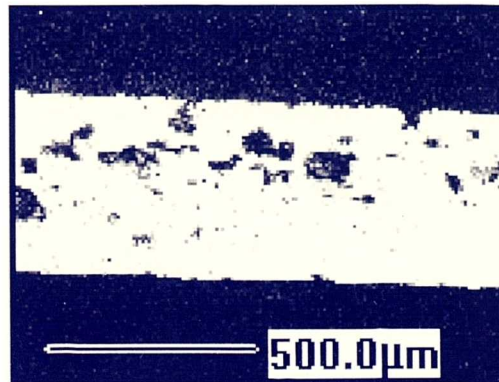
Figure 5.9   EDX elemental map of Fecralloy-silicon nitride joint (900°C, 15 minutes, 30 MPa)
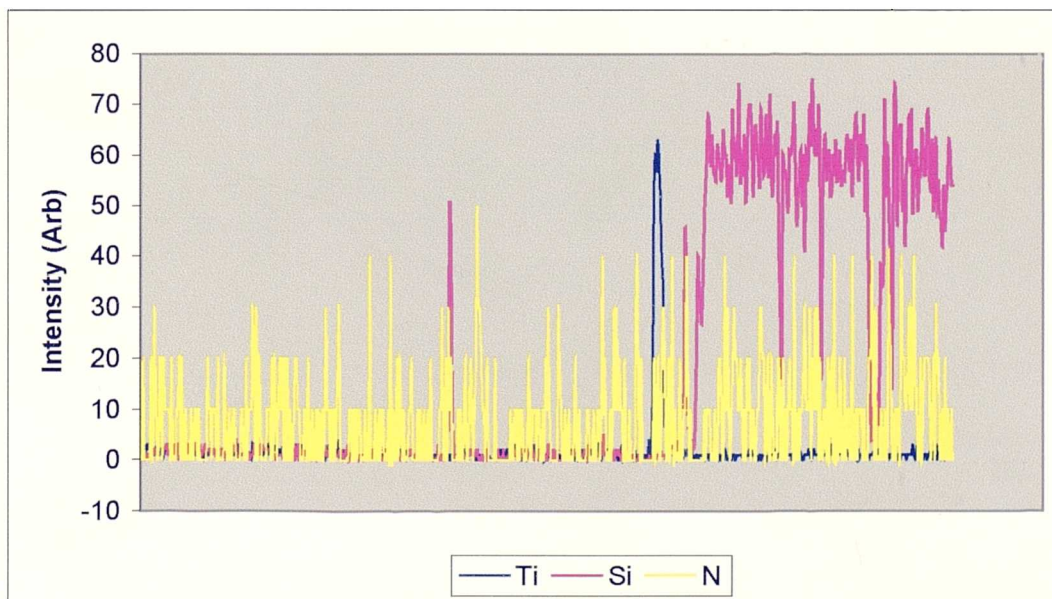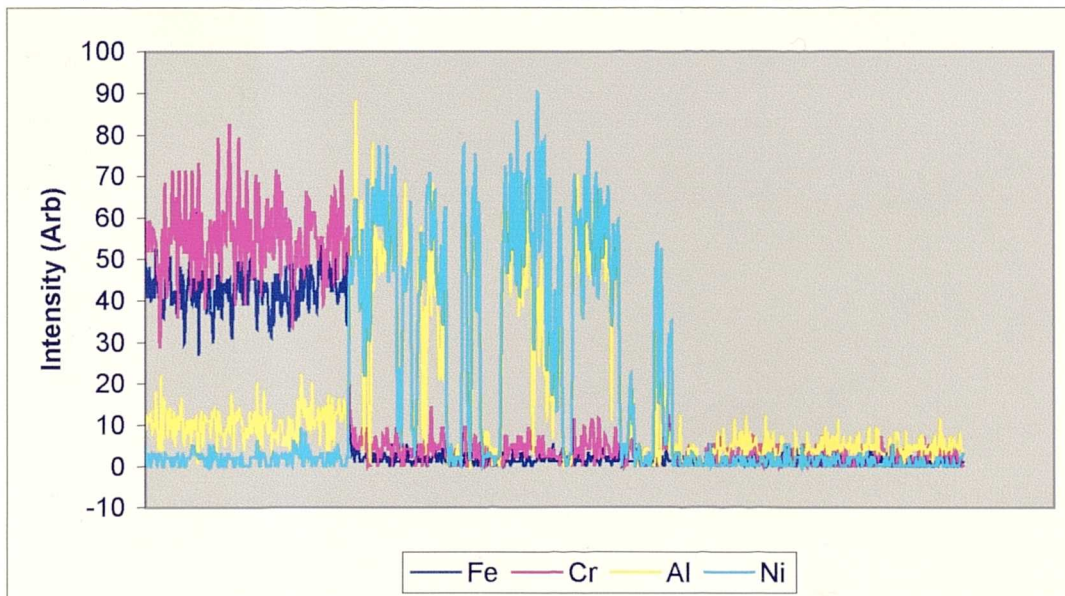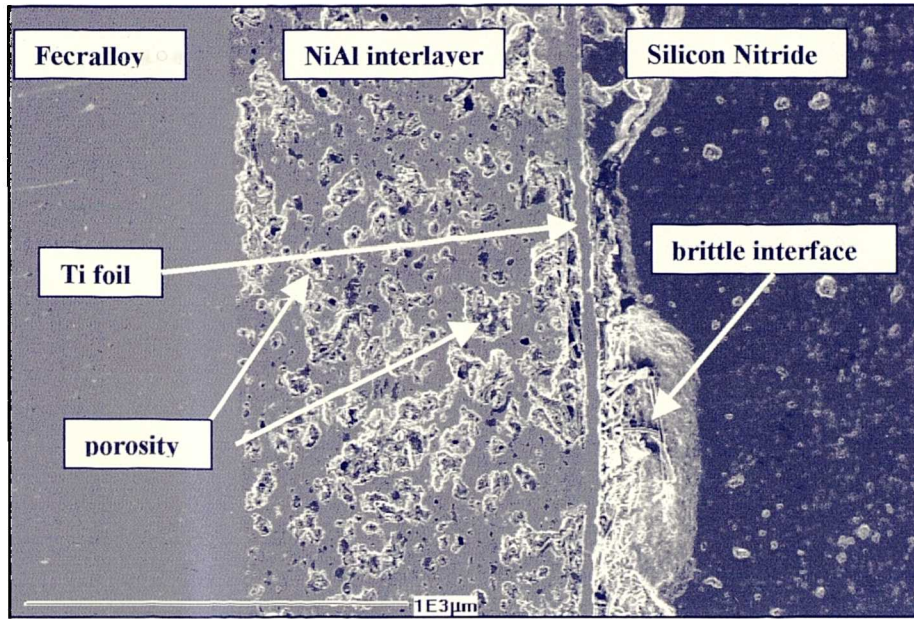
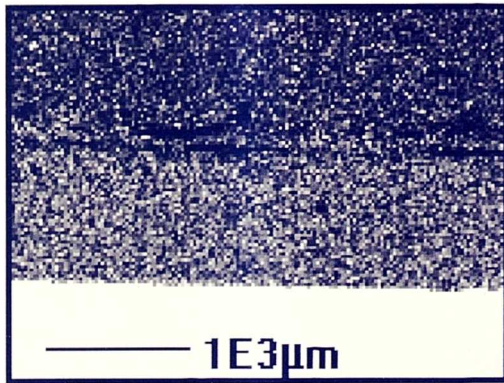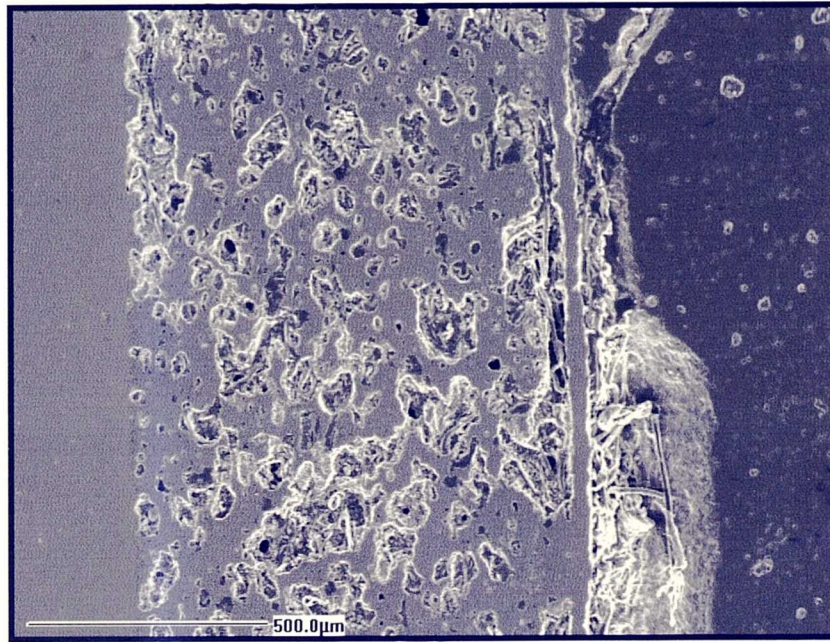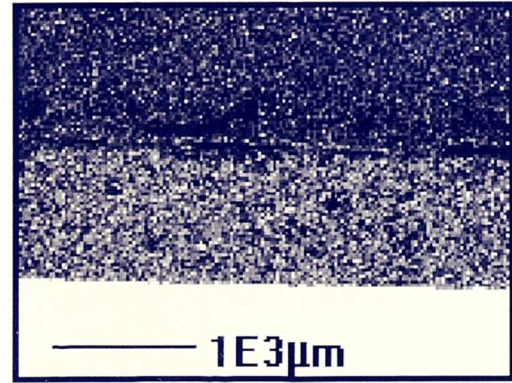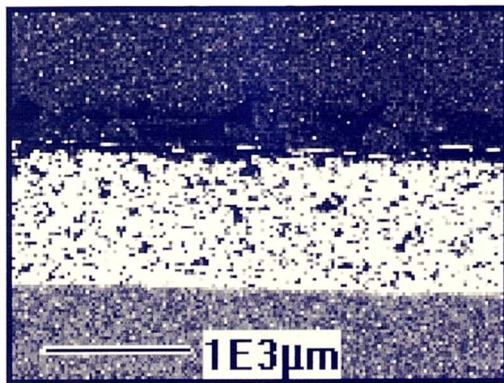**Figure 5.10**   **Micrograph & EDX linescan of a failed Fecralloy-silicon nitride joint with a Ti foil insert (900°C, 15 minutes, 45 Mpa).**
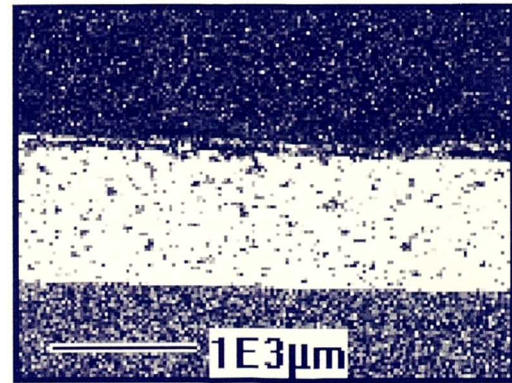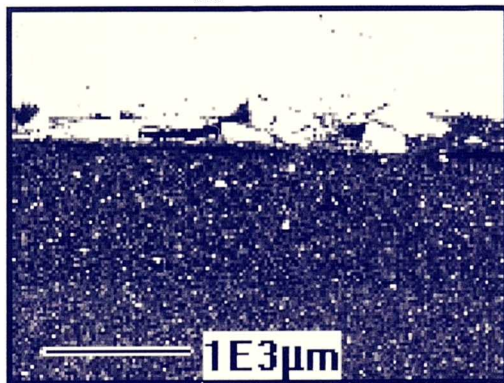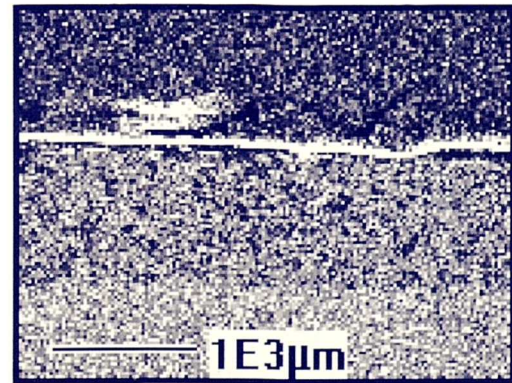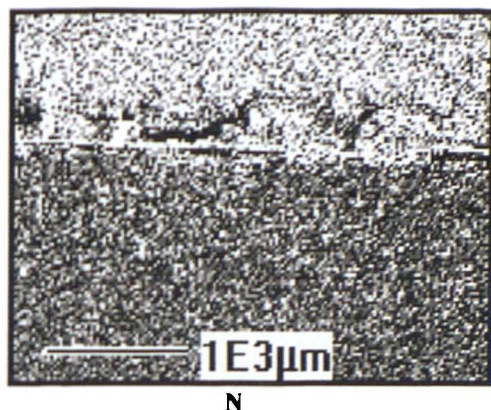
Fe

Cr

Al

Ni

Si

Ti

Figure 5.11 **EDX elemental map of Fecralloy-silicon nitride joint with Ti foil insert (900°C, 15 minutes, 45 MPa) showing presence of TiN reaction product layer.**

5.2.2 *Thermal Behaviour*

5.2.2.1 *Effect of Heating Rate*

Using the Perkin-Elmer 7 DTA, the effects of heating rate between 5-20 K/minute were investigated on the 1.1 molar Ni-Al as-compacted powder. Fig 5.12 shows the DTA plots.

The ignition temperature, T_{ig}, is the temperature at which the exothermic reaction is initiated, while the peak maximum temperature, T_p, corresponds to the temperature at which the rate of transformation of the viscous liquid into a crystal becomes a maximum. The combustion temperature, T_c, is the maximum temperature reached during the exothermic reaction and only lasts for a short period of time, usually a few seconds

In all the DTA plots a large exotherm is evident at approximately 500-600°C demonstrating the onset of reactive synthesis. The first eutectic temperature in the Ni-Al binary system is at 640°C and Al melts at 660°C and so our results show that exothermic peaks prior to liquid formation. The reactions are initiated in the solid state (solid-solid) and are followed by solid-liquid interactions. The NiAl formation can be divided into several steps, the first of which is solid-state inter-diffusion that causes the formation of $NiAl_3$ and Ni_2Al_3 at 520°C. In all samples heated up to the T_{ig}, small amounts of $NiAl_3$ and Ni_2Al_3 were detected, but the major XRD peaks were of Ni and Al.

These reactions are exothermic which subsequently heat the compact to the eutectic temperature of 640-660°C triggering further reactions and melting of Al. The liquid consumes the elemental powders and inter-diffusion of Ni and Al is rapid in the liquid phase and the compound generates sufficient heat that further assists the reaction. Under ideal conditions the liquid becomes self-propagating through the compact and lasts for a few seconds. The solid-solid reactions liberate heat and the heat release rate is kinetically controlled. The liquid can be termed as transient as the process occurs below the melting temperature of the NiAl. The liquid provides a capillary force on the interlayer that leads to eventual densification. Due to the rapid spreading and reaction of the liquid, pore formation is common.

In the reaction synthesis of NiAl using a low heating rate, numerous papers have characterised the behaviour in to several steps [123]. The solid–solid reactions lead to the formation of a dense layer of $NiAl_3$ and Ni_2Al_3. These prevent the reaction from further proceeding and so the system cannot produce enough heat to reach the eutectic temperature. Once the furnace reaches the eutectic temperature of 640°C the eutectic liquid forms and spreads allowing more Ni and Al to react. With increased furnace temperature the $NiAl_3$ and Ni_2Al_3 phases react with the remaining Ni and Al forming NiAl. From all of this it is clear that the synthesis of NiAl is very sensitive to numerous factors, the most important of which are the heating rate and particle size. It was therefore deemed important for us to characterize our as-compacted Ni-Al mixture in order to produce a dense NiAl interlayer and successful metal–ceramic joining.

As to the influence of heating rate, our results show that the T_{ig} increases with heating rate, as shown in the graph of Fig 5.13. This demonstrates that the reaction mechanism results from a competition between thermal effects (heating rate) and kinetic effects (activation energy). At lower heating rates the solid-solid diffusion process prevails with the formation of Ni_2Al_3 and $NiAl_3$ products. These can act as a physical barrier to liquid spreading and the heat generation rate will be small compared to the heat loss rate, the reaction will stop at this intermediate stage. Higher heating rates kinetically disallows the formation of $NiAl_3$ and the heat generation rate is larger than the heat loss rate, so enough liquid phase is produced for the reaction to proceed with the formation of monophase and homogenous NiAl.

XRD was used to characterise and analyse the reaction product after all the DTA heating rate trials. In all cases monophase NiAl was formed in the same quantity. This is surprising as the ΔT value (from y-axis DTA plots) is found to increase with heating rate. Therefore, the

difference in ΔT must relate to the extent of formation of the product through liquid-phase reactions. For the samples heated at a lower rate significant amounts of the product form through solid-state reactions. When this occurs the amount of free Al is decreased which leads to a lower exothermicity of the liquid phase reaction and hence a lower ΔT, as observed experimentally. With higher heating rates the opposite is true where most of the product is formed through liquid-phase reactions giving rise to a higher ΔT. The ΔT value is a function of composition, heating rate and particle size.

The interlayer formed using a lower heating rate (5 K/minute) and a higher heating rate (30 K/minute) all attempting to join Fecralloy with silicon nitride (900°C, 15 minutes, 45 MPa) are shown in Fig 5.14 and Fig 5.15. The higher heating rate results in the formation of monophase NiAl, which is confirmed by the accompanying XRD plot (Fig 5.14) and this is metallic in look and contains large pores. The lower heating rate produces an interlayer that is very porous and powder like in nature (Fig 5.15). The accompanying XRD plot confirms the presence of unreacted Ni, in addition to NiAl. An increase in heating rate increases the reactivity of the liquid. In terms of reaction kinetics, increased heating rate increases the activation energy and accelerate the self-propagating reaction. However, too high a heating rate leads to a loss of process control and one of the results is the formation of large pores as was demonstrated. An intermediate heating rate of 15 K/minute was chosen as the optimum and resulted in good joining with limited interlayer porosity, as shown in Fig 5.6.

While DTA results accurately characterised the behaviour of the Ni-Al as-compacted powder joining trials using varied heating rates had to be carried out. This is because additional factors such as applied pressure (discussed in section 5.4.4), heat loss and processing conditions all have an effect upon the reaction bonding process., which the DTA trials cannot take account of this. This was found to be the case with a heating rate of 5 K/minute. The DTA results deemed this heating rate as sufficient to produce NiAl by a self-propagating mode. However, under joining conditions the self-propagating mode did not prevail but rather solid-solid reactions, as was described previously. This is believed to be due to greater heat loss experienced under joining conditions that prevented the self-propagating mode to occur.

It has been shown that heating rate is an important parameter for the reaction synthesis of NiAl by the self-propagating mode in order to produce sound Fecralloy-silicon nitride joints.
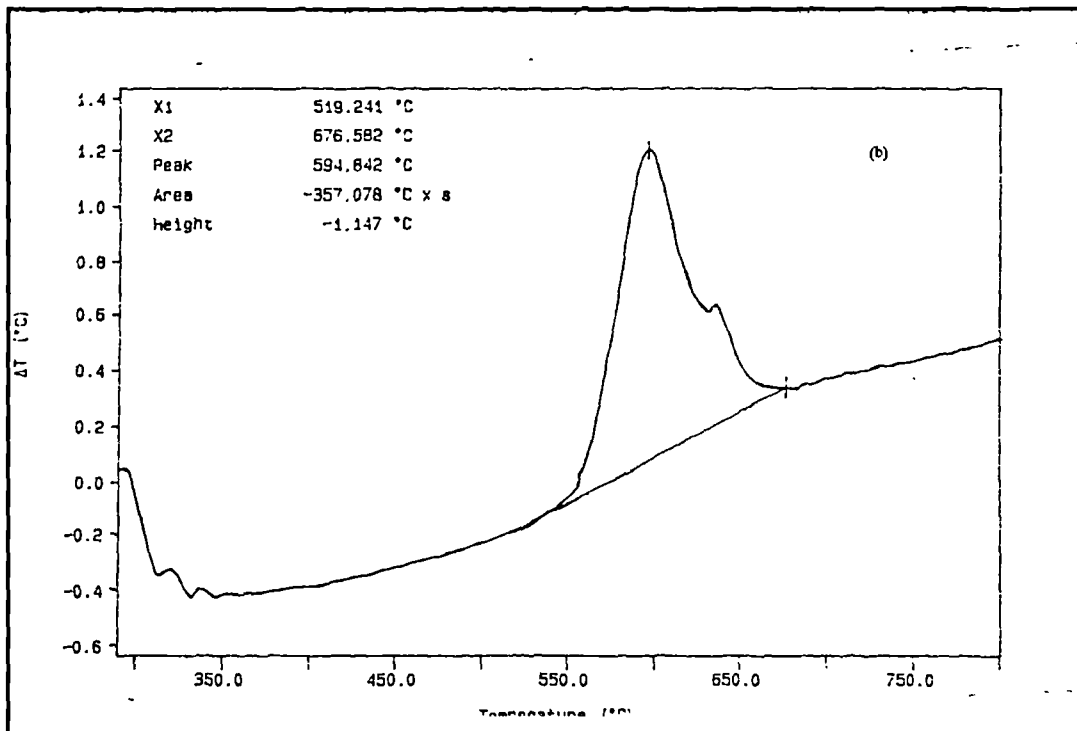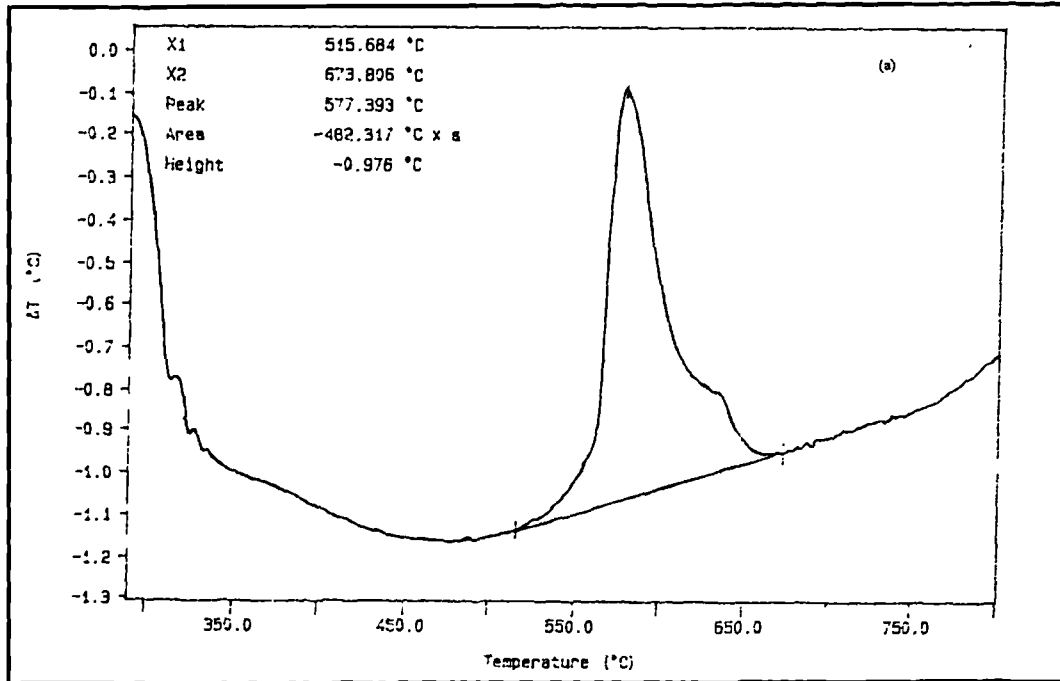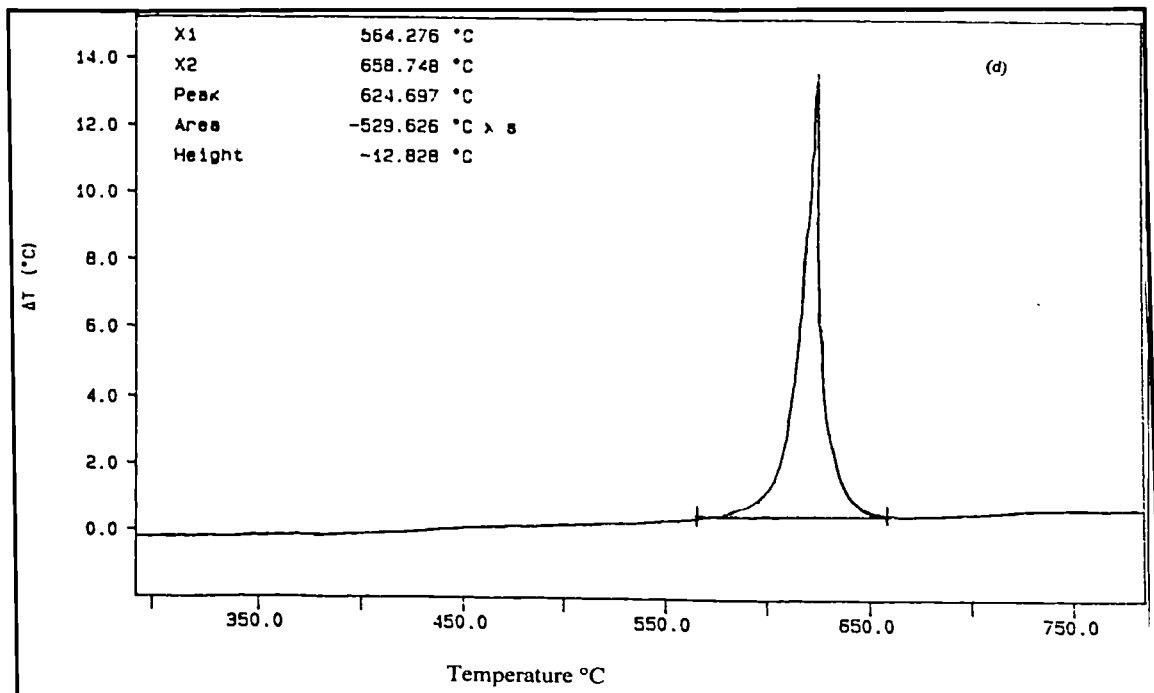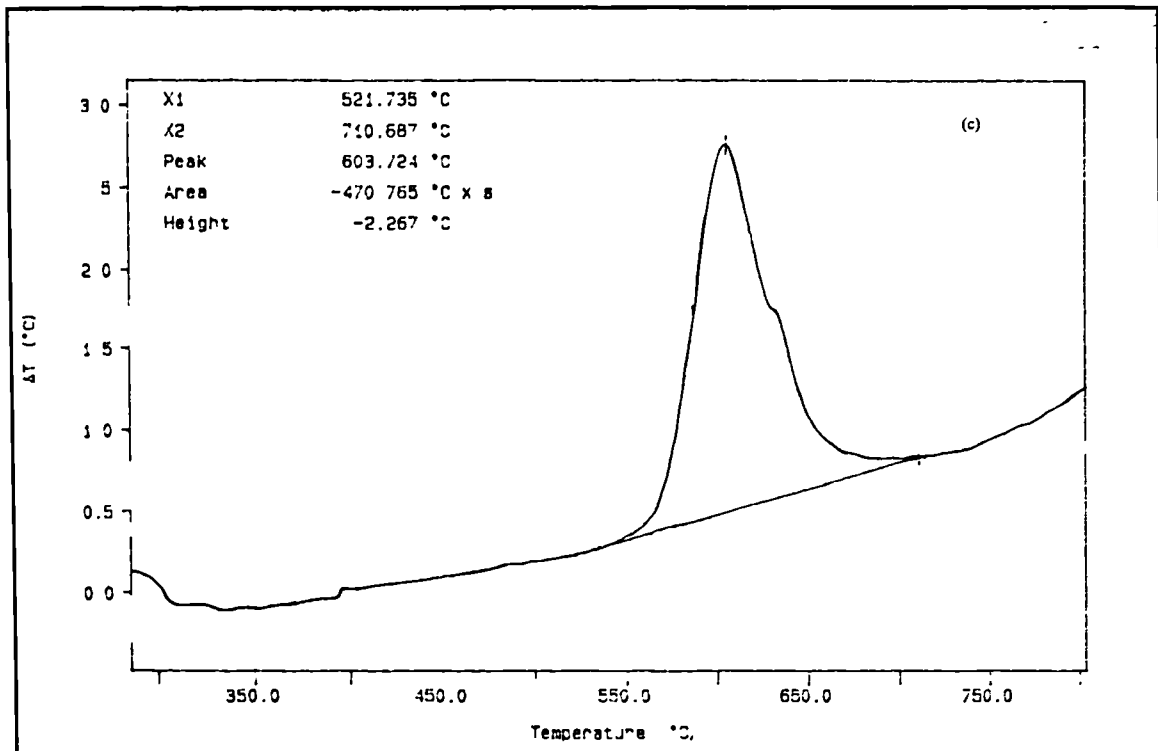
Figure 5.12   DTA plots of Ni-Al (molar 1:1) at heating rates (a) 5 K/minutes (b) 10 K/minute (c) 15 K/minute (d) 20 K/minute

103
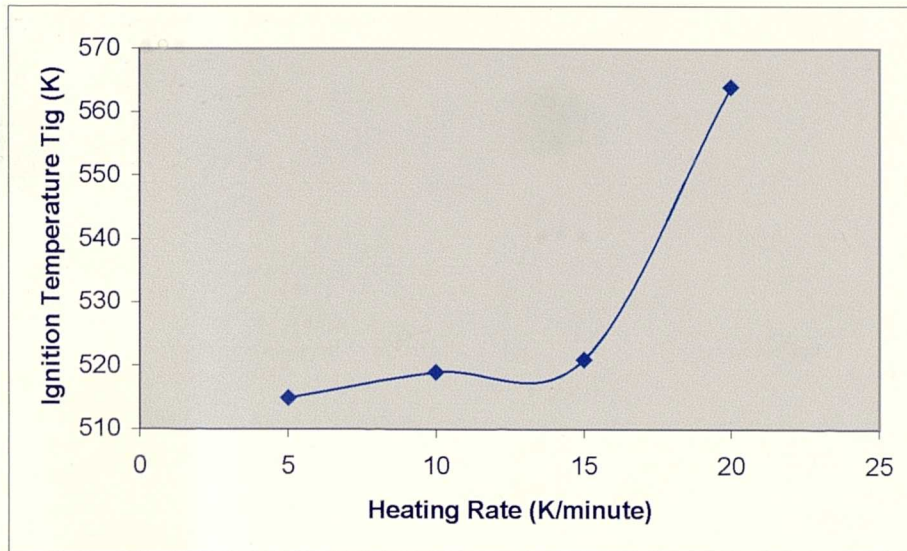
Figure 5.13   Graph showing variation of Ignition temperature, T_{ig}, with heating rate.
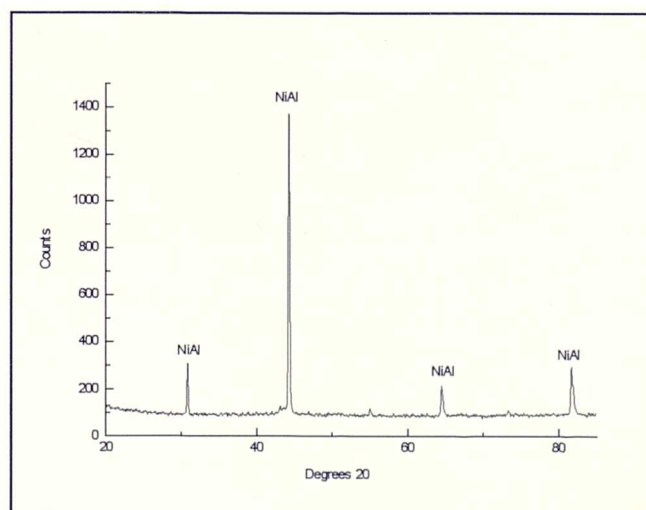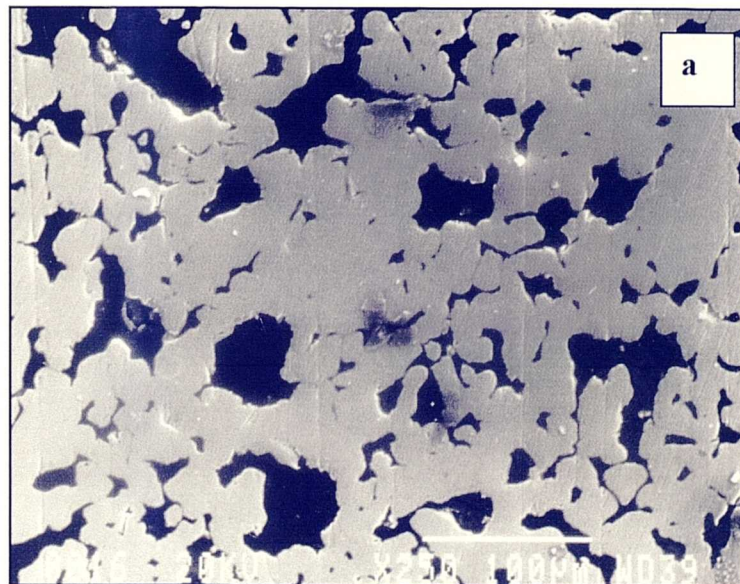
Figure 5.14   Micrograph showing the interlayer formed at a heating rate of 30 K/minute. XRD plot confirms that monophase NiAl is formed.

104
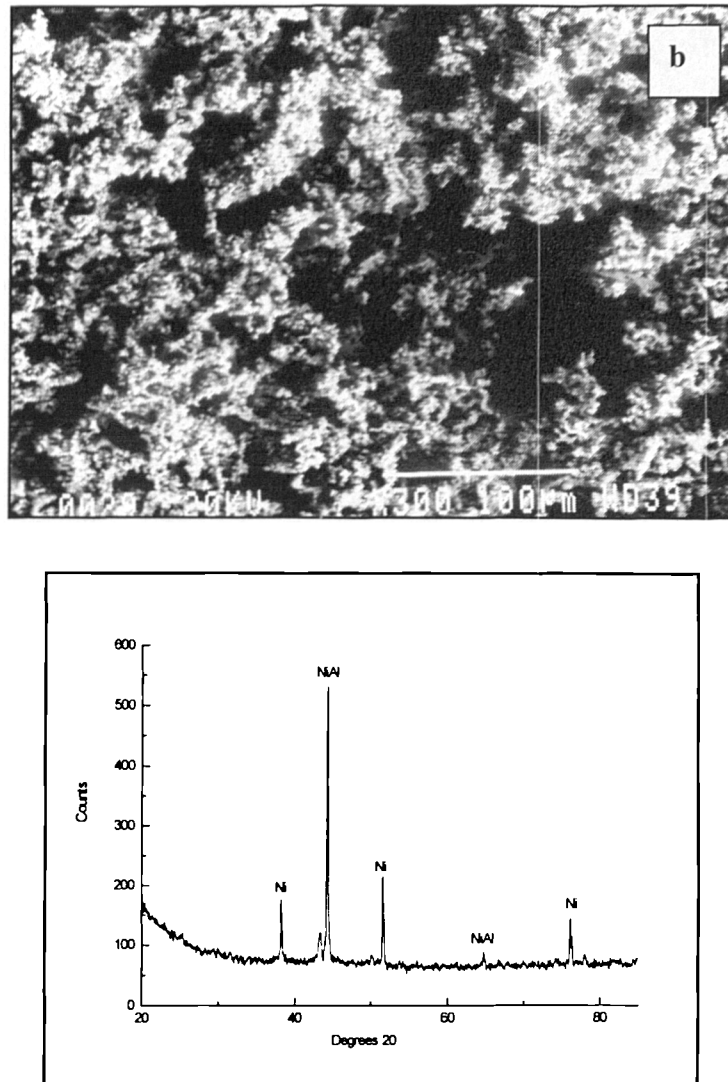
Figure 5.15   Micrograph showing the interlayer formed at a heating rate of 5 K/minute. XRD plot confirms that unreacted Ni particles remain.

5.2.2.2   *Effect of Particle Size*

The Ni and Al powder that was used had a small particle size and this was to help the intermixing and to achieve good particle–particle contact after cold pressing. Work by Philpot *et al.* [124] conclusively showed that Ni particle size had a profound effect on the reaction synthesis of $NiAl_3$ from its constituents. It was therefore important to investigate the effects of increased Ni particle size on the reaction synthesis using DTA and also joining trials.

Fig 5.16 shows the DTA plots, where Ni particles with an average diameter of 50μm were used. The T_{ig} is found to occur at a higher temperature, compared to those where smaller Ni particles are used, as shown in the graph of Fig 5.17. Fig 5.18 shows the interlayer from a

failed joining trial using larger Ni particles in the compact (900°C, 15 minutes, 45 MPa). The interlayer is porous and agglomerated, indicating that the self-propagating mode did not occur and no liquid phase densification. Unreacted Ni particles are present in addition to multi-phase nickel aluminides that are indistinguishable.

For the reaction to proceed with densification, the transient liquid has to propagate through the structure. It is important that the Al is interconnected through the interlayer, as porosity will arise in areas where there is no liquid phase at temperature. This interconnection ensures uniform long-range capillary action on the liquid phase through the interlayer compact and promotes uniform densification. Interconnectivity is influenced by many factors such as the stoichiometry and reactant particles size ratio.

Lebrat *et al.* [125] found that if the correct particle size ratio was not chosen, this was likely to lead to an incomplete reaction. Increased particle size leads to a decrease on the capillary force and the T_c is reduced. The effect of Ni particle size can be explained in terms of available reacting surface area. A smaller particle size has a higher surface area in contact with the Al and this facilitates the reaction synthesis process. Smaller particle size also results in shorter diffusion distance with a faster reaction rate.

However, too fine particle size is also detrimental to the interlayer as it results in rapid consumption of the liquid and poor densification. This was found to be the case by Dong *et al.* [126] who looked into the use of Ni and Al nanoparticles for the reaction synthesis fabrication of NiAl. Apart from poor microstructural and mechanical properties of the fabricated NiAl, nanoparticle powders are expensive making processing uneconomical.

Our results highlight the importance of reactant particle size ratio. Increased Ni particle size was detrimental to the synthesis of the NiAl interlayer and did not result in joining. Due to the reasons mentioned above, the self-propagating reaction synthesis mode did not occur, rather localized solid-state reactions that result in a porous and weak multi-phase interlayer. It is therefore important to determine and use the correct particle size in order to optimise the self-propagating reaction synthesis.
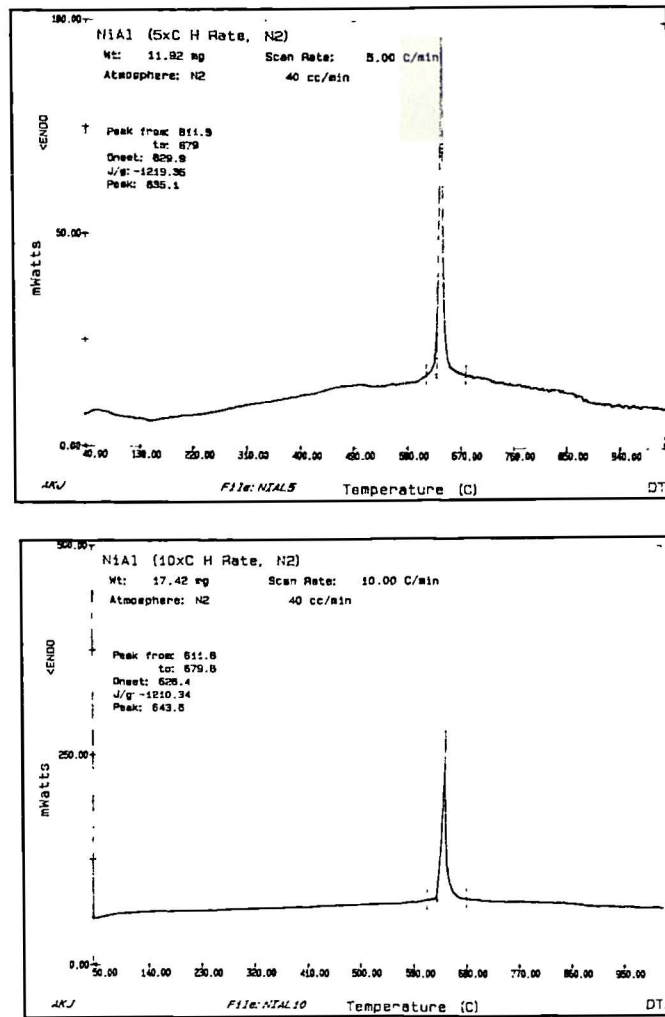
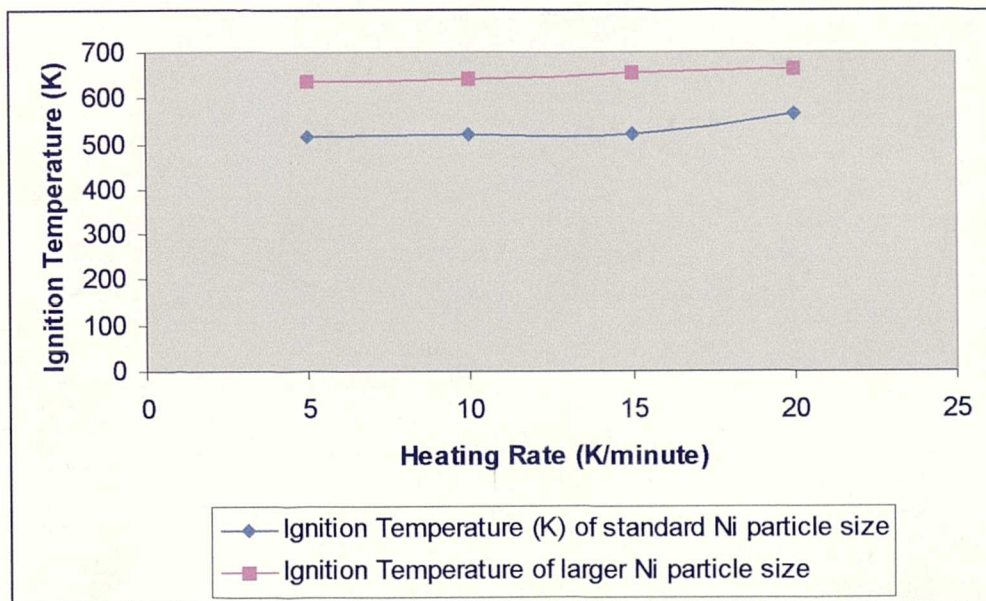**Figure 5.16**   DTA plots of Ni-Al compacted powder with larger Ni particle size.

Figure 5.17   Graph showing effect of Ni particle size on heating rate.
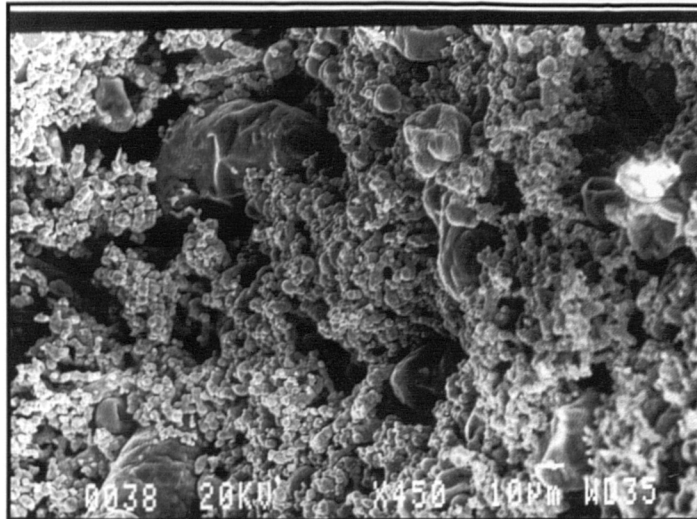
Figure 5.18   **Micrograph showing interlayer of failed Fecralloy-silicon nitride joint using larger Ni particles (900°C, 15 minutes, 45 Mpa).**

5.2.2.3   *Determination of Reaction Kinetics*

A number of models have been put forth over the years, all attempting to describe and quantify the kinetics of reactive synthesis of NiAl from its constituents.

In 1957 Kissinger [127] used DTA data to calculate the activation energy of the process. More recently Atzom [128] suggested an approach to predict the T_{ig} for the formation of Ni_3Al. He calculated the evolution of temperature during slow uniform heating taking into account heat generation due to the formation of $NiAl_3$, the presence of diffusion barriers at the Ni and Al interfaces and heat exchange between the sample and the environment. This approach obtained good agreement between the model and experimental results.

Recent work by Farber *et al.* [129] extended Atzmons approach to describe the kinetics of synthesis of NiAl intemetallics from fine elemental powders. In this rather confusing study a model is presented based on spherical geometry and takes into account the presence of oxides at the Ni and Al particle surface and heat exchange between the sample and environment. The focus was on the solid-solid reactions up to the T_{ig}, where a $NiAl_3$ reaction product formed around a Ni particle later followed by an additional Ni_2Al_3 layer.

The reaction constant M was described by an equation of Arhenius type.

$$M = M_0 \exp\left(-\frac{E}{RT}\right)$$ **Equation 5.1**

108

Where

E = Activation energy

R   Gas constant

T = Temperature

M_0 Pre-exponential factor.

It was suggested that the pre-exponential factor, Mo, could not be determined experimentally and will be a variable in the treatment. The value inversely proportional to the M_0, $1/M_0$. was regarded as the barrier thickness.

Theoretically derived DTA plots were compared with experimental ones, and good agreement was found. Without any surface barriers, it was theoretically shown that two DTA exothermic peaks would occur at 350°C and 440°C, corresponding to the formation of $NiAl_3$ and Ni_2Al_3. The introduction of a barrier was theoretically shown to increase the start and finish formation temperature of $NiAl_3$. When Ni_2Al_3 starts to form its growth rate and heat generation rate were higher.

The theoretical plot where a strong barrier was presumed that the powder particle interface was almost identical to the experimentally derived plot, suggesting the presence of such barriers.

The activation energy was calculated to be 116 kJ mol.

Recent work by Biswas *et al.* [130] looked in to the reactive synthesis of NiAl and proposed a two-stage model. The first stage was similar to that of Farber *et al.* [129]. where the solid state interaction up to T_{ig} was considered. The second stage considered the reaction sequence that leads to the formation of densified NiAl.

With regards to the first stage, Atzmon studied the effects of interfacial diffusion barriers on the T_{ig} using computed temperature profiles. Modifying this approach, Biswas *et al* [130] calculated the thickness of $NiAl_3$ at different time and temperatures using experimentally derived time-temperature profiles up to 640°C. It was found that thickness of the $NiAl_3$ layer increased at slower heating rates. Also, that beyond a certain heating rate the growth of the $NiAl_3$ layer reaches a maximum and is not affected by a further increase in heating rate.

The second stage was concerned with the formation of a liquid phase and the densification of NiAl. From the DTA results it was assumed that as soon as the temperature reached 640°C, the

Al-rich eutectic melts and engulfs the Ni particles and an intermediate complex layer of a composition of NiAl forms around it. Increased temperature causes further diffusion until monophase NiAl is formed. The activation energy, E, was experimentally determined to be 170 kJ/mol.

The difference in the DTA plot of Biswas *et al.* [130] and the plots obtained in our work can be explained by different reaction mechanisms. In all our DTA trials the powder was compacted ensuring good particle-particle contact. This was not carried out by Biswas *et al.* [130] and so different reaction mechanisms occurred.

These models are based on results with particular parameters, in that small particle size, no compaction, etc were used. So these models are valid for those conditions and cannot be assumed/applied for trials that have different parameters. Therefore a need was identified to determine the kinetic parameters from our results, the most important of which is the activation energy. A different approach and model is put forth and the validity determined using our DTA results.

Bansal and Doremus [131] put forth a kinetic model for evaluating the kinetic parameters from non-isothermal DSC/DTA data. This model is an extension of the Johnsan-Mehl-Avremi (JMA) kinetic model for non-isothermal conditions. Apart from determining the kinetic parameters, it was proposed that the Bansal-Doremus equation could be used to calculate the T_p. The Bansal-Doremus kinetic model is expressed in logarithmic form as;

$$\ln\left(\frac{T_p^2}{\alpha}\right) = \ln\left(\frac{E}{R}\right) - \ln \nu + \frac{E}{R.T_p} \qquad \textbf{Equation 5.2}$$

Where

T_P = Peak maximum temperature

α = Heating rate

E = Activation energy

R = Gas constant

ν = Frequency factor

The kinetic parameters E and ν are related to the reaction rate constant, K, by an Arrhenius equation;

110

$$K = \nu \exp\left(-\frac{E}{RT}\right)$$

Equation 5.3

In isothermal conditions ν and E are usually not functions of time or degree of transformation. Over a narrow range of temperature ν and E can be constant but over wider ranges of temperature, transformations can depend on nucleation and growth rates that have complicated temperature dependencies. If we consider nucleation and growth rate, for instance, they often have maxima as a function of temperature and do not fit Equation 5.2. Bansal-Doremus assumed ν and E to be independent of temperature, which should be valid for transformations with a constant number of nuclei and a growth rate with ν and E constant.

A Plot of $\ln\left(\dfrac{T_P{}^2}{\alpha}\right)$ versus $\left(\dfrac{10^3}{T_P}\right)$ obtained at various heating rates should be linear with slope $\dfrac{E}{R}$ and intercept $\left[\ln\left(\dfrac{E}{R}\right) - \ln\nu\right]$. If $\dfrac{E}{R}$ is calculated from the slope, the frequency factor ν can be calculated from the intercept.

In the derivation of Equation 5.2, many assumptions were made, the most important of which is that the rate of reaction is maximum at T_p.

Experimentally derived Bansal-Doremus plots using the optimum and increased Ni particle size are shown in Fig 5.19. The activation energy was 103 kJ/mol and 170 kJ mol for the increased Ni particle size. These values are in agreement with those reported by other authors [128,130]. The good agreement of the results verifies the applicability of the Bansal-Doremus kinetic model. The model does not take into account of factors such as stoichiometry and particle size variations, as demonstrated. This suggests that the main features controlling the behaviour of the compacted powder were taken into account. Increased Ni particle size does not allow the reaction to proceed optimally due to reduced surface area and hence the higher activation energy. This demonstrates the sensitivity of the kinetic model. The value of 170 kJ mol is identical to that obtained by Biswas *et al.* [130] who also used considerably larger Ni particle size.
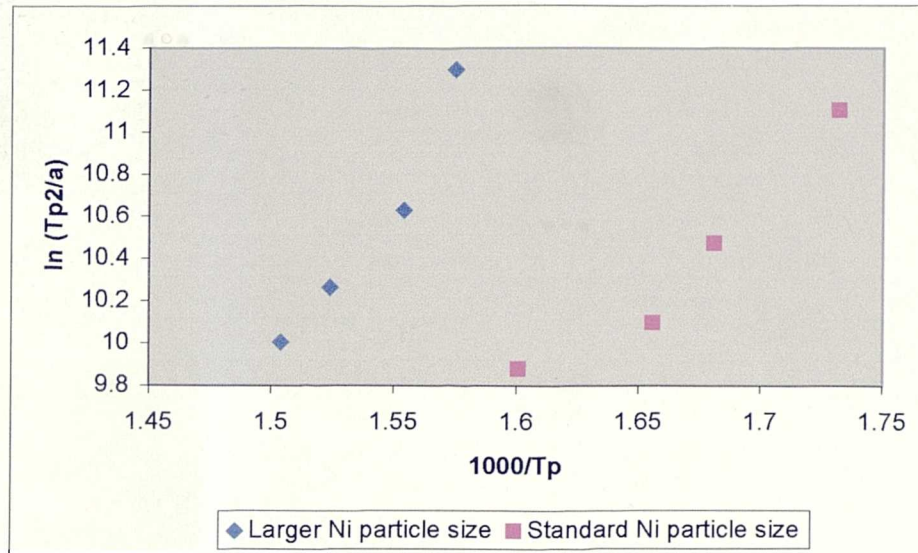
Figure 5.19 **Graph showing plot of $\ln(T_P^2/\alpha)$ versus $1000/T_P$ for optimum and increased Ni particle size**

5.2.2.4   TGA

TGA was carried out on the Ni-Al as-compacted powder in both air and nitrogen to see how the mass gain varied with temperature and to see if the results conferred those of the DTA. It was also used to demonstrate the oxidation resistant nature of the formed NiAl.

Due to the exothermic nature of the reaction where a great amount of heat is released, Pt pans were used in the TGA trials. An alumina pan would crack due to the large amount heat released.

Under both atmospheres there is substantial mass gain in the 500-680C temperature range, as shown in Fig 5.20. This confers the DTA results, where the reaction is initiated by solid-solid interactions at about 500°C and these then proceed by solid–liquid reactions where the NiAl product is formed at a relatively low temperature (about 700°C). While the reaction mechanism and reaction products are different due to different atmosphere, it is believed that the general trend is the same under vacuum like conditions. As was previously mentioned, the large amount of heat liberated at T_c is due to the exothermic reduction of NiO by liquid Al. Under non-vacuum conditions, where the partial pressure of O_2 is high, it is the exothermic oxidation of Al that causes the large amount of heat liberation at T_c.

Fig 5.21 confirms the oxygen resistant nature of the NiAl interlayer, where the NiAl shows negligible mass gain in air over a period of 100 hours at 850°C.
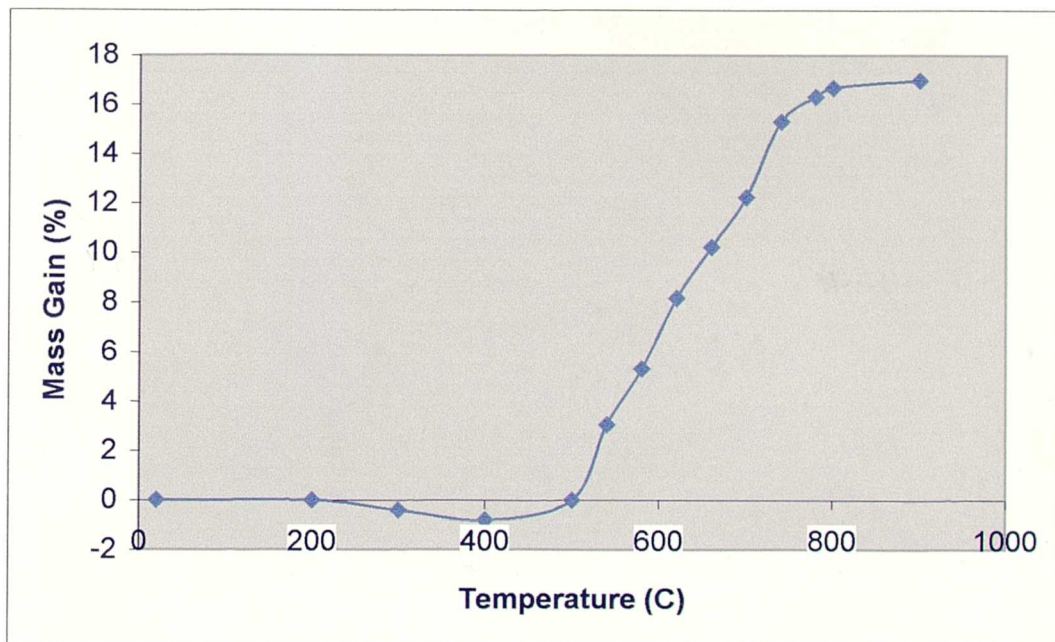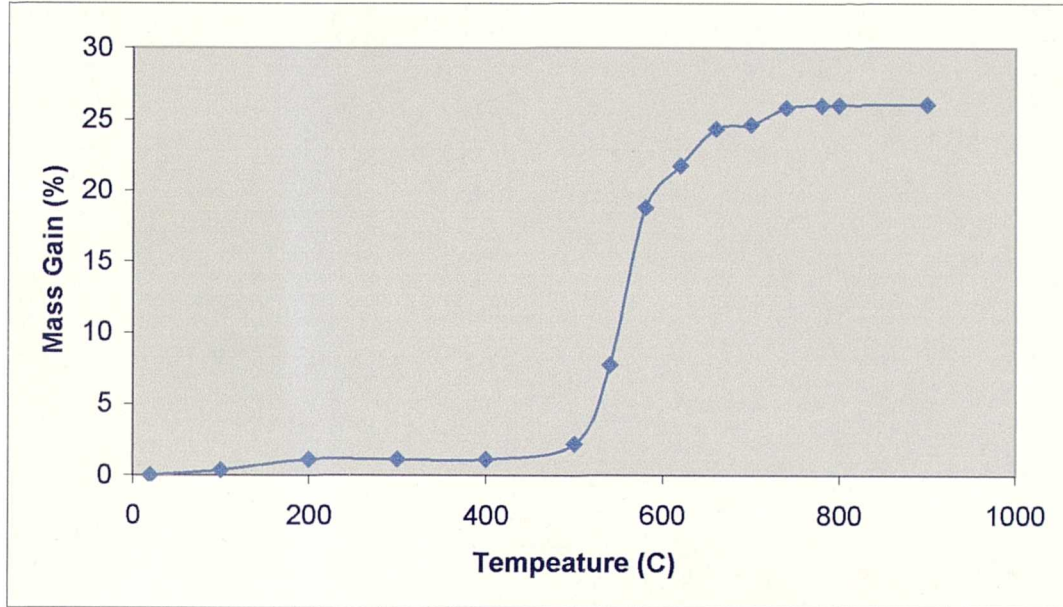
Figure 5.20   TGA plots for Ni-Al compacted powder at a heating rate of 10 K/minute in (a) air (b nitrogen
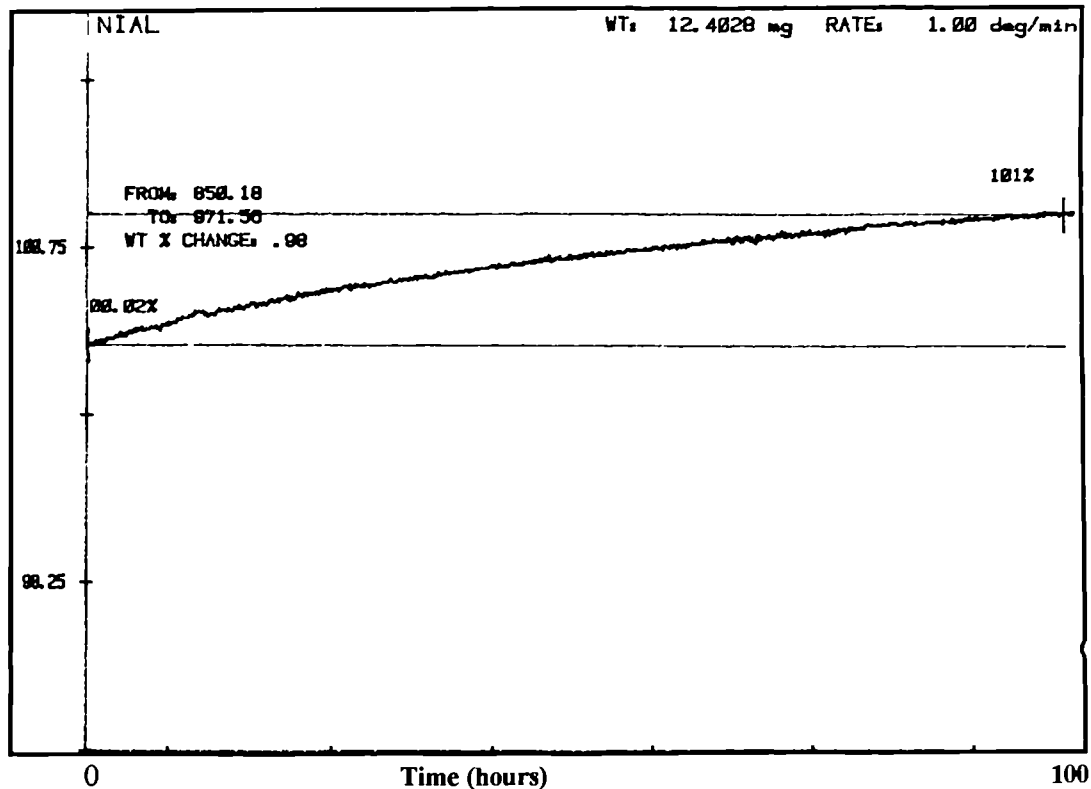
Figure 5.21 **TGA plot showing oxidation resistance of formed NiAl interlayer (neglible mass gain).**

5.3 Reaction Bonding Mechanism

In this section the most likely sequence of events that lead to successful joining with a dense and monophase NiAl interlayer are presented. This is schematically illustrated in Fig 5.22.

A pre-requisite is the dry mixing and high-pressure compaction of the Ni-Al powder into a compact that ensures good inter-particle mixing and contact. As shown in stage 1, a butt joint configuration is employed with a high uni-axial pressure (45 MPa) applied from room temperature. This provides intimate contact and aids the breaking of surface oxides at temperature.

With a moderate heating rate (15 K/minute) the configuration is heated under vacuum and at approximately 500°C the solid state reactions start to occur forming $NiAl_3$ and Ni_2Al_3, as shown in stage 2. This is mildly exothermic heating the interlayer to 640-660°C, where the Al becomes molten and it is this transient liquid that leads to densification of the interlayer.

114

It is the oxidation-reduction reaction of the NiO (on Ni particle surface) by the molten Al that is highly exothermic. The heat released from the reaction heats up the interlayer to the T_c and this can be calculated from the enthalpy of the reaction and the heat capacity of the product phases, with the assumption of adiabatic conditions. The exothermic reaction that occurs is given below (Equation 5.4) and Wang *et al.* [120] calculated the T_c to be 3250°C, higher that the melting temperature of all the phases present.

$$Al + 3/2\ NiO \Rightarrow 3/2\ Ni + 1/2\ Al_2O_3 \hspace{2cm} \textbf{Equation 5.4}$$
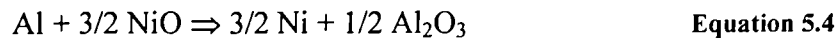
Plazanet and Nardou [84] experimentally determined the T_c of NiAl as 1680°C in argon and 1795°C in air. The discrepancy between a theoretically derived and experimentally measured T_c is possibly due to the theoretical derivation not taking account for the vaporization of the product phases. However, this work was carried out under different atmospheres and it is the exothermic oxidation of the molten Al that takes the temperature up to T_c. Although the large amount of heat released (T_c) is by different mechanisms, the main point is that a high temperature is reached (T_c).

Munir [133] found that as a general rule for a reaction to self propagate under ideal conditions, the T_c should exceed 1700°C. While the exact figure may be disputed and a more realistic figure of 1400-1500°C would be appropriate, a high temperature is reached. The T_c provides not only a quantitative measure of the exothermicity of the reaction but also a quick means to determine whether the reaction will self propagate.

It is the high T_c that causes partial melting of the Fecralloy interface and aids the wetting/dissolution of the silicon nitride interface by the liquid Al, as shown in stage 3. Small amounts of Fe infiltrate the interlayer, while the dissolution of the silicon nitride interface caused by the reactive wetting of molten Al causes Si and N to diffuse into the interlayer and Al to infiltrate the silicon nitride. Good interfacial bonding is attained with no interfacial reaction products and mechanical interlocking forces hold the joint together. The introduction of mainly Fe into the interlayer improves the yield strength, fracture toughness and most importantly the room temperature ductility that reduces the residual stress, in addition to lower processing temperatures and times, as reported by Miracle *et al.* [121].

115

In effect it is a variant of the transient liquid phase sintering (TLPS) process that leads to the formation and densification of the interlayer. This process should not be confused with TLP bonding, which is totally different. With TLPS several variables have to be considered for the process to be optimised. From a thermodynamic view, the melting behaviour, solubility and interfacial energies are most important. The interfacial energies dictate the dihedral angle and wetting of the solid by the liquid. The liquid must form a film around the solid phase, with a small contact angle and the solid must be soluble in the liquid.

The kinetics of the process depends on spreading, capillarity and penetration of the liquid. Diffusion of the solid phase through the liquid determines the coarsening and intermediate stage densification rates. Processing factors greatly influence this process, the most important of which are; particle size, stoichiometry/homogeneity, green density, temperature, time and atmosphere.

The major advantage of TLPS over conventional solid-state sintering is that a dense structure is obtained at a lower temperature and shorter time.

Stage 1. Butt joint configuration at room temperature:
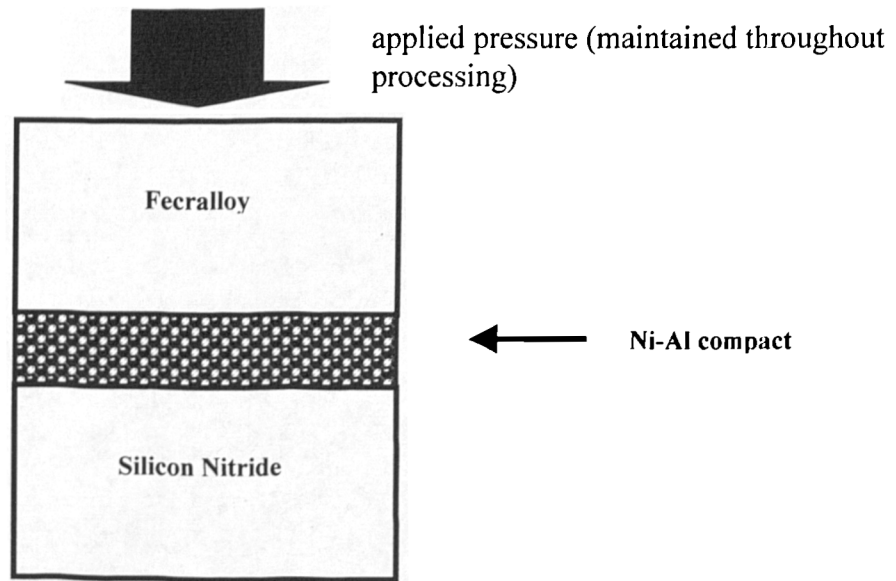
Stage 2. Solid state reactions at 500°C:
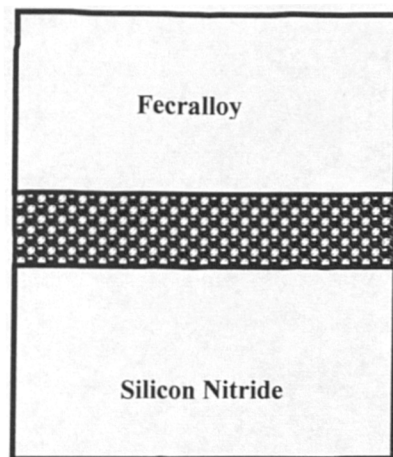
schematic of interlayer with increasing temperature:
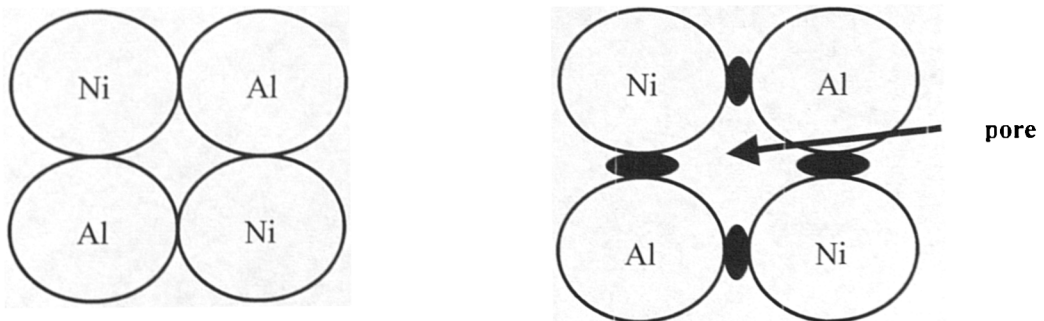
At room temperature

Initial solid state reactions that yield small amount of product

Formation of reaction products arounc
particles
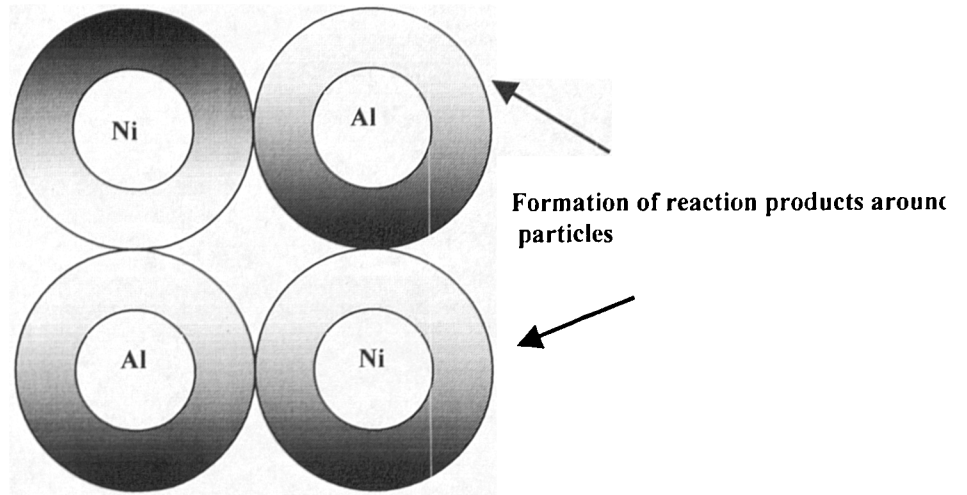
The formation of the solid-state reaction products produces enough heat to take the interlayer temperature up to 640-660°C, causing the Al to melt.

Transient liquid phase
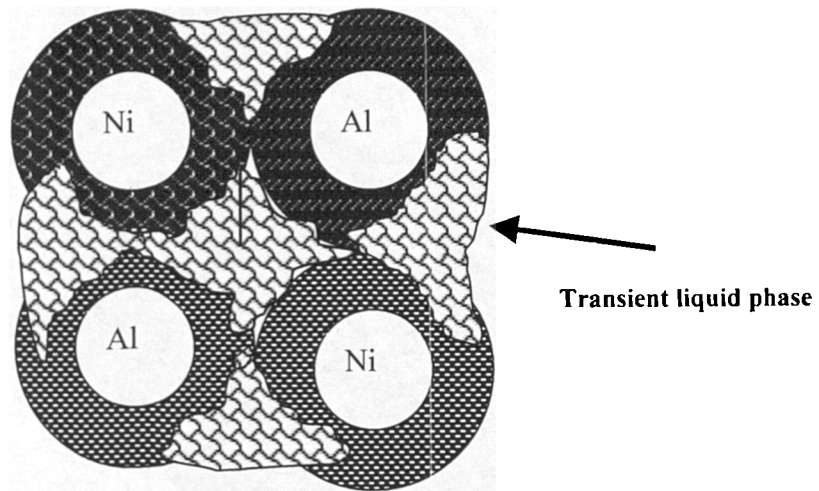
At 640-660°C, the Al melts and a transient liquid phase is formed that wets reacts leading to densification and monophase NiAl by self-propagating reactive synthesis.

Dense and monophase NiAl is formed mostly by the self-propagating reactive synthesis mode, while classical solid state sintering forms a small amount.

Stage 3. High T_c causes partial melting of Fecralloy interface.
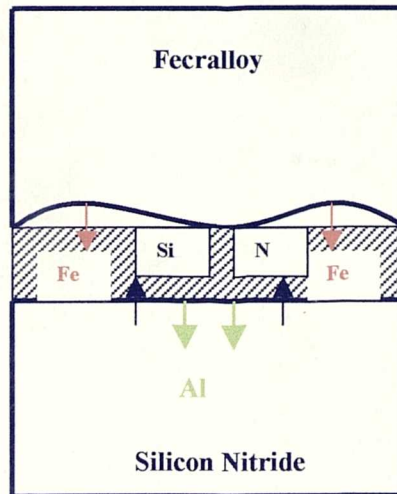
The T_c causes partial melting of the Fecralloy interface causing mostly Fe to infiltrate the interlayer. At this high temperature, the molten Al reactively wets the silicon nitride interface, with Si and N diffusing into the interlayer due to dissolution of the silicon nitride interface.

Stage 4. At room temperature,
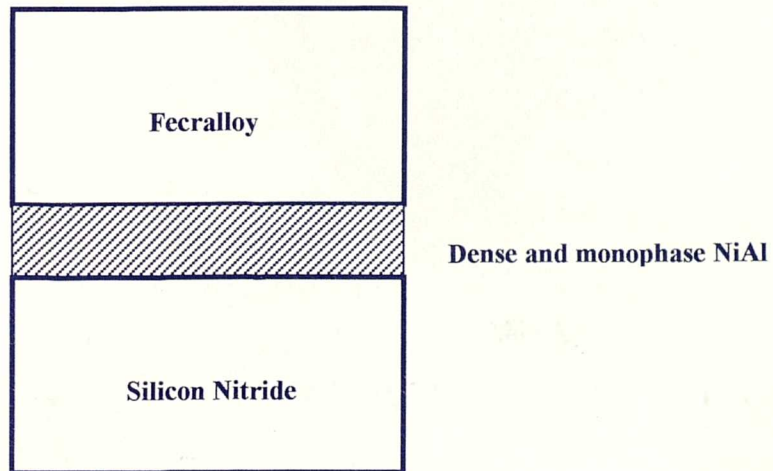
Upon cooling to room temperature, a strong joint is formed with good interfacial bonding and no reaction product layers at the ceramic interface.

Fig 5.22.   **Schematic illustrating sequence for reaction bonding using a cold pressed Ni-Al compact (not to scale).**

5.4   Processing Conditions

The key to successful joining by reaction bonding is the production of a dense monophase NiAl interlayer by reaction synthesis. It is therefore important to optimise all process conditions to produce the interlayer during the joining process. Processing conditions that influence the reaction between the constituent powders will alter the amount of transient liquid, length of time the liquid is present and its distribution. The various process factors effect the final density and mechanical properties of the interlayer and these can mostly be explained in terms of their effects on the liquid phase and reaction synthesis.

The most important factors are discussed, briefly in some instances, outlining their effects upon the interlayer and joining. Two very important factors, heating rate and particle size have been discussed in some depth.

5.4.1   Dry Mixing

This was carried out in a Turbula™ mixer in order to ensure good intermixing and particle-particle contact. Milling was ruled out as it would reduce particle size and due to large particle interfacial area, a more rapid reaction would occur with increased porosity.
Good intermixing ensures the interconnected Al matrix exist and it is this interconnectivity that promotes long range capillary action upon the liquid phase ensuring uniform densification.

5.4.2   Atmosphere

The role of the process atmosphere can be explained by its ability to conduct heat from the interlayer and to out trapped air/gas from the pores. Vacuum reduces heat loss to the surroundings and maintains T_c for slightly longer times. Higher densification is also achieved as pores are evacuated. The use of an atmospheric gas such as argon tends not to be beneficial as the atmosphere carries heat away. If the rate of heat loss is greater than that of heat generation, self-propagating synthesis will not occur. Argon can also be trapped inside the pores and hinder densification.

5.4.3   Temperature

The main requirement of temperature is to initiate the self-propagating synthesis at T_{ig}, where a transient liquid forms. Temperature over this increases the diffusion rate, increases wetting, increases solubility of the solid in the liquid, decreases the liquid viscosity and increases the amount of liquid. All of these factors favour more rapid densification, however, the time-temperature combination has to be controlled to optimise the densification. According to classical sintering theory, the optimal sintering time decreases with increased sintering temperature due to greater diffusion and greater liquid content [133]. Our results found that at temperature and pressure (900°C, 45 MPa) increasing dwell time from 5 to 15 minutes not only eliminated porosity but also increased joint shear strength.

As has been previously discussed, the heating rate is very important and has a direct effect upon joining. Joining was carried out at 800°C, 900°C, and 1000°C. The joints that exhibited the highest shear strength with a dense and monophase NiAl were produced at 900°C. The DTA results shows that with the appropriate heating rate monophase NiAl is produced by 700°C. In the joining trials the exothermic heat that is released and helps propagate the reaction synthesis is also absorbed by the metal and ceramic. This is shown by the partial melting of the Fecralloy interface and infiltration of Fe into the NiAl. Increased temperature causes a decrease in average shear strength and this is due to the build up of residual thermal stress primarily at the interlayer-ceramic interface.

5.4.4   Pressure

The application of uni-axial pressure was important and used in two steps. The first was the compaction of the Ni-Al powder to produce a compact and the second was during the joining process. Matsuura *et al.* [92] conclusively showed that increased pressure on the green compact (Ni-Al powder) was beneficial in reducing porosity, and to assist in the reactive synthesis of NiAl. Therefore, a compaction pressure close to 1GPa was used.

The effects of pressure during the joining process were investigated upon the interlayer and average shear strength. From the micrographs shown in Fig 5.6-5.8 and the graph showing average shear strength (±8 MPa) versus bonding pressure (Fig 5.23), it is clear that increased

pressure is beneficial in reducing porosity and increasing shear strength. The increased pressure ensures good particle-particle contact and helps to break up any surface oxides. This assist the self-propagating reaction synthesis and the applied pressure also help the liquid phase to propagate through the compact.

With the application of an external pressure, the rearrangement processes plays a greater role in densification. In the rearrangement stage the rate of densification increases with capillary force. Increased pressure generally increases the capillary force and this aids the densification process. Large particle size is known to have low capillary forces as they have an inverse relationship, but as pressure increases the particle size effects becomes smaller.

Apart from aiding the reaction synthesis of NiAl, the applied pressure also forms joints with increased shear strength. This is due to the intimate contact brought about by increased pressure between the interlayer and metal/ceramic interface. Pressure aids the break up of the detrimental surface oxides and oxynitrides and helps the wetting process. It is the molten Al that wets the ceramic interface and previous work [43] has shown that the non-wetting to wetting transition of an Al drop on silicon nitride occurs at about 1100°C. Process temperatures lower than this were used, but the T_c reaches temperatures well above this and aids the reactive wetting process.
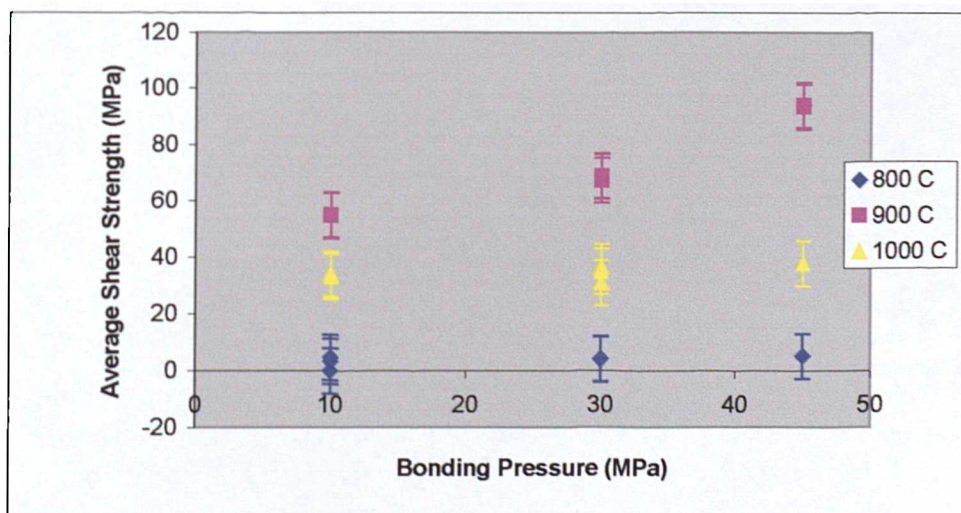

Figure 5.23   **Graph showing relationship between bonding pressure and temperature on average shear strength of joint.**

5.4.5 Time

This is an important process variable and our results shows that dwell time at temperature has a direct effect upon the joint shear strength. The time needed to attain a densified structure depends on several processing factors, the most important of which is the volume fraction of solid present and the process temperature. At temperature and pressure, an increase in dwell time to 15 minutes is beneficial as shear strength increases and porosity is reduced. From this one is led to believe that while the bulk of the interlayer is formed by self-propagating reactive synthesis, there are some areas of incomplete densification and porosity. Although not detected by XRD, this could be due to their small concentration. Thus, increased temperature and dwell time are beneficial as pores elimination occurs.

Work by Sims *et al.* [135] concluded that time was negligible on the exothermic formation of Ni₃Al as it was produced in a matter of seconds. Recent work by Matsuura *et al.* [94] found that monophase NiAl formed after 7 minutes at the reaction synthesis temperature. Numerous factors such as heating rate and particle size all effects the formation time.

There is a major difference between the reaction synthesis time and the process joining time (dwell time). The process joining time occurs at a temperature above which the NiAl forms and so has more of a homogenisation and annealing effect upon the interlayer. However, prolonged time would be detrimental to the interlayer as pore growth and microstructural coarsening become favourable. Also the formation of detrimental phases at the interlayer-ceramic interface can occur. Such a detrimental time was not identified during the course of this work.

5.5 Mechanical Properties

5.5.1 Shear Strength

From table 5.1 it can be seen that shear strength values of up to 94.3 MPa were possible using a NiAl interlayer. The maximum shear strength obtained using a Cu interlayer (previous chapter) was 67.5 MPa and this is a considerable improvement.

The introduction of small amounts of Fe into the interlayer from the partial melting of the Fecralloy interface greatly improves the mechanical properties of the NiAl, the most important of which is the increased room-temperature ductility. The residual stress depends on numerous factors, the most notable being; (a) the difference between processing and ambient temperature (b) the CTE mismatch (c) ability of interlayer to plastically deform and absorb some of the evolved residual strain.

The lower processing temperature and dwell time (900°C, 15 minutes), higher pressure (45 MPa) and remaining ductile NiAl interlayer all help to reduce the residual thermal stress that is induced during processing. The use of higher pressures ensures good interfacial bonding with intimate interfacial contact (no un-bonded regions) and the absence of any reaction product layer at the silicon nitride interface is believed to contribute to increasing the shear strength. As was discussed in the previous chapter, the presence and thickness of a reaction product layer at the silicon nitride interface can either be beneficial or detrimental to joint strength. Generalization is difficult as this varies from system to system, but a thick reaction product layer does induce growth stresses due to volume changes during formation.

Zhang *et al.* [136] investigated the influence of CTE mismatch on bond strength for a metal-ceramic joint. FEA was used to stimulate the stress distribution along the joint, where alumina was joined to 304 stainless steel by a PTLP method using a Ni-Cr interlayer (1150-1250°C, 180 minutes, 4 /1 K/minute heating/cooling rate). Their work showed that the residual stress is tensile in nature on the ceramic side and this gradually changes in to compressive stress on the ceramic side. Accordingly, the thermal stress is more detrimental for the ceramic. The tensile stresses in the ceramic side were found to be maximum in the vicinity of the interface, the shear stresses also being found to be maximum near to this location. The presence of shear stress at the ceramic side near to the joint interface may in combination with the tensile stress induce fracture along the ceramic interface. Ceramics tend to have poor fracture toughness and cannot provide enough energy to prevent crack progression. Their work showed that a compliant interlayer does reduce the residual stress and improve joint strength. This was found to be dependent upon interlayer thickness and ductility, where a thicker interlayer reduced the residual stress. This can be related to our joining results, where the NiAl interlayer was of considerable thickness and ductility.

As was discussed in section 5.4, the processing conditions greatly influence the shear strength. This can be used to optimise the joining process in order to produce high strength metal-ceramic joints.

Optical analysis of the shear test samples found that two-fracture types exist in the metal-ceramic joints. In the first type, as shown in Fig 5.24, the crack propagates along the interlayer-ceramic region separately the two. This type of fracture was associated with joints of low/moderate shear strength. This suggests that this is a weak zone and that adhesion between the interlayer-ceramic is poor.

In the second type of fracture the crack initiates and propagates in the silicon nitride only, close to the joint interface (Fig 5.25). This type of fracture behaviour was associated with joints that exhibited high shear strength, where adhesion between interlayer-ceramic was good usually due to greater applied pressure. This confirms the predicted behaviour put forth by Zhang *et al.* [135] where the residual stress is high in the ceramic near to the interface and from where crack propagation is most likely.

In the joining of dissimilar materials residual stresses are inevitable due to CTE mismatch. This problem cannot be eliminated but has to be addressed. The use of lower processing temperatures, short dwell time and a ductile interlayer improve the shear strength by reducing the residual stress.
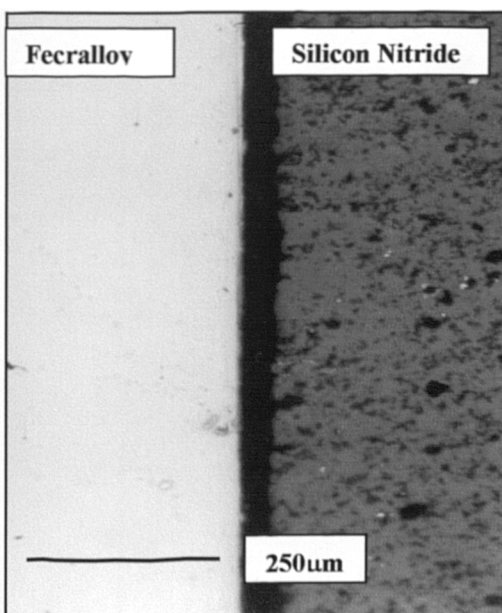
Figure 5.24. Micrograph showing failure due to first type of failure mode during shear test (deattachment).
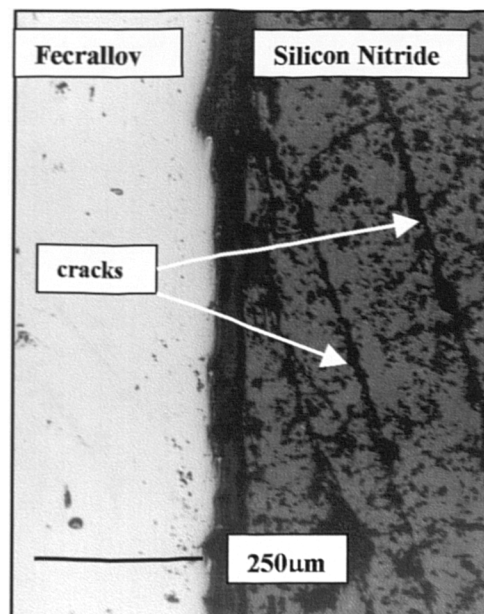
Figure 5.25. Micrograph showing shear test failure due to second type of failure (cracking in ceramic).

125

Temperature (°C)	Time (minutes)	Pressure (MPa)	Average Shear Strength (± 8 MPa)	No. thermal cycles till failure
800°C	5	10	0	0
800°C	10	10	4.63	0
800°C	15	10	3.28	0
800°C	5	30	4.11	0
800°C	10	30	4.18	0
800°C	15	45	5.20	0
900°C	5	10	54.90	3
900 C	10	10	55.23	3
900 C	15	10	55.02	2
900 C	5	30	68.90	5
900 C	10	30	67.56	6
900 C	15	30	69.11	6
900 C	5	45	93.66	10
900°C	10	45	94.12	10
900°C	15	45	94.30	10
1000°C	5	10	34.16	2
1000 C	10	10	33.29	2
1000°C	15	10	34.33	2
1000°C	5	30	36.87	1
1000°C	10	30	31.29	1
1000°C	15	30	35.34	2
1000°C	15	45	38.21	2

Table 5.1   **Summary of results**

5.5.2   *Thermal Cycling*

On reviewing literature related to metal-ceramic joining, one finds that joint strength is measured by various techniques but no thermal cycling is carried out. This is an important parameter that should be used in conjunction with strength measurements to characterise the mechanical properties of the metal-ceramic joint. In this work materials known for their high temperature oxidation resistance were used and while they would not be effected by oxidation, the effects of thermal cycling were looked at.

The thermal cycling results given in Table 5.1 are good, with some joints withstanding up to 10 thermal cycles till failure. This is due to good interfacial bonding and reduced residual thermal stress. These results can be directly related to the shear strength results. Joints that exhibit high shear strength are also able to withstand a greater number of thermal cycles till failure. This demonstrates the link between shear strength and thermal shock resistance of the joints.

Unalloyed NiAl is brittle at room temperature and ductile at higher temperatures, exhibiting a ductile to brittle transition temperature (DBTT) between 350-400°C. This is still the case with alloyed NiAl, where there is an increase in high-temperature ductility from $6^o o$ to $40^o o$ after DBTT [136]. The exact reason for the increased ductility is not known but proposed explanations for this behaviour include the onset of dislocation climb, thermally activated slip and additional slip systems [136].

With the high strength joints there is good interfacial bonding and it is the excellent high-temperature ductility of the interlayer that is responsible for the good thermal shock resistance of the joint. This demonstrates the strength of the interfacial bonding where the interlayer elastically plastically deforms in order to counteract the residual stress caused by the CTE mismatch. Failure was always due to crack propagation always in the ceramic close to the joint interface. The crack initiated from the pores present and then propagated till failure, as shown by the micrograph of Fig 5.26. These are regions from where stress concentrates and when the stress in a pore reaches a critical value, a crack forms and propagates. There are no large energy absorbing process in ceramics such as those that operate in ductile metals during deformation and so a crack propagates till failure. Pores decrease the cross-sectional area over which a load is applied and hence lowers the stress a material can support.

Thus, it is important to reduce porosity in the interlayer and ceramic to improve the mechanical properties. RBSN is inherently 15-20% porous and so it's mechanical properties will be lower compared to SSN where porosity is almost non-existent.

For the low/moderate strength joints, failure was usually due to the detachment of the interlayer from the ceramic. This is due to poor interfacial bonding where the interface is unable to withstand the residual stresses that take effect with the thermal cycling.
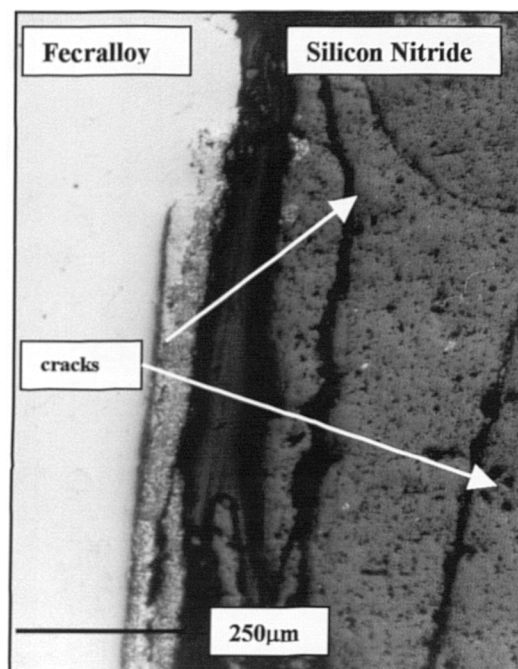
Figure 5.26. **Micrograph showing joint failure after thermal cycling, where cracking is in the ceramic only.**

5.5.3   *Microhardness*

Microhardness profiling is a useful mechanical parameter that can be used to characterise and compare the effects of joining on the metallic substrates. It was used to measure the variation of microhardness across the Fecralloy-NiAl interface in order to assess the effects of the joining process had and to see if homogenisation occurs.

Microhardness was found to vary with distance from the interface, as shown in the various profiles of Fig 5.27. At the NiAl interface the microhardness was $392H_v$ and this decreased with distance away to $378H_v$ at $800\mu m$. This can be explained by the presence of Fe that has

infiltrated the NiAl and whose concentration levels off with distance away from the interface. The Fe causes an increase interfacial microhardness due to solution hardening.

At the Fecralloy interface the microhardness is lower and increases with distance from the interface. The interfacial melting due to the reactive synthesis of NiAl is believed to cause the lowered interfacial microhardness.

Dwell time and temperature had little effect on the microhardness profiles and so it is difficult to comment on homogenisation from this.
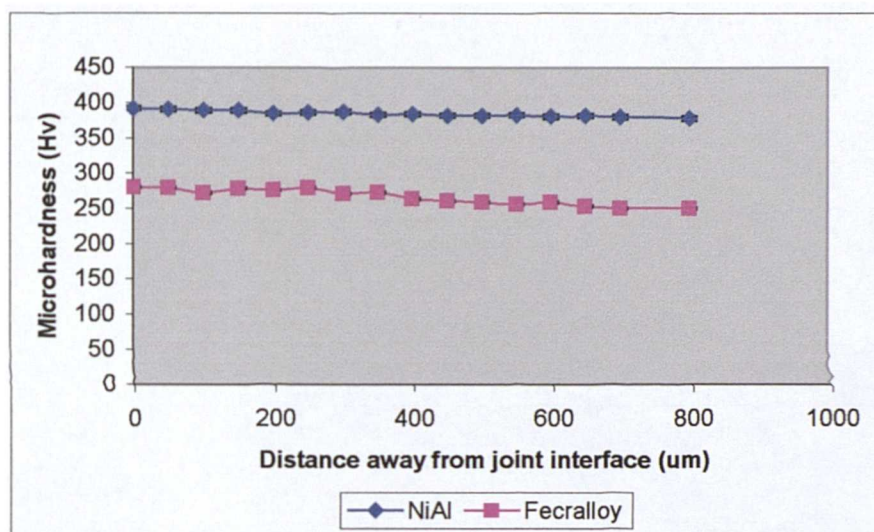
Figure 5.27.   **Graph showing microhardness variation at and away from Fecralloy-NiAl interface.**

5.6   *Summary*

A powder metallurgy route achieved joining between Fecralloy-silicon nitride with some joints exhibiting high shear strength and thermal shock resistance.

Optimising the process conditions, namely moderate temperature, dwell time and high applied pressure all helped to reduce the residual stress, improve interfacial contact/bonding and produce a monophase and densified interlayer. All of these factors led to the production of joints with high shear strength and thermal shock resistance.

However, this process is dependant upon the highly exothermic formation of the NiAl interlayer from its constituents. The high temperature reached (T_c) causes partial melting of the Fecralloy interface and dissolution/reactive wetting at the silicon nitride interface. Mostly Fe infiltrates the NiAl interlayer improving the room temperature ductility, fracture toughness and yield strength, as reported by Miracle *et al.* [121]. Molten Al from the interlayer reacts and wets the silicon nitride interface, with small amount of infiltration into the silicon nitride. There was no reaction product layer formed at the silicon nitride interface. Good interfacial bonding, no reaction layer products, moderate process temperature and dwell time, high pressure, formation of a monophase and densified NiAl interlayer that is ductile at both room temperature and high temperature all were responsible for the production of joints that exhibited high shear strength and good thermal shock resistance.

The exothermic formation of the NiAl is highly dependant upon particle size and heating rate, as was demonstrated.

The Bansal-Doremus kinetic model was found to be valid as the results obtained conferred those by other authors who used a different model and approach.

Joining by a powder metallurgy route using a NiAl interlayer has been shown to be a valid method of producing integral Fecralloy-silicon nitride joints. Due to the oxidation resistant nature of the materials used the joints produced are not easily susceptible to moderate temperature oxidation (850°C), with the potential of withstanding temperatures up to 1000°C.

A viable and low cost technique has been put forth that offers a realistic opportunity of joining Fecralloy with silicon nitride.

6.   *Conclusion*

The importance of Joining Technology and benefits of joining dissimilar materials such as metal to ceramic has been emphasised throughout this work.

The objective of this study was to successfully join Fecralloy to silicon nitride, of which there are no reports to date. The primary focus was on the effects of process conditions upon the microstructure-mechanical properties of the joint. Also to identify and study the joining mechanism.

The ultimate aim of this study has been achieved, namely the successful joining of Fecralloy to silicon nitride by two different joining techniques. Two different joining interlayers were employed and the effects of the process conditions (eg. applied pressure, temperature, interlayer thickness, particle size, etc) were investigated with regards to the microstructure and mechanical properties of the joint.

Attempting not to repeat the summaries of chapters 4 and 5, the main conclusions of this work can be summarised as;

- Fecralloy was successfully joined to silicon nitride via two novel techniques.

- The first technique employed a thin Cu foil that did not remain after processing. At 1100°C (9.5 MPa, 30 minutes) the joint exhibiting the highest shear strength was produced (67.5 MPa).

- A reaction product layer was present at the silicon nitride interface and our results indicate that this is AlN.

- The free surface Si and porosity of the silicon nitride and temperature above 1100°C are all vital factors for this joining process.

- No correlation could be established between the theoretically derived values for melt-back distance and the microhardness profiles.

- The second technique was that of a powder metallurgy one, where NiAl successfully joined Fecralloy to silicon nitride.

131

- High shear strength and thermal shock resistant joints were produced. The highest joint shear strength was 94.30 MPa and it withstood 10 thermal cycles at 850°C in air (900°C, 15 minutes, 45 MPa).

- The moderate process temperature and dwell time and high-applied pressure all improve the shear strength of the joint by reducing the residual stress and improve interfacial contact/bonding.

- This process is highly dependant upon the exothermic formation of NiAl from its constituents. The high temperature reached (T_c) causes partial melting of the Fecralloy interface and dissolution/reactive wetting at the silicon nitride interface. Mostly Fe infiltrates the NiAl and improves its properties, most importantly room temperature ductility.

- The exothermic formation of the NiAl is highly dependant upon particle size and heating rate, as was demonstrated. The NiAl has to be densified and monophase to produce a good joint.

- The Bansal-Doremus kinetic model was found to be valid as the results obtained in this work were similar to those by other authors who used a different model and approach.

- It was shown that optimising the process conditions for both techniques did improve the mechanical properties of the joint.

In a recent International Materials Review on the Progress in joining of advanced materials [138], it was stated that 'sound joint quality for any new or advanced material has always been considered a milestone in research and development. Better understanding of the microstructure-mechanical properties relationship of the joint will feed back to the materials development activities both in conventional and new material areas'. It is hoped that this is the case and that this work has made a contribution to the field of joining technology by presenting an instep to low cost and commercially viable techniques for producing metal-ceramic joints for higher temperature applications.

7.   Future Work

With regards to recommendations for future work numerous areas have been identified. The first is to see the effects of increasing sample size from 10mm x 10 mm x 8 mm to 50mm x 50 mm x 20mm, for instance. Sample size is known to have an effect upon the mechanical properties of the joint and it would be interesting to see exactly how on these two joining systems.

It is felt that the joint interface should be studied more comprehensively by use of techniques such as transmission electron microscopy (TEM) in order to conclusively identify the reaction product layer, precipitate formation/distribution and elemental migration.

The measurement of residual stress by a technique such as the indentation fracture method or XRD method, as outlined by Lee *et al.* [137] would be beneficial. This would quantify the residual stresses and show its variation with process conditions. Relationships could be identified with a view to improving joint integrity.

Extending the joining techniques from this work to other metal-ceramic combinations would be of interest. This would show if these two joining routes are confined only to join Fecralloy-silicon nitride. It is believed that the Ni-Al compact route has the potential to produce integral joints with other metal-ceramic combinations.

Metal to ceramic joining via a FGM interlayer is an exiting challenge that has to be investigated. The theoretical advantages and the processing difficulties are known, but they have to be practically investigated. A comprehensive investigation could be the initiation of greater commercial and academic interest or show that their use in metal-ceramic joining is not feasible.

References

[1].   R.W.MESSLER, "Joining of advanced materials" (Butterworth-Heinemann, 1994).

[2].   I. E. REIMANIS, C. H. HENAGER and A. P. TOMSIA, Proceedings of the Ceramic Joining symposium, 98th Annual Meeting of the American Ceramic Society, Indiana, April 1996.

[3].   M. G. NICHOLAS, "Joining of Ceramics" (Chapman and Hall, 1990).

[4].   S. MUSKANT, "What every engineer should know about ceramics" (Chapman and Hall, 1991).

[5].   O. M. AKSELEN, *J. Mater. Sci.* **27** (1992) p.569.

[6].   L. ESPOSITO, A. BELLOSI, S. GUICCIASDI and G. DE PORTU, *J. Mater. Sci.* **33** (1998) p.1827.

[7].   J. P. KRUGERS and G. DEN OUDEN, *Int. J. Join. Mater.* **3** (1992) Vol 4 p.73.

[8].   J. P. KRUGERS and G. DEN OUDEN, *Int. J. Join. Mater.* **3** (1994) Vol 6 (3) p.88.

[9].   K. SUGANAMA, T. OKAMOTO, Y. MIYAMOTO, M. SHIMADA and M. KOIZUMI, *Mater. Sci.Tech.* **2.** (1986) p.1156.

[10].   A. KRAJEWSKI, *J. Mater. Proc. Tech.* **54** (1995) p.103.

[11].   B. T. J. STOOP and G. Den Ouden, Metal.and Mat.Trans.A, Vol 26 A p.203-208 (1995).

[12].   L. ESPOSITO, A BELLOSI and G. CELDITTI, *Acta. Mater.* **12** (1997) Vol 45, p.5087.

[13].   L.ESPOSITO, A. BELLOSI and G. DE PORTU, *J. Mater. Sci.* **33** (1998) p.1827.

[14].   R. S. BUSHBY and V. D. SCOTT, *Mater. Sci and Tech.* **11** (1995) p.753.

[15].   J. A. FERNIE, "Ceramic Joining", (American Ceramic Society 1997) Vol 77 p.3.

[16].   K. SUGANAMA, *Ceram. Mater.* **1** (1986)p356.

[17].   H. TABATA, *Proc. Int. Symp. Ceram. Comp. Eng.* (1984) p.387.

[18].   K. BHANUMURTHY and R SCHMID-FETZER, *Mater. Sci. Eng.* A (1996) p.35.

[19].   L. HUIJIE, *J. Mater. Sci. Lett.* **18.** (1999) p.1011.

[20].   K. OZTURK, R. N. BASU, C. A. RANDULL and M. J. MAYO, *Scripta Materialia.* **11** (1999) Vol 41,p.1191.

[21].   W. D. MACDONALD, *Mater. Sci. Ann. Rev.* **22** (1992) p.23.

[22].   Y. ZHOU, *Intl. Mater.Rev.* **40.** (1995) p.181.

[23].   I. TUAH-POKU, M. DOLLAR and T. B. MASSALKI, *Met. Trans.* **A.** (1998) Vol.19A p.675.

[24].   N. EUSTATHPOULOS, M. G. NICHOLAS and B. DREVET, "Wettability at High Temperatures" (Pergamon Materials Series, 1999).

[25]. J. R. ASKEW, J. F. WILDE and T. I. KHAN, *Mater. Sci. and Tech.* **14**. (1998) p.920.

[26]. J. R. ASKEW and T. I. KHAN, in Proceedings for the Joining of Materials conference JOM-9 (1999).

[27]. Z. LI, W. FEARIS and T. H. NORTH, *Mater. Sci and Tech.* **11**. (1995) p.363.

[28]. Y. N. AKAO and K.SHINOZAKI, *Mater. Sci and Tech.* **11** (1995) p304

[29]. Y. ZHOU, K. I. KEUCHI, T. H. NORTH and Z. WANG, *Metall.Trans.* **22A** (1991) p.2822.

[30]. G.CECCONE, *Acta. Materialia.* **44** (1995) p.657.

[31]. M. PAULASTO, G. CECCONE and S. D. PETEVES, *Scripta Materilia.* **10** (1997) Vol 36. p1167

[32]. C. ZHENG, H. LOU and Z. LI, *J. Mater. Sci. Lett.* **16** (1997) p.2026.

[33]. Y. ZHAI and J. REN, *J. Mater. Sci.* **32** (1997) p.1399.

[34]. Y. ZHAI, H. NORTH and J. SERRATO-RODRIGUES, *J. Mater. Sci.* **32** (1997) p.1393.

[35]. O. M. AKSELSEN, *J. Mater. Sci.* **27**. (1992) p1989.

[36]. M. G. NICHOLAS, "Joining of Ceramics" (Chapman and Hall, 1990) p.76.

[37]. K.LANDRY, C. RADO, R. VOITOVICH and N. GUSTO *Acta. Materialia.* **45.** (1997) p.3079.

[38]. J. A. WARREN, W. J. BOETTINGER and A. R. ROSEN *Acta. Materialia.* **46.** (1998) p.3247.

[39]. Y. S. CHUNG, *Eng. Frac. Mech.* **415** (1991) Vol 40. p.941.

[40]. Y. V. NAIDICH, N. Y. TARANET, in Proceedings of International conference on high temperature capillarity (ASM, USA 1994).

[41]. N. EUSTATHPOULOS, M. G. NICHOLAS and B. DREVET, "Wettability at High Temperatures" (Pergamon Materials Series, 1999) p. 360.

[42]. M. G. NICHOLAS, "Joining of Ceramics" (Chapman and Hall, 1990) p.178.

[43]. N. EUSTATHPOULOS, M. G. NICHOLAS and B. DREVET, "Wettability at High Temperatures" (Pergamon Materials Series, 1999) p. 294.

[44]. J. R. MCDERMAID, *Met. Trans. A* **20** (1989) p.1803.

[45]. S. D. PETEVES, M. PAULASTO, G. CECCONE and V. STAMOS, *Acta. Materilia.***7** (1998) Vol.46. p.2407.

[46]. M. W. FINNIS, *J. Phys. Cond. Matter.* (1996) p.5811.

[47]. F. G. YOST, R. A. SACKINGER and E. J. O'TOOLE, *Acta. Materilia.* **7** (1998) Vol 46 p.2329.

[48]. J. A. YEOMANS and T. F. PAGE, *J. Mater. Sci.* **25** (1990) p.2312.

[49]. K.LANDRY, C. RADO, R. VOITOVICH and N. GUSTO *Acta. Materialia.* **45.** (1997) p.3079

[50]. G. ROSAZZA PRIN, *Mater. Sci. Eng A* **298** (2001) p.34.

[51]. S. D PETEVES, M. PAULASTO, G. CECCONE and V. STAMOS, *Acta. Materilia.* **7** (1998) Vol 46 p.2407.

[52]. P. XIAO and B. DERBY, *J. Mater. Sci.* **30** (1995) p.5915.

[53]. P. XIAO and B. DERBY, *Acta.Materialia.* **10** (1998) Vol 46 p.3491.

[54]. X. B. ZHOU and J.T. M. DETRLOSSON, *Acta.Materilia.* **2** (1996) Vol.44. p.421.

[55]. W. C. LEE, *J. Mater. Sci.* **32** (1997) p.221.

[56]. J. H. CHEN, E. Z WANG NOG, M. KAMI, N. SATO, and N. IWAMOT, *J. Mater. Sci.* **28** (1993) p.293.

[57]. A. II. ELSAURY and M. F. FAHURY, *J. Mater. Proc. Tech.* **77** (1998).p.266.

[58]. K. SUGANUMA, T. OKAMOTO, M. FOIZUM, M. SHIMADA, *J. Mater. Sci.* (1987) p.1359.

[59]. M. G. NICHOLAS, "Joining of Ceramics" (Chapman and Hall, 1990) p.175.

[60]. M. PANLASTO, *Scripta Materialia.* **10** (1997) Vol 36. p.1167.

[61]. Y. MATSOU, M. HO, and M. TAMGUCHI, *Industrial Ceramics* **3** (1999) Vol .19.

[62]. H. XIONG, C.WAN, Z. ZHON, *J. Mater. Proc. Tech.* **75** (1998) p.137.

[63]. M. HEIM, *Ceram. Eng. Sci.* **19** (1999) p3.

[64]. M. SINGH, in Proceedings from Joining of Advanced and Speciality Materials, October 1998, USA, edited by M. Singh, J. E. Indacochea and D. Hauser, p.1.

[65]. W. B. HANSON, K. I. IRONSIDE and J. A. FERNIE, *Acta. Materilia.* **48** (2000) p.4673.

[66]. H HAO, Y. WANG, Z JIN and X. Wang, *J. Am.Ceram. Soc.* **78** (1995) No.8 p.2157.

[67]. H. HAO, Y. L.WANG, Z. H. JIN, and X. T. WANG, *J.Mater. Proc. Tech.* **52** (1995). p.238.

[68]. A. V. DUROV, B. D. KOS, A. V. S. CHEUKO and Y. V. NAIDICH, *Mat. Sci. Eng A* **290** (2000) p.186.

[69]. H. HAO, Y. WANG, Z. JIN and X. WANG, *J. Mater. Sci.* **30** (1995) p.4107.

[70]. R. A. MARKS, D. R. CHAPMAN, D. T. DANIELSON, A. M. GlAESSER, *Acta. Materilia* **48** (2000) p.4425.

[71]. J. H KIM, Y. C. YOO, *J. Mater. Sci. Lett.* **16** (1997) p.1212.

[72]. S. P. KOVALEV, P. MIRAN, and M. OSCENDI, *J. Am. Ceram. Soc.* **81** (1998) (9) p.2342.

[73].   D. MUNZ, M. A. SCKHUR and Y. YANG, *J. Am. Ceram. Soc.***78** (1995) (2) p.185.

[74].   M. G. NICHOLAS, "Joining of Ceramics" (Chapman and Hall, 1990) p.184.

[75].   J. A. FERNIE, "Ceramic Joining", (The American Ceramic Society, 1996) p.8.

[76].   J. A. FERNIE and W.B. HANSON, in proceedings of 8th.World Ceramic Congress p.165 (1996).

[77].   J. LI and P. XIAO, *J. Mater. Sci.* **36** (2001) p.1383.

[78].   K. MORSI, *Mat. Sci. Eng A.***299** (2001) p.1.

[79].   Y. MIYAMOTO, *J. Mater. Res.* **1** (1986) Vol 1 p.7.

[80].   B. H. RABIN, *Int. J. Self Prop. High Temp. Syn.* **1** (1992).

[81].   V. M. ROSARIO, M. C. CHATURVEDI, G. J. KIPOROUS and W. F. CALEY, *Mat. Sci. Eng A***270** (1999) p.283.

[82].   A. K. JADOON, in Proceedings of the 6th International Symposium on Advanced Materials, Pakistan, September 1999, edited by M. A. Khan, K. Hussain and A. Q .Khan, p.304.

[83].   ASM handbook, Vol 3 (1992), Alloy phase diagrams (ASM International).

[84].   L. PLAZANET and F. NARDOU, *J. Mater. Sci* **33** (1998) p.2129.

[85].   K. A. PHILPOT and Z. A. MUNIR, *J. Mater. Sci* **22** (1987) p.159.

[86].   D. E. ALMAN and N. S. STOLOFF, *Int. J. Powd. Met.* **1** (1997) Vol 27.

[87].   K. MATSUURA, T. KITAMUTRA and M. KUDOH, *J. Mater. Proc. Tech.* **63** (1997) p.298.

[88].   Z. A. MUNIR, *Solid State Phen.* **37** (1989) p.8.

[89].   T. S. DYER and Z. A. MUNIR, *Metall. Mater. Trans. B* **26** (1995) p.603.

[90].   H. C. YI and J. J. MOORE, *J. Mater. Sci.* **25** (1990) p.1159.

[91].   K. MATSUURA, K. OHSASA, N. SUEKO, M. KUDOH, *Met. Mater. Trans. A.* **30** (1999) p.1605.

[92].   K. MATSURA, K. OHSASA, N. SUEOHA, M. KUDOH, *ISIJ. Int.* **3** (1998)Vol 38, p.310.

[93].   K. MATSUURA, H. JINMON, Y. HIRASHISHMA, T. I. KHAN and M. KUDOH, *ISIJ. Int.* **2** (2000) Vol 40 p.161 .

[94].   K. MATSUURA, H. JINMON, T. OHMI and M. KUDOH, *Int. J. Self. Prop. High. Temp. Syn.* **3** (1999) No.3 p.307.

[95].   K. MATSUURA, H. JINMON and M. KUDOH, *ISIJ.Int* **2** (2000).Vol.40. p.167.

[96].   K. MATSUURA and M. KUDOH, in proceedings from 2nd International conference on Materials for Propulsion, TMS, USA 2000, p.1053.

[97]. J. P. KAY and J. HURLEY, in Proceedings from Joining of Advanced and Speciality Materials, October 1998, USA, edited by M. Singh, J. E. Indacochea and D. Hauser, p.7.

[98]. M. SINGH, *Scripta Materilia.* **34** (1997) 8, p.1151.

[99]. M. SINGH, *Industrial Ceramics* **3** (1999) Vol 19.

[100]. M. KOIZUMI, *Composites Part B* **28B** (1997), p.1.

[101]. A. M. GLAESER, *Composites Part B* **28B** (1997) p.71-84.

[102]. K. KAKEGAWA and A. M. GLAESER, *Composites Part B* **28B** (1997) p.85.

[103]. Y. W. GU and K. A. KHOR, Y. Q. FU and Y. WANG, *Surface and Coatings Tech.* **96** (1997)p. 305.

[104]. J. F. GROVES and H. N. G. WADLEY, *Composites Part B* **28B** (1997) p.57-69.

[105]. S. K. MUKHERJEE and S. BANDYOPAGHUAY, *Composites Part B* **28B** (1997) p.45-48.

[106]. J. JEDLINSKI, *Solid State Ionics 101-103* (1997) p.1033.

[107]. J. JEDLINSKI, B. COHAT and G. BORCHARDT, *High Temperature Materials and Processes 13* (1994) p.241.

[108]. H. E. EVANS, *Mater. Sci. Tech. 4* (1988) p.415.

[109]. L. LJUNGBERG, *Ceram. Eng. Sci. Proc.* **10** (1989) p.1655..

[110]. P. Tomsia, *Ceram. Eng. Sci. Proc.* **10** (1989) p.1631.

[111]. ASM handbook, Vol 3 (1992), Alloy phase diagrams (ASM International)

[112]. A. KUBO, K. MAEKAWA and T. KITAGAWA, *Wear* 2 Vol. 22 (1997) p.142.

[113]. T. R. JONAS, J. A. CORNIC and K. C. RUSSELL, *Metall. and Mat. Trans. A*, Vol 26A (1995) p.1491.

[114]. R. H. VEGETER, *J. Mater. Sci.* **33** (1998) p.4525.

[115]. N. EUSTATHPOULOS, M. G. NICHOLAS and B. DREVET, "Wettability at High Temperatures" (Pergamon Materials Series, 1999) p. 294.

[116]. Y. IINO, *J. Mater. Sci. Lett.* **10** (1990) p.104.

[117]. C. ZHENG, H. LOU and Z. LI, *J. Mater. Sci. Lett.* **16** (1997) p.2026.

[118]. A. H. CARIM, *J. Am. Ceram. Soc.* **73** (1990) p.2764.

[119]. "Physical metallurgy and processing of intermetallic compounds", edited by N S Stoloff, (Chapman and Hall, 1996).

[120]. L. L. WANG, Z. A. MUNIR and Y. M. MAXIMOV, *J. Mater. Sci.* **28** (1993) p.3693.

[121]. D. B. MIRACLE and R. DAROLIA, "Intermetallic Compounds", edited by J. H.

Westbrook and R. L. Fleischer (John Wiley and Sons, 1994) p. 53.

[122]. K. MATSUURA, T. KITAMURA and M. KUDOH, *J. Mater. Proc. Tech.* **63** (1997) p.298.

[123]. J. X. ZHANG, R. S. CHANDEL, Y. Z. CHEN and H. P. SEOW, *J. Mater. Proc. Tech.* **122** (2002) p.220.

[124]. A. PHILPOT, Z. A. MUNIR and B. HOLT, *J. Mater. Sci.* **22** (1987) p.159.

[125]. J. P. LEBRAT, A. VARMA and A. E. MILLER, *Met. Trans. A* **2A** (1992) p.69.

[126]. S. DONG, P. HOU, H. YANG and G. ZOU, *Intermetallics* **10** (2002) 217.

[127]. H. E. KISSINGER, *Anal. Chem.* **29** (1957) p.1702.

[128]. M. ATZMON, *Metall. Trans. A* **23** (1992) p.49

[129]. L. FARBER, L. KLINGER and I. GOTMAN, *Mat. Sci. Eng. A* **234** (1998) p.155.

[130] A. BISWAS, S. K. Roy, K. R. GURUMURPHY, N. PRABHU and S. BANERJEE, *Acta Materilia* **50** (2002) p.757.

[131]. N. P. BANSAL and R. H. DOREMUS, *J Ther. Ana.* Vol 29 (1984) p.115.

[132]. P. R. MUNROE, M. GEORGE, I. BAKER and F. E. KENNEDY, *Mater. Sci. and Eng.* **A235** (2002) 1.

[133]. Z. A. MUNIR, *Amer. Ceram. Soc. Bull.* **67** (1988) p.342.

[134]. R. M. GERMAN, "Sintering Theory and Practise", (John Wiley and Sons, 1997).

[135]. D. M. SIMS, A. BOSE and R. M. GERMAN, *Prog. in Powder Metall.,* **4** (1987) p.575.

[136]. J. X. ZHANG, R. S. CHANDEL, Y. Z. CHEN and H. P. SEOW, *J. Mater. Proc. Tech.* **122** (2002) p.220.

[137]. S. B. LEE and J. H. KIM, *J. Mater. Proc. Tech.* **67** (1997) p.167.

[138]. G. CAM and I. KOCAK, *Int. Mater. Rev* **1** (1998) Vol 43.